A LETTERS JOURNAL EXPLORING THE FRONTIERS OF PHYSICS

LETTER • OPEN ACCESS

# Breakdown of the conventional spin-wave dynamics and its double-constraint modification in the spin-$\frac{1}{2}$ triangular-prism Heisenberg antiferromagnet

To cite this article: Shoji Yamamoto and Jun Ohara 2025 *EPL* **151** 36003

View the article online for updates and enhancements.

You may also like

- Topological aspects of antiferromagnets
V Bonbien, Fengjun Zhuo, A Salimath et al.
- Magnetization process of the *S* = 1/2 Heisenberg antiferromagnet on the floret pentagonal lattice
Rito Furuchi, Hiroki Nakano, Norikazu Todoroki et al.
- The kagome Heisenberg antiferromagnet $YCu_3(OH)_{6.5}Br_{2.5}$: a review
Xun Chen, Haijun Liao and Yuesheng Li

This content was downloaded from IP address 106.155.63.144 on 22/08/2025 at 01:53

A Letters Journal Exploring the Frontiers of Physics

August 2025

EPL, **151** (2025) 36003
doi: 10.1209/0295-5075/adedaf

www.epljournal.org

# Breakdown of the conventional spin-wave dynamics and its double-constraint modification in the spin-$\frac{1}{2}$ triangular-prism Heisenberg antiferromagnet

Shoji Yamamoto[(a)] and Jun Ohara

*Department of Physics, Hokkaido University - Sapporo 060-0810, Japan*

received 9 May 2025; accepted in final form 9 July 2025
published online 21 August 2025

**Abstract** – Spontaneous magnon decays in an $S = \frac{1}{2}$ Heisenberg antiferromagnet on the equilateral triangular prism are investigated in terms of modified magnon Green's functions. In one dimension, the so-called infrared divergence prevents us from calculating any —whether static or dynamic— structure factor within the conventional spin-wave theory even at zero temperature. The well-known modified spin-wave theory initiated by Takahashi completely fails to treat anharmonicities to cause transverse-to-longitudinal coupling which are quite characteristic of noncollinear antiferromagnets. We propose imposing a double-constraint condition on spin waves to solve all these difficulties and get a full view of the nonlinear spin-wave dynamics in one-dimensional frustrated noncollinear antiferromagnets. We reveal a novel instability of the single-particle spectrum in the absence of any well-defined magnetically ordered ground state.

open access Copyright © 2025 The author(s)

Published by the EPLA under the terms of the Creative Commons Attribution 4.0 International License (CC BY). Further distribution of this work must maintain attribution to the author(s) and the published article's title, journal citation, and DOI.

There are such surprises on the way from one- to two-dimensional quantum magnets [1–6] that the $S = \frac{1}{2}$ antiferromagnetic Heisenberg model on ladders exhibits an excitation gap immediately above the ground state when consisting of an even number of legs whereas that reproduces the quantum critical Tomonaga-Luttinger liquid behavior [7] of a single chain [8,9] when consisting of an odd number of legs. We can verify this theoretical scenario in various ladder materials such as two-legged $LaCuO_{2.5}$ [10], two-legged $CaV_2O_5$ [11], and $\frac{1}{2}(n+1)$-legged $Sr_{n-1}Cu_{n+1}O_{2n}$ $(n = 3, 5, \ldots)$ [12,13]. There are more interesting approaches to form these ladder materials into a cylindrical shape. Examples of such practices include three-legged $[(CuCl_2tachH)_3Cl]Cl_2$ (tach = *cis*, *trans*-1, 3, 5-triamino-cyclohexane) [14,15] and $CsCrF_4$ [16,17], four-legged $Cu_2Cl_4$-$D_8C_4SO_2$ [18,19], and nine-legged $Na_2V_3O_7$ [20–22].

Such chemical explorations motivated numerical investigations of the spin-$\frac{1}{2}$ nearest-neighbor antiferromagnetic Heisenberg model on a triangular prism [23–26]. Surprisingly, its ground state is no longer critical, breaking a translational symmetry in the leg direction [23,24]. $S = 1$ [27] and $S = \frac{3}{2}$ [28] analogs also exhibit an excitation gap immediately above their ground states with spontaneous dimerization. With decreasing coupling between triangles, however, the $S = 1$ ground state turns unique but the $S = \frac{3}{2}$ one stays degenerate, though both remain gapped from their excitation spectra. Despite such theoretical findings, experimental observations of the excitation gap to the lowest-lying triplet state are limited to more-than-three-legged tubes [18,22]. $[(CuCl_2tachH)_3Cl]Cl_2$ of $S = \frac{1}{2}$ is not a triangular prism [14,15] but an alternating stack of triangles [29–31] to behave as an effective spin-$\frac{3}{2}$ antiferromagnetic Heisenberg chain [31,32]. $CsCrF_4$ of $S = \frac{3}{2}$ seems a three-legged straight tube [16] but substantial magnetic anisotropies [33] hinder our detecting so small a gap of intrinsic origin [28].

A three-leg spin tube can give rise to a rich phase diagram [27] and therefore varied low-lying excitations, even if we limit our focus to an equilateral triangular prism consisting of Heisenberg-exchange–coupled identical spins. We are encouraged to calculate the dynamic

[(a)] E-mail: yamamoto@phys.sci.hokudai.ac.jp (corresponding author)

spin structure factor, which can be accessed directly by inelastic neutron scattering, for such a fascinating system, but it is far from straightforward to do so in the thermodynamic limit. Density-matrix renormalization group (DMRG) [24,34] and tensor network [35] are really powerful tools, but a direct access to the thermodynamic limit is still hard even with them. *Magnetic frustration* generally demands an increasing number $M$ of states kept in matrix renormalization [24,36] and several excited as well as the ground states must be included as targets in *dynamical* density-matrix renormalization at each frequency $\omega$ [24,37], both causing an increase in computational cost. We may consider a spin-wave (SW) theory in this context, but its naivest application to one-dimensional $SU(2)$ Heisenberg antiferromagnets ends in a fiasco. In one dimension, the conventional SW (CSW) theory [38] has no way of describing either static or dynamic structure factor even in the ground state, whether it is collinear or noncollinear, unless hardening of soft antiferromagnons. The staggered magnetization diverges logarithmically, to say nothing of the antiferromagnetic structure factor as its fluctuation [39], in a Heisenberg antiferromagnet on the triangular prism lattice within the CSW theory. We can overcome this difficulty by modifying CSWs so as to keep the total staggered magnetization zero [40–44]. Hartree-Fock (HF) approximation of such modified SW (MSW) Hamiltonian truncated at the order of $S^0$ yields an excellent low-temperature thermodynamics for collinear antiferromagnets [40,41], which turns out to be essentially the same as a Schwinger-boson mean-field description [45], but it still ends in failure when applied to frustrated noncollinear antiferromagnets. Since the total uniform magnetization is no longer commutable with any SW Hamiltonian, whether modified or not, MSWs conditioned as the above awfully overestimate the otherwise moderate intra-triangular ferromagnetic spin correlation. Then we devise a new MSW scheme [46] capable of suppressing such a ferromagnetic divergence and featuring cubic as well as quartic anharmonicities peculiar to frustrated noncollinear antiferromagnets [46,47].

A SW language is characterized by its "$1/S$ expansion" and is therefore suited for visualizing quantum renormalization of the harmonic spectrum on the order of $S$. $O(S^0)$ quantum corrections to harmonic antiferromagnons on the square and triangular lattices contribute toward upward and downward renormalizations of their energies, respectively. In the triangular-lattice antiferromagnet, this first-order renormalization causes such drastic effects on SW excitations that their lifetimes no longer remain infinite in a major part of the hexagonal Brillouin zone [47–49] and rotonlike minima develop at some points outside the decay region [50,51]. In the square-lattice antiferromagnet, on the other hand, the lowest-order spectrum renormalization brings about neither a finite lifetime nor a rotonlike minimum [52,53]. Since the classical ground state of a triangular-prism antiferromagnet is a collinear (180°-Néel) stack of coplanar (120°-Néel) states,

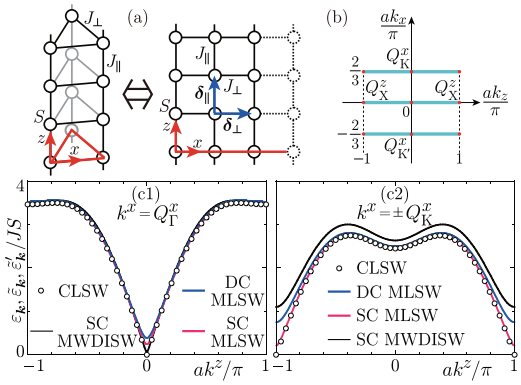



Fig. 1: An equilateral triangular prism may be identified with a planar three-leg ladder with the periodic boundary condition in the rung direction (a) whose first Brillouin zone consists of three parallel line segments at equal intervals in two dimensions (b). CLSW $\varepsilon_{\boldsymbol{k}}$ (5), SC-MLSW $\tilde{\varepsilon}^{\mathrm{SC}}_{\boldsymbol{k}}$ (7), SC-MWDISW $\tilde{\varepsilon}'^{\mathrm{SC}}_{\boldsymbol{k}}$ (S24) in the Supplementary Material `Supplementarymaterial.pdf`, and DC-MLSW $\tilde{\varepsilon}^{\mathrm{DC}}_{\boldsymbol{k}}$ (9) dispersions as functions of $k^z$ with $k^x = Q^x_\Gamma$ (c1) and $k^x = \pm Q^x_K$ (c2) in the $N \to \infty$ limit.

quantum renormalization of its harmonic SW spectrum may have characteristics of both one-dimensional collinear antiferromagnets [8,9] in a Luttinger liquid state [7] and two-dimensional coplanar antiferromagnets in an ordered state [54–61]. We shall evaluate various MSW schemes in comparison with DMRG calculations, intending to find out the best MSW language that has the potential to reveal such a subtle spectrum.

We set the spin-$S$ nearest-neighbor antiferromagnetic Heisenberg model $\mathcal{H} = \sum_{l=1}^{L} \sum_{\sigma=\parallel,\perp} J_\sigma \boldsymbol{S}_{\boldsymbol{r}_l} \cdot \boldsymbol{S}_{\boldsymbol{r}_l+\boldsymbol{\delta}_\sigma}$ on an equilateral triangular prism of $L \equiv 3N$ sites (cf. figs. 1(a) and (b)). Henceforth we set $J_\parallel$ and $J_\perp$ both equal to $J\,(>0)$ and accordingly suppose $|\boldsymbol{\delta}_\parallel| = |\boldsymbol{\delta}_\perp| = a$. In order to express the spin Hamiltonian in terms of Holstein-Primakoff bosons, we first transform it into the rotating frame with its "moving" $z$-axis pointing along each local spin direction in the classical ground state designated by the ordering vector $(q^z, q^x, q^y) = \frac{\pi}{a}(1, \frac{2}{3}, 0)$. With a tacit understanding of $q^y$ being 0, we henceforth use a shorthand notation in the two-dimensional reciprocal space,

$$\boldsymbol{Q}_{\Gamma,\Gamma} = (Q^z_\Gamma, Q^x_\Gamma) \equiv \frac{\pi}{a}\,(0,0)\,,\ \boldsymbol{Q}_{X,K} = (Q^z_X, Q^x_K) \equiv \frac{\pi}{a}\left(1, \frac{2}{3}\right). \tag{1}$$

We denote the local coordinate system by $(\tilde{z}, \tilde{x}, \tilde{y})$ distinguishably from the laboratory frame $(z, x, y)$. Note that every local $\tilde{z}$-$\tilde{x}$ plane coincides with the global $z$-$x$ "plane", which consists of the side faces of the triangular prism in practice. For coplanar antiferromagnets with their spins lying in the thus-made $z$-$x$ plane, the spin components in the laboratory and rotating frames are related with each other as

$$\begin{bmatrix} S^z_{\boldsymbol{r}_l} \\ S^x_{\boldsymbol{r}_l} \\ S^y_{\boldsymbol{r}_l} \end{bmatrix} = \begin{bmatrix} \cos\phi_{\boldsymbol{r}_l} & -\sin\phi_{\boldsymbol{r}_l} & 0 \\ \sin\phi_{\boldsymbol{r}_l} & \cos\phi_{\boldsymbol{r}_l} & 0 \\ 0 & 0 & 1 \end{bmatrix} \begin{bmatrix} S^{\tilde{z}}_{\boldsymbol{r}_l} \\ S^{\tilde{x}}_{\boldsymbol{r}_l} \\ S^{\tilde{y}}_{\boldsymbol{r}_l} \end{bmatrix}, \tag{2}$$

where $\phi_{\boldsymbol{r}_l} \equiv \boldsymbol{Q}_{\rm X,K} \cdot \boldsymbol{r}_l$ is the angle formed by the axes $z$ ($x$) and $\tilde{z}$ ($\tilde{x}$) at $\boldsymbol{r}_l$. Then we introduce Holstein-Primakoff bosons,

$$S^{\tilde{z}}_{\boldsymbol{r}_l} = S - a^\dagger_{\boldsymbol{r}_l} a_{\boldsymbol{r}_l},\ S^{\tilde{x}}_{\boldsymbol{r}_l} - iS^{\tilde{y}}_{\boldsymbol{r}_l} \equiv S^{\tilde{+}\dagger}_{\boldsymbol{r}_l} \equiv S^{\tilde{-}}_{\boldsymbol{r}_l} = \sqrt{2S} a^\dagger_{\boldsymbol{r}_l} \mathcal{R}_{\boldsymbol{r}_l}(S);$$
$$\mathcal{R}_{\boldsymbol{r}_l}(S) \equiv \sqrt{1 - \frac{a^\dagger_{\boldsymbol{r}_l} a_{\boldsymbol{r}_l}}{2S}} = 1 - \sum_{l=1}^{\infty} \frac{(2l-3)!!}{l!} \left( \frac{a^\dagger_{\boldsymbol{r}_l} a_{\boldsymbol{r}_l}}{4S} \right)^l, \tag{3}$$

to expand the Hamiltonian as $\mathcal{H} = \sum_{m=0}^{4} \mathcal{H}^{(\frac{m}{2})} + O(S^{-\frac{1}{2}})$, where $\mathcal{H}^{(\frac{m}{2})}$, on the order of $S^{\frac{m}{2}}$, consists of $4-m$ boson operators (see the Supplementary Material `Supplementarymaterial.pdf` (SM), sect. S1) and those on the order of $S$ to a fractional power are peculiar to noncollinear antiferromagnets. $\mathcal{H}^{(\frac{3}{2})}$ automatically vanishes because the Holstein-Primakoff boson vacuum corresponds to a minimum of the classical energy [47].

We start from the naivest SW description of the triangular-prism antiferromagnet. We move to the reciprocal space, $a^\dagger_{\boldsymbol{k}_{\nu,\sigma}} = \sum_{l=1}^{L} e^{i\boldsymbol{k}_{\nu,\sigma}\cdot\boldsymbol{r}_l} a^\dagger_{\boldsymbol{r}_l}/\sqrt{L}$, and define the Bogoliubov bosons $\alpha^\dagger_{\boldsymbol{k}_{\nu,\sigma}} = u_{\boldsymbol{k}_{\nu,\sigma}} a^\dagger_{\boldsymbol{k}_{\nu,\sigma}} - v_{\boldsymbol{k}_{\nu,\sigma}} a_{-\boldsymbol{k}_{\nu,\sigma}}$ so as to make the linear SW (LSW) Hamiltonian diagonal,

$$\sum_{m=1}^{2} \mathcal{H}^{(m)} \equiv \mathcal{H}_{\rm harm} = \sum_{l=1}^{2} E^{(m)} + \sum_{\sigma=0,\pm} \sum_{\nu=1}^{N} \varepsilon_{\boldsymbol{k}_{\nu,\sigma}} \alpha^\dagger_{\boldsymbol{k}_{\nu,\sigma}} \alpha_{\boldsymbol{k}_{\nu,\sigma}}, \tag{4}$$

where $E^{(2)} \equiv -\frac{3}{2}LJS^2$ is the classical ground-state energy and $E^{(1)} \equiv -\frac{3}{2}LJS + \sum_{\sigma=0,\pm}\sum_{\nu=1}^{N} \frac{\varepsilon_{\boldsymbol{k}_{\nu,\sigma}}}{2}$ is its $O(S^1)$ quantum correction, while $\alpha^\dagger_{\boldsymbol{k}_{\nu,\sigma}}$ creates a SW with wave vector $\boldsymbol{k}_{\nu,\sigma} \equiv (k^z_\nu, k^x_\sigma) = \frac{\pi}{a}(\frac{2\nu}{N} - 1, \frac{2}{3}\sigma)$ and energy

$$\begin{aligned} \varepsilon_{\left(k^z_\nu, k^x_0\right)} &= JS\sqrt{2(1-\cos ak^z_\nu)(5+2\cos ak^z_\nu)}\,, \\ \varepsilon_{\left(k^z_\nu, k^x_\pm\right)} &= JS\sqrt{2(1+\cos ak^z_\nu)\left(\tfrac{7}{2} - 2\cos ak^z_\nu\right)}. \end{aligned} \tag{5}$$

The complete breaking of the global $SO(3)$ rotational symmetry results in three Nambu-Goldstone modes [47,62] of linear dispersion (figs. 1(c1) and (c2)), one at the zone center $\boldsymbol{Q}_{\Gamma,\Gamma}$ with velocity $v_{\boldsymbol{Q}_{\Gamma,\Gamma}} = \sqrt{7}JSa$ and two at the zone corners $\pm\boldsymbol{Q}_{X,K}$ with velocity $v_{\boldsymbol{Q}_{X,K}} = \sqrt{\frac{11}{2}}JSa$. On the equilateral triangular prism [23,24,27,28], however, these acoustic antiferromagnons are fictitious characters and make structure factors diverge.

Then we consider modifying CSW Hamiltonians. The naivest MSW scheme [40–43] consists of diagonalizing the conventional LSW (CLSW) Hamiltonian (4) subject to the single-constraint (SC) condition $S - \langle a^\dagger_{\boldsymbol{r}_l} a_{\boldsymbol{r}_l} \rangle^{\rm SC}_T = 0$,

$$\begin{aligned} &\mathcal{H}_{\rm harm} + \sum_{l=1}^{L} \mu_l (S - a^\dagger_{\boldsymbol{r}_l} a_{\boldsymbol{r}_l}) \equiv \widetilde{\mathcal{H}}^{\rm SC}_{\rm harm} = \sum_{m=1}^{2} E^{(m)} \\ &+\mu L\left(S + \frac{1}{2}\right) + \sum_{\sigma=0,\pm}\sum_{\nu=1}^{N} \tilde{\varepsilon}^{\rm SC}_{\boldsymbol{k}_{\nu,\sigma}} \alpha^\dagger_{\boldsymbol{k}_{\nu,\sigma}} \alpha_{\boldsymbol{k}_{\nu,\sigma}}, \end{aligned} \tag{6}$$

where $\langle \cdots \rangle^{\rm SC}_T$ denotes a thermal average at temperature $T$ with respect to $\widetilde{\mathcal{H}}^{\rm SC}_{\rm harm}$, the $L$ Lagrange multipliers $\mu_l$ degenerate into $\mu$, and then $\alpha^\dagger_{\boldsymbol{k}_{\nu,\sigma}}$ creates a modified LSW (MLSW) with wave vector $\boldsymbol{k}_{\nu,\sigma}$ and energy

$$\begin{aligned} \frac{\tilde{\varepsilon}^{\rm SC}_{\left(k^z_\nu, k^x_0\right)}}{JS} &= \sqrt{2\left(1-\cos ak^z_\nu - \frac{\mu}{2JS}\right)\left(5+2\cos ak^z_\nu - \frac{\mu}{JS}\right)}, \\ \frac{\tilde{\varepsilon}^{\rm SC}_{\left(k^z_\nu, k^x_\pm\right)}}{JS} &= \sqrt{2\left(1+\cos ak^z_\nu - \frac{\mu}{2JS}\right)\left(\frac{7}{2} - 2\cos ak^z_\nu - \frac{\mu}{JS}\right)}. \end{aligned} \tag{7}$$

Since its extension up to $O(S^0)$ within the HF approximation [40,41], which we call the SC-modified HF-decomposition-based-interacting-SW (SC-MHFISW) scheme, yields a good thermodynamics of one-dimensional Haldane-gap antiferromagnets [63–66], we try this too on the present system. Here we perform all calculations at $T = 0$, and then, MHFISWs are no different from modified Wick-decomposition-based-interacting SWs (MWDISWs) [67,68]. Such calculated MSWs no longer have any soft mode (see figs. 1(c1) and (c2)) to enable us to calculate the dynamic spin structure factor (see eq. (S44) in the SM).

We lead the argument off with the SC-MLSW findings. A major portion of the spectral weight concentrates at $\boldsymbol{q} = \boldsymbol{Q}_{X,K}$ (figs. 2(a2) and (c2)), claiming that while the coplanar 120°-Néel structure predominates in each cross-sectional triangle, the collinear 180°-Néel structure remains significant in the leg direction. Even so, SC-MLSWs overestimate this single-magnon scattering intensity $S(\boldsymbol{Q}_{X,K}, \omega)$ (see eq. (S62) in the SM) with such a small excitation energy that $\tilde{\varepsilon}^{\rm SC}_{\boldsymbol{Q}_{\Gamma,\Gamma}} \ll JS$. Another serious fault of SC MLSWs is a spurious intensity at $\boldsymbol{q} = \boldsymbol{Q}_{X,\Gamma}$ (fig. 2(a1)), claiming a one-dimensional antiferromagnetic configuration of spins coupled ferromagnetically within each triangle. SC MLSWs overestimate this two-magnon scattering intensity $S(\boldsymbol{Q}_{X,\Gamma}, \omega)$ (see eq. (S63) in the SM) as well with a still smaller excitation energy $\tilde{\varepsilon}^{\rm SC}_{\pm\boldsymbol{Q}_{X,K}} \ll JS$. Indeed SC-MLSWs at $\boldsymbol{Q}_{\Gamma,\Gamma}$ and $\pm\boldsymbol{Q}_{X,K}$ are both gapped, but their gaps seem to be still too small to reproduce the correct spectral weighting. DMRG calculations show that the $S(\boldsymbol{q}, \omega)$ spectral weighting is well dispersive with $q^z$ moving from $Q^z_\Gamma$ to $Q^z_X$ at every $q^x$ (figs. 2(c1) and (c2)), but SC MLSWs can hardly reproduce such features especially along the lines connecting $(Q^z_\Gamma, \pm Q^x_K)$ and $(\frac{1}{2}Q^z_X, \pm Q^x_K)$. So how about the SC-MWDISW findings? The increased gaps at $\pm\boldsymbol{Q}_{X,K}$ suppress the too strong SC-MLSW intensity $S[\boldsymbol{Q}_{X,\Gamma}, (\tilde{\varepsilon}^{SC}_{\boldsymbol{Q}_{X,K}} + \tilde{\varepsilon}^{\rm SC}_{-\boldsymbol{Q}_{X,K}})/\hbar]$ (fig. 2(a1″)), whereas the diminished gap at $\boldsymbol{Q}_{\Gamma,\Gamma}$ even more enhances the almost divergent SC-MLSW intensity $S(\boldsymbol{Q}_{X,K}, \tilde{\varepsilon}^{\rm SC}_{\boldsymbol{Q}_{\Gamma,\Gamma}}/\hbar)$ (fig. 2(a2″)). In any case, the SC-MWDISW findings are still far from the DMRG calculations or may even be a change for the worse.

In order to make cubic as well as quartic anharmonicities effective in sophisticating harmonic SWs, we have to treat them perturbatively rather than variationally. We correct the SC-MLSW Hamiltonian to first order in

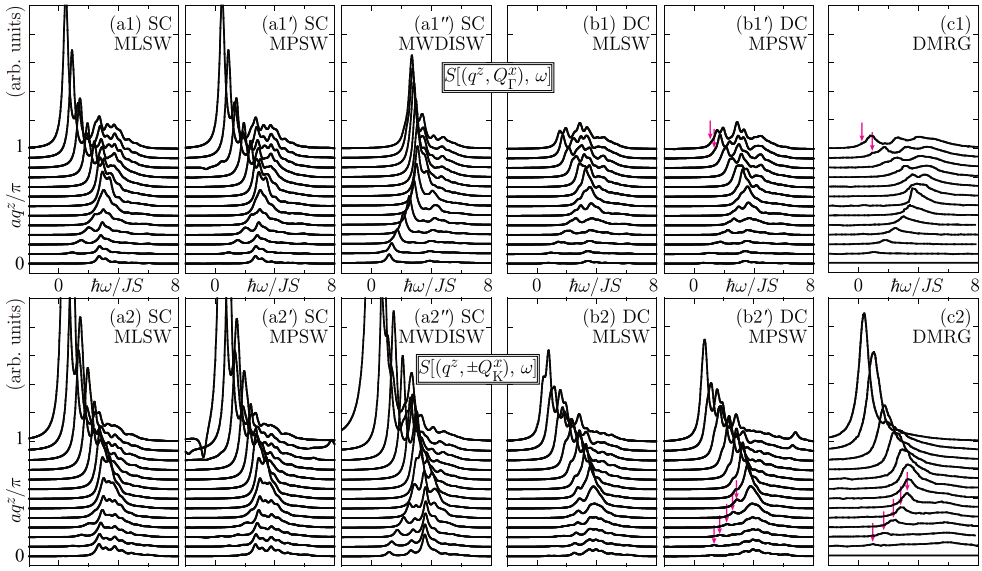



Fig. 2: Various MSW ((a1) to (b1′): $(q^x = Q^x_\Gamma)$; (a2) to (b2′): $(q^x = \pm Q^x_K)$) *vs.* DMRG ((c1) and (c2)) [24] calculations of the total dynamic structure factor $S(\boldsymbol{q},\omega) \equiv \sum_{\lambda=z,x,y} S^{\lambda\lambda}(\boldsymbol{q},\omega)$ ((S44), (S50), and (S51) in the SM) for $S = \frac{1}{2}$ at $N = 24$. Arrows to $S[(q^z, Q^x_\Gamma),\omega]$ at $\frac{Q^z_X}{2} \ll |q^z| \lesssim Q^z_X$ ((b1′) and (c1)) and $S[(q^z, \pm Q^x_K),\omega]$ at $Q^z_\Gamma \lesssim |q^z| \lesssim \frac{Q^z_X}{2}$ ((b2′) and (c2)) indicate particular spectral features describable only with pertinent single-magnon energies, $\tilde{\varepsilon}^{\rm DC}_{\boldsymbol{k}} + \overline{\Sigma}^{(0)}_1(\boldsymbol{k}) + \overline{\Sigma}^{(0)}_2(\boldsymbol{k}; \tilde{\varepsilon}^{\rm DC}_{\boldsymbol{k}}/\hbar)$ ((9) and (S42) in the SM) especially at $\boldsymbol{k} \simeq \pm\boldsymbol{Q}_{\Gamma,K}$.

$1/S$ [47,69], *i.e.*, to first order in $\mathcal{H}^{(0)}$ and to second order in $\mathcal{H}^{(\frac{1}{2})}$. We employ magnon Green's functions [51,70] to renormalize the spectrum and accordingly correct the dynamic structure factor. Since the longitudinal component of the structure factor, which probes the two-magnon continuum, is a factor of $1/S$ smaller than the leading terms in the transverse correlation functions, it may be calculated in terms of bare magnon Green's functions. The effect of interactions between antiferromagnons is taken into its transverse components through the lowest-order self-energies $\Sigma^{(0)}(\boldsymbol{k};\omega+i\epsilon)$ [46,47] consisting of the frequency-independent contribution $\Sigma^{(0)}_1(\boldsymbol{k})$ of first order in $\mathcal{H}^{(0)}$ and the frequency-dependent contribution $\Sigma^{(0)}_2(\boldsymbol{k};\omega+i\epsilon)$ of second order in $\mathcal{H}^{(\frac{1}{2})}$, both on the order of $S^0$. Figures 2(a1′) and (a2′) show such corrected calculations to (S44) in the SM in terms of modified perturbed SWs (MPSWs). Even though any two-magnon correlation remains the same, yet some sort of change may be coming to the one-magnon contributions. However, the MLSW and MPSW findings look almost the same at least within the SC modification. This is because the real parts of the two primary self-energies, $\overline{\Sigma}^{(0)}_1(\boldsymbol{k})$ and $\overline{\Sigma}^{(0)}_2(\boldsymbol{k};\tilde{\varepsilon}^{\rm SC}_{\boldsymbol{k}}/\hbar)$, balance each other at $|k^z| \lesssim \frac{Q^z_X}{2}$ (see SM, sect. S3). Considering that neither SC MWDISWs nor SC MPSWs can hardly reproduce the DMRG calculations, we are now in a position to reconsider the way of modifying CSWs.

Then we should figure out two serious problems of SC MSWs in noncollinear antiferromagnets [46]. First, they break the $U(1)$ rotational symmetry about each local $\tilde{z}$-axis. Quantum averages $\langle a^\dagger_{\boldsymbol{r}_l} a^\dagger_{\boldsymbol{r}_l} + a_{\boldsymbol{r}_l} a_{\boldsymbol{r}_l}\rangle^{\rm SC}_0$ in a noncollinear ground state are generally nonzero to cause $\langle S^{\tilde{x}}_{\boldsymbol{r}_l} S^{\tilde{x}}_{\boldsymbol{r}_l}\rangle^{\rm SC}_0 \neq \langle S^{\tilde{y}}_{\boldsymbol{r}_l} S^{\tilde{y}}_{\boldsymbol{r}_l}\rangle^{\rm SC}_0$. Demanding that MSWs should keep these unreasonable expectation values as well as the total staggered magnetization zero causes to increase their otherwise stable ground-state energy. In order to solve this composite problem, we diagonalize the LSW Hamiltonian subject to the double-constraint (DC) condition $S - \langle a^\dagger_{\boldsymbol{r}_l} a_{\boldsymbol{r}_l}\rangle^{\rm DC}_0 = \delta$ and $\langle a^\dagger_{\boldsymbol{r}_l} a^\dagger_{\boldsymbol{r}_l} + a_{\boldsymbol{r}_l} a_{\boldsymbol{r}_l}\rangle^{\rm DC}_0 = 0$,

$$\begin{aligned}
&\mathcal{H}_{\rm harm} + \sum_{l=1}^{L}\left[\mu_l\left(S - \delta - a^\dagger_{\boldsymbol{r}_l} a_{\boldsymbol{r}_l}\right) + \eta_l \frac{a^\dagger_{\boldsymbol{r}_l} a^\dagger_{\boldsymbol{r}_l} + a_{\boldsymbol{r}_l} a_{\boldsymbol{r}_l}}{2}\right] \equiv \\
&\widetilde{\mathcal{H}}^{\rm DC}_{\rm harm} = \sum_{m=1} E^{(m)} \\
&+\mu L\left(S - \delta + \frac{1}{2}\right) + \sum_{\sigma=0,\pm}\sum_{\nu=1}^{N} \tilde{\varepsilon}^{\rm DC}_{\boldsymbol{k}_{\nu,\sigma}} \alpha^\dagger_{\boldsymbol{k}_{\nu,\sigma}} \alpha_{\boldsymbol{k}_{\nu,\sigma}},
\end{aligned} \tag{8}$$

where $\mu_l$'s and $\eta_l$'s both degenerate to be set to $\mu$ and $\eta$, respectively, $\delta$ is determined so as to minimize the ground-state energy, and then $\alpha^\dagger_{\boldsymbol{k}_{\nu,\sigma}}$ creates an MSW with energy

$$\begin{aligned}
\frac{\tilde{\varepsilon}^{\rm DC}_{(k^z_\nu, k^x_0)}}{JS} &= \sqrt{2\left(1 - \cos ak^z_\nu - \frac{\mu-\eta}{2JS}\right)\left(5 + 2\cos ak^z_\nu - \frac{\mu+\eta}{JS}\right)}, \\
\frac{\tilde{\varepsilon}^{\rm DC}_{(k^z_\nu, k^x_\pm)}}{JS} &= \sqrt{2\left(1 + \cos ak^z_\nu - \frac{\mu+\eta}{2JS}\right)\left(\frac{7}{2} - 2\cos ak^z_\nu - \frac{\mu-\eta}{JS}\right)}.
\end{aligned} \tag{9}$$

Note that the DC condition reduces to the original SC condition for collinear antiferromagnets without any frustration. Such DC-MLSW calculations $S[\boldsymbol{Q}_{X,\Gamma}, (\tilde{\varepsilon}^{\rm DC}_{\boldsymbol{Q}_{X,K}} + \tilde{\varepsilon}^{\rm DC}_{-\boldsymbol{Q}_{X,K}})/\hbar]$ (fig. 2(b1)) and $S(\boldsymbol{Q}_{X,K}, \tilde{\varepsilon}^{\rm DC}_{\boldsymbol{Q}_{\Gamma,\Gamma}}/\hbar)$ (fig. 2(b2)) are remarkable improvements compared to any of the SC-MSW overestimates. This is more or less thanks to the enhanced gaps at $\pm\boldsymbol{Q}_{X,K}$ (fig. 1(c2)) and $\boldsymbol{Q}_{\Gamma,\Gamma}$ (fig. 1(c1)),

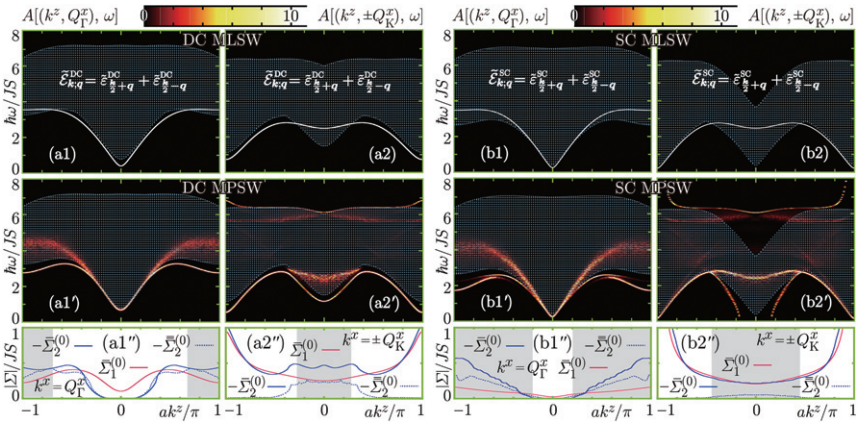



Fig. 3: DC-MLSW ((a1) and (a2)), DC-MPSW ((a1′) and (a2′)), SC-MLSW ((b1) and (b2)), and SC-MPSW ((b1′) and (b2′)) calculations of the spectral function $A(\boldsymbol{k},\omega)$ (10) plotted against the background of the two-magnon continuum $\widetilde{\mathcal{E}}_{\boldsymbol{k};\boldsymbol{q}} = \tilde{\varepsilon}_{\frac{\boldsymbol{k}}{2}+\boldsymbol{q}} + \tilde{\varepsilon}_{\frac{\boldsymbol{k}}{2}-\boldsymbol{q}}$ with running $\boldsymbol{q}$ dotted finely and homogeneously for $S=\frac{1}{2}$ in the $N\to\infty$ limit. An excitation with wave vector $\boldsymbol{k}$ is unstable when the minimum of $\widetilde{\mathcal{E}}_{\boldsymbol{k};\boldsymbol{q}}$, denoted by $\widetilde{\mathcal{E}}_{\boldsymbol{k};\boldsymbol{q}_{\min}(\boldsymbol{k})}$, is lower than $\tilde{\varepsilon}_{\boldsymbol{k}}$ (see (a1) to (b2)), explicitly shown by shading in (a1″) to (b2″), and then the quasiparticle dispersion $\tilde{\varepsilon}_{\boldsymbol{k}} + \overline{\Sigma}_1^{(0)}(\boldsymbol{k}) + \overline{\Sigma}_2^{(0)}(\boldsymbol{k};\tilde{\varepsilon}_{\boldsymbol{k}}/\hbar)$ is pushed out below the lower edge of $\widetilde{\mathcal{E}}_{\boldsymbol{k};\boldsymbol{q}}$ (see (a1′) to (b2′)) with emergent imaginary self-energy correction $\overline{\Sigma}_2^{(0)}(\boldsymbol{k};\tilde{\varepsilon}_{\boldsymbol{k}}/\hbar)$. Note that in the triangular-prism antiferromagnet $\overline{\Sigma}_2^{(0)}(\boldsymbol{k};\tilde{\varepsilon}_{\boldsymbol{k}}/\hbar)$ can be finite even if the inequality $\widetilde{\mathcal{E}}_{\boldsymbol{k};\boldsymbol{q}_{\min}(\boldsymbol{k})} < \tilde{\varepsilon}_{\boldsymbol{k}}$ is not met (see (a1″) in particular).

indeed, but we should be reminded of the spurious peak in $S(\boldsymbol{Q}_{X,\Gamma},\omega)$ fabricated by SC-MWDISWs with even larger gaps at $\pm\boldsymbol{Q}_{X,K}$ (fig. 1(c2)) to learn that the DC modification scheme —restoration of the local $U(1)$ rotational symmetry and then required ground-state optimization— must be more essential.

DC-MLSWs are no doubt much better than any of SC-MSWs but still lack subtlety in reproducing the DMRG calculations. They are totally ignorant of the subtle shoulder (fig. 2(c1)) and curved ridge (fig. 2(c2)) on the lower-energy side of the two-magnon scattering continuum, both originating in the renormalized one-magnon spectrum. There is no such observation without sufficiently strong renormalization of magnon energies via the cubic interaction $\mathcal{H}^{(\frac{1}{2})}$ which serves to couple one-magnon transverse and two-magnon longitudinal fluctuations. The $\mathcal{H}^{(\frac{1}{2})}$-driven $O(S^0)$ self-energy $\overline{\Sigma}_2^{(0)}(\boldsymbol{k};\tilde{\varepsilon}^{\rm DC}_{\boldsymbol{k}}/\hbar)$ causes a strong downward renormalization of the bare magnon energies $\tilde{\varepsilon}^{\rm DC}_{\boldsymbol{k}}$ for $k^x=\pm Q^x_K$ and $|k^z| \lesssim \frac{Q^z_X}{2}$. The thus-obtained DC-MPSWs (see eqs. (S66) and (S67) in the SM) successfully reproduce the DMRG calculations, as are illustrated with vertical arrows in figs. 2(b1′) and 2(b2′), respectively.

Noncollinear magnets generally have a propensity of their elementary excitations to spontaneous decays into pairs of other magnons [48,49,71]. The present system is also the case and hence the complicated dynamic structure factor. In order to understand such decay-induced magnon dynamics in more detail, we calculate a spectral function, which is an analytic continuation of the one-magnon Green's function and explicitly written as

$$A(\boldsymbol{k},\omega) = \begin{cases} \mathrm{Im}\dfrac{-1/\pi}{\hbar\omega-\tilde{\varepsilon}_{\boldsymbol{k}}+i\hbar\epsilon} = \delta(\hbar\omega-\tilde{\varepsilon}_{\boldsymbol{k}}) & \text{(MLSW)}, \\ \mathrm{Im}\dfrac{-1/\pi}{\hbar\omega-\tilde{\varepsilon}_{\boldsymbol{k}}-\Sigma^{(0)}(\boldsymbol{k};\omega+i\epsilon)+i\hbar\epsilon} & \text{(MPSW)}, \end{cases} \tag{10}$$

where $\tilde{\varepsilon}_{\boldsymbol{k}}$ is assumed to be either $\tilde{\varepsilon}^{\rm SC}_{\boldsymbol{k}}$ (7) or $\tilde{\varepsilon}^{\rm DC}_{\boldsymbol{k}}$ (9). Figure 3 shows $A(\boldsymbol{k},\omega)$ in the DC-MLSW ((a1) and (a2)), DC-MPSW ((a1′) and (a2′)), SC-MLSW ((b1) and (b2)), and SC-MPSW ((b1′) and (b2′)) ground states. MLSWs have an infinite lifetime without damping and, therefore, their energy spectrum consists of delta functions. If we denote the energy sum of two free MLSWs with wave vectors $\boldsymbol{k}_1$ and $\boldsymbol{k}_2$ by $\widetilde{\mathcal{E}}_{\boldsymbol{k};\boldsymbol{q}} \equiv \tilde{\varepsilon}_{\frac{\boldsymbol{k}}{2}+\boldsymbol{q}} + \tilde{\varepsilon}_{\frac{\boldsymbol{k}}{2}-\boldsymbol{q}}$ and plot it as a function of the conserved quantity $\boldsymbol{k} \equiv \boldsymbol{k}_1+\boldsymbol{k}_2$ with the free parameter $2\boldsymbol{q} \equiv \boldsymbol{k}_1-\boldsymbol{k}_2$ running over the full Brillouin zone, $\widetilde{\mathcal{E}}_{\boldsymbol{k};\boldsymbol{q}}$ becomes a continuum band, as is dotted finely and homogeneously in fig. 3. If a single-magnon energy exceeds the bottom of the two-magnon continuum at each value of $\boldsymbol{k}$, $\widetilde{\mathcal{E}}_{\boldsymbol{k};\boldsymbol{q}_{\min}(\boldsymbol{k})} < \tilde{\varepsilon}_{\boldsymbol{k}}$, such a quasiparticle is no longer stable but tends to decay into a pair of quasiparticles with their relative wave vector being $2\boldsymbol{q}_{\min}(\boldsymbol{k})$. Figures 3(a1) and (a2) demonstrate that the single DC-MLSW delta-function spectrum $\tilde{\varepsilon}^{\rm DC}_{\boldsymbol{k}}$ indeed penetrates their pair excitation continuum $\widetilde{\mathcal{E}}^{\rm DC}_{\boldsymbol{k};\boldsymbol{q}}$. The CLSW spectrum contains three Nambu-Goldstone modes to be buried in its pair excitation continuum, as is shown in figs. S3(a1) and S3(a2) of the SM. Modifying CLSWs causes a hardening of their dispersion as $0 < \tilde{\varepsilon}^{\rm SC}_{\pm\boldsymbol{Q}_{X,K}} < \tilde{\varepsilon}^{\rm SC}_{\boldsymbol{Q}_{\Gamma,\Gamma}} < \tilde{\varepsilon}^{\rm DC}_{\boldsymbol{Q}_{\Gamma,\Gamma}} < \tilde{\varepsilon}^{\rm DC}_{\pm\boldsymbol{Q}_{X,K}}$ and pushes out the single-magnon branch below the two-magnon continuum according to the modification scheme (fig. 3). The sufficient hardening of the DC-MLSW mode $\tilde{\varepsilon}^{\rm DC}_{\pm\boldsymbol{Q}_{X,K}}$ results in substantially lifting up its pair excitation energy $\tilde{\varepsilon}^{\rm DC}_{\pm\boldsymbol{Q}_{X,K}} + \tilde{\varepsilon}^{\rm DC}_{\pm\boldsymbol{Q}_{X,K}} = \widetilde{\mathcal{E}}^{\rm DC}_{\mp\boldsymbol{Q}_{\Gamma,K};\boldsymbol{q}_{\min}(\mp\boldsymbol{Q}_{\Gamma,K})}$ so that the perturbed single-magnon branch $\tilde{\varepsilon}^{\rm DC}_{\mp\boldsymbol{Q}_{\Gamma,K}} + \left|\overline{\Sigma}_1^{(0)}(\mp\boldsymbol{Q}_{\Gamma,K})\right| - \left|\overline{\Sigma}_2^{(0)}(\mp\boldsymbol{Q}_{\Gamma,K};\tilde{\varepsilon}^{\rm DC}_{\mp\boldsymbol{Q}_{\Gamma,K}}/\hbar)\right|$ can appear below that (fig. 3(a2′)). However, an overlap of the single-magnon branch with the two-magnon continuum does not necessarily lead to a strong downward renormalization

of the bare magnon energies and a rotonlike dip in the single-magnon dispersion emergent below the two-magnon continuum. DC-MSWs owe their such behaviors at $\boldsymbol{k} \simeq \boldsymbol{Q}_{X,\Gamma}$ and $\boldsymbol{k} \simeq \pm\boldsymbol{Q}_{\Gamma,K}$ to cubic dominant anharmonicities, $\left|\overline{\varSigma}_1^{(0)}(\boldsymbol{k})\right| < \left|\overline{\varSigma}_2^{(0)}(\boldsymbol{k};\tilde{\varepsilon}_{\boldsymbol{k}}^{\mathrm{DC}}/\hbar)\right|$. Note that at $\boldsymbol{k} \simeq \boldsymbol{Q}_{\Gamma,\Gamma}$, $\left|\overline{\varSigma}_1^{(0)}(\boldsymbol{k})\right|$ predominates over $\left|\overline{\varSigma}_2^{(0)}(\boldsymbol{k};\tilde{\varepsilon}_{\boldsymbol{k}}^{\mathrm{DC}}/\hbar)\right|$ to renormalize the single-magnon branch upward, which is the case with single-chain [67] and square-lattice [52] collinear antiferromagnets, for instance. SC-MLSWs with $\boldsymbol{k} \simeq \pm\boldsymbol{Q}_{\Gamma,K}$ fail to enjoy a quantum rotonlike stabilization (fig. 3(b2′)) with their balanced self-energy corrections, $\left|\overline{\varSigma}_1^{(0)}(\boldsymbol{k})\right| \simeq \left|\overline{\varSigma}_2^{(0)}(\boldsymbol{k};\tilde{\varepsilon}_{\boldsymbol{k}}^{\mathrm{SC}}/\hbar)\right|$ (fig. 3(b2″)).

The inequality $\widetilde{\mathcal{E}}_{\boldsymbol{k};\boldsymbol{q}_{\min}(\boldsymbol{k})} < \tilde{\varepsilon}_{\boldsymbol{k}}$, which is shown by shading in figs. 3(a1″) to (b2″), guarantees the single-magnon branch to overlap with the two-magnon continuum and then the cubic interaction makes its lifetime finite to cause one-to-two-magnon decays even at zero temperature. At $\boldsymbol{k} \simeq \pm\boldsymbol{Q}_{\Gamma,K}$, the decay rate $-\overline{\varSigma}_2^{(0)}(\boldsymbol{k};\tilde{\varepsilon}_{\boldsymbol{k}}^{\mathrm{DC}}/\hbar)$ stays finite well consistently with the shaded region, whereas on the way from $\boldsymbol{Q}_{X,\Gamma}$ to $\boldsymbol{Q}_{\Gamma,\Gamma}$, the imaginary part survives far beyond the shaded region possibly with a different decay scenario such as fractionalization of spin excitations into spinons. The present wave vector $\boldsymbol{Q}_{X,\Gamma}$ represents such a collinear spin configuration as ferromagnetic and antiferromagnetic in the rung and leg directions, respectively, while the midedges of the hexagonal Brillouin zone of the triangular-lattice antiferromagnet, which are often referred to as the $M$ points, also represent such collinear configurations as ferromagnetic and antiferromagnetic in the directions of certain two primitive translation vectors with a relative angle of 60°. These two ordering vectors thus correspond well to each other, and interestingly enough, the renormalized antiferromagnon spectra in one and two dimensions have similar appearances in their vicinities [51]. Series expansion calculations for the triangular-lattice antiferromagnet [50,72] reveal that the bare magnon energies are strongly renormalized downward by quantum fluctuations so as to form rotonlike minima near $M$. Bosonic [73] and fermionic [74] spinon language analyses both claim that these rotonlike minima should be collective modes of a spinon condensate, *i.e.*, two-spinon bound states that spontaneously break the $SU(2)$ symmetry. In the triangular-lattice antiferromagnet, the inequality condition of bare magnons being kinematically unstable towards decays into pairs of other magnons and the region of the lowest-order self-energy corrections to bare magnons having an imaginary part coincide to form a hexagram, which is inscribed in the hexagonal Brillouin zone occupying two-thirds of it but not including the $M$ points [47–49]. In the triangular-prism antiferromagnet, the magnon decay rate $-\overline{\varSigma}_2^{(0)}(\boldsymbol{k};\tilde{\varepsilon}_{\boldsymbol{k}}^{\mathrm{DC}}/\hbar)$ remains finite far beyond the spontaneous two-magnon decay region on the way from $\boldsymbol{Q}_{X,\Gamma}$ to $\boldsymbol{Q}_{\Gamma,\Gamma}$. Then, there is a possibility of bare magnons decaying into two spinons instead, but if so why is the magnon decay rate vanishing near $M$ on the hexagonal Brillouin zone? We find a probable key to this mystery in general arguments on frustrated quantum antiferromagnets in terms of lattice gauge theories [75] for which spinons are necessarily confined in their ordered phases [76] but should be deconfined in their disordered phases [77]. Calculating the dynamic structure factor of the triangular-lattice antiferromagnet in terms of spinon Green's functions [73,74] indeed shows that when coming closer to the $M$ points, single magnons are no longer allowed to decay into two spinons but stabilize below the lower edge of the two-spinon continuum with their line width disappearing. The present system on the way from $\boldsymbol{Q}_{X,\Gamma}$ to $\boldsymbol{Q}_{\Gamma,\Gamma}$ behaves as an effective spin-$\frac{3}{2}$ chain rather than spin-$\frac{1}{2}$ frustrated triangles, wherein the instability of its single-magnon spectrum may change in character, from spontaneous two-magnon decays to two-spinon decays. Unlike the collective antiferromagnon modes with their decay rates vanishing at the $M$ points on the triangular lattice, here one-dimensional antiferromagnon modes are persistently accompanied by nonvanishing decay rates on the way from $\boldsymbol{Q}_{X,\Gamma}$ to $\boldsymbol{Q}_{\Gamma,\Gamma}$, suggesting their possible decays into some other elementary excitations. Deconfined spinons are indeed the case with the spin-$\frac{1}{2}$ antiferromagnetic Heisenberg chain [78], whose eigenstates necessarily contain an even number of kinks without forming any bound state of them, each with quasimomentum running through half the Brillouin zone. Though its $O(S^0)$ self-energy is independent of frequency to have no imaginary part, higher-order self-energy corrections necessarily have an imaginary part without cubic interactions. Note that the well-known rotonlike dip in the single-magnon dispersion of the spin-$\frac{1}{2}$ square-lattice Heisenberg antiferromagnet [53] is never describable without $O(S^{-1})$ self-energy corrections [52,79]. It is worth noting further that a recently developed bond operator technique is quite efficient in reproducing such a quantum rotonlike stabilization [80]. Considering that spinon observations are qualitatively common to all fractional-spin chains [9,81], two-spinon bound states as stable triplet magnons are unlikely in the present system. It should also be noted that a strong-rung-coupling effective Hamiltonian [82,83] for the triangular-prism antiferromagnet yields massive spinon-like as well as magnon-like excitation spectra with varying interchain and intrachain couplings. Ordered but noncollinear magnets have cubic anharmonicities, *i.e.*, coupling of transverse and longitudinal fluctuations, hence the ubiquitous propensity of their excitations to spontaneous decays. The ground states of fractional-spin antiferromagnetic Heisenberg chains are neither ordered nor disordered completely, hence deconfined spinons. The spin-$\frac{1}{2}$ triangular-prism antiferromagnet is possessed of both characteristics and may exhibit a novel *mixed instability* of the single-particle spectrum.

* * *

This work is supported by JSPS KAKENHI Grant No. 22K03502.

*Data availability statement*: All data that support the findings of this study are included within the article (and any supplementary files).

REFERENCES


[1] Reigrotzki M. *et al.*, *J. Phys.: Condens. Matter*, **6** (1994) 9235.
[2] Gopalan S. *et al.*, *Phys. Rev. B*, **49** (1994) 8901.
[3] Azzouz M. *et al.*, *Phys. Rev. B*, **50** (1994) 6233.
[4] Dagotto E. and Rice T. M., *Science*, **271** (1996) 618.
[5] Dai X. and Su Z., *Phys. Rev. B*, **57** (1998) 964.
[6] Hori H. and Yamamoto S., *J. Phys. Soc. Jpn.*, **71** (2002) 1607.
[7] Schulz H. J., *Fermi liquids and non-Fermi liquids*, in *Mesoscopic Quantum Physics, Les Houches, Session LXI, 1994*, edited by Akkermans E. *et al.* (Elsevier, Amsterdam) 1995, p. 533.
[8] Haldane F. D. M., *Phys. Rev. Lett.*, **45** (1980) 1358.
[9] Hallberg K. *et al.*, *Phys. Rev. Lett.*, **76** (1996) 4955.
[10] Hiroi Z. and Takano M., *Nature*, **377** (1995) 41.
[11] Iwase H. *et al.*, *J. Phys. Soc. Jpn.*, **65** (1996) 2397.
[12] Azuma M. *et al.*, *Phys. Rev. Lett.*, **73** (1994) 3463.
[13] Kojima K. *et al.*, *Phys. Rev. Lett.*, **74** (1995) 2812.
[14] Schnack J. *et al.*, *Phys. Rev. B*, **70** (2004) 174420.
[15] Seeber G. *et al.*, *Chem. Commun.*, **2004** (2004) 1580.
[16] Manaka H. *et al.*, *J. Phys. Soc. Jpn.*, **78** (2009) 093701.
[17] Manaka H. *et al.*, *J. Phys. Soc. Jpn.*, **80** (2011) 084714.
[18] Garlea V. O. *et al.*, *Phys. Rev. Lett.*, **100** (2008) 037206.
[19] Garlea V. O. *et al.*, *Phys. Rev. B*, **79** (2009) 060404(R).
[20] Millet P. *et al.*, *J. Solid State Chem.*, **147** (1999) 676.
[21] Lüscher A. *et al.*, *Phys. Rev. B*, **70** (2004) 060405(R).
[22] Gavilano J. L. *et al.*, *Phys. Rev. B*, **72** (2005) 064431.
[23] Kawano K. and Takahashi M., *J. Phys. Soc. Jpn.*, **66** (1997) 4001.
[24] Nishimoto S. and Arikawa M., *Phys. Rev. B*, **78** (2008) 054421.
[25] Sakai T. *et al.*, *Phys. Rev. B*, **78** (2008) 184415.
[26] Sakai T. *et al.*, *J. Phys.: Condens. Matter*, **22** (2010) 403201.
[27] Charrier D. *et al.*, *Phys. Rev. B*, **82** (2010) 075108.
[28] Nishimoto S. *et al.*, *Phys. Rev. B*, **83** (2011) 224425.
[29] Okunishi K. *et al.*, *Prog. Theor. Phys. Suppl.*, **159** (2005) 297.
[30] Okunishi K. *et al.*, *Int. J. Mod. Phys. C*, **20** (2009) 1423.
[31] Fouet J.-B. *et al.*, *Phys. Rev. B*, **73** (2006) 014409.
[32] Ivanov N. B. *et al.*, *Phys. Rev. Lett.*, **105** (2010) 037206.
[33] Kikuchi H. *et al.*, *Phys. Rev. B*, **107** (2023) 184405.
[34] Dargel P. E. *et al.*, *Phys. Rev. B*, **85** (2012) 205119.
[35] Chen X. *et al.*, *Science Bull.*, **63** (2018) 1545.
[36] Maisinger K. and Schollwöck U., *Phys. Rev. Lett.*, **81** (1998) 445.
[37] Jeckelmann E., *Phys. Rev. B*, **66** (2002) 045114.
[38] Kubo R., *Phys. Rev.*, **87** (1952) 568.
[39] Schmidt B. *et al.*, *Phys. Rev. B*, **83** (2011) 075123.
[40] Takahashi M., *J. Phys. Soc. Jpn.*, **58** (1989) 1524.
[41] Takahashi M., *Phys. Rev. B*, **40** (1989) 2494.
[42] Hirsch J. E. and Tang S., *Phys. Rev. B*, **40** (1989) 4769.
[43] Tang S. *et al.*, *Phys. Rev. B*, **40** (1989) 5000.
[44] Yamamoto S., *Phys. Rev. B*, **69** (2004) 064426.
[45] Auerbach A. and Arovas D. P., *Phys. Rev. Lett.*, **61** (1988) 617.
[46] Yamamoto S. and Ohara J., *J. Phys. Commun.*, **7** (2023) 065004.
[47] Chernyshev A. L. and Zhitomirsky M. E., *Phys. Rev. B*, **79** (2009) 144416.
[48] Starykh O. A. *et al.*, *Phys. Rev. B*, **74** (2006) 180403(R).
[49] Chernyshev A. L. and Zhitomirsky M. E., *Phys. Rev. Lett.*, **97** (2006) 207202.
[50] Zheng W. *et al.*, *Phys. Rev. B*, **74** (2006) 224420.
[51] Mourigal M. *et al.*, *Phys. Rev. B*, **88** (2013) 094407.
[52] Syromyatnikov A. V., *J. Phys.: Condens. Matter*, **22** (2010) 216003.
[53] Zheng W. *et al.*, *Phys. Rev. B*, **71** (2005) 184440.
[54] Huse D. A. and Elser V., *Phys. Rev. Lett.*, **60** (1988) 2531.
[55] Jolicoeur Th. and Guillou J. C. L., *Phys. Rev. B*, **40** (1989) 2727(R).
[56] Singh R. R. P. and Huse D. A., *Phys. Rev. Lett.*, **68** (1992) 1766.
[57] Bernu B. *et al.*, *Phys. Rev. Lett.*, **69** (1992) 2590.
[58] Azaria P. *et al.*, *Phys. Rev. Lett.*, **70** (1993) 2483.
[59] Bernu B. *et al.*, *Phys. Rev. B*, **50** (1994) 10048.
[60] Capriotti L. *et al.*, *Phys. Rev. Lett.*, **82** (1999) 3899.
[61] White S. R. and Chernyshev A. L., *Phys. Rev. Lett.*, **99** (2007) 127004.
[62] Bauer D.-V. and Fjærestad J. O., *Phys. Rev. B*, **101** (2020) 195124.
[63] Rezende S. M., *Phys. Rev. B*, **42** (1990) 2589.
[64] Wang H. *et al.*, *Phys. Rev. B*, **42** (1994) 12805.
[65] Yamamoto S. and Hori H., *J. Phys. Soc. Jpn.*, **72** (2003) 769.
[66] Yamamoto S. and Hori H., *J. Phys. Soc. Jpn.*, **72** (2004) 822.
[67] Noriki Y. and Yamamoto S., *J. Phys. Soc. Jpn.*, **86** (2017) 034714.
[68] Yamamoto S. and Noriki Y., *Phys. Rev. B*, **99** (2019) 094412.
[69] Veillette M. Y. *et al.*, *Phys. Rev. B*, **72** (2005) 134429.
[70] Canali C. M. and Wallin M., *Phys. Rev. B*, **48** (1993) 3264.
[71] Zhitomirsky M. E. and Chernyshev A. L., *Rev. Mod. Phys.*, **85** (2013) 219.
[72] Zheng W. *et al.*, *Phys. Rev. Lett.*, **96** (2006) 057201.
[73] Ghioldi E. A. *et al.*, *Phys. Rev. B*, **98** (2018) 184403.
[74] Zhang C. and Li T., *Phys. Rev. B*, **102** (2020) 075108.
[75] Fradkin E. and Shenker S. H., *Phys. Rev. D*, **19** (1979) 3682.
[76] Chubukov A. V. and Starykh O. A., *Phys. Rev. B*, **53** (1996) 14729(R).
[77] Read N. and Sachdev S., *Phys. Rev. Lett.*, **66** (1991) 1773.
[78] Faddeev L. D. and Takhtajan L. A., *Phys. Lett. A*, **85** (1981) 375.
[79] Uhrig G. S. and Majumdar K., *Eur. Phys. J. B*, **86** (2013) 282.
[80] Syromyatnikov A. V., *Phys. Rev. B*, **98** (2018) 184421.
[81] Affleck I. and Haldane F. D. M., *Phys. Rev. B*, **36** (1987) 5291.
[82] Cabra D. C. *et al.*, *Phys. Rev. B*, **58** (1998) 6241.
[83] Wang H.-T., *Phys. Rev. B*, **64** (2001) 174410.

*Supplemental Material for*

# Breakdown of the conventional spin-wave dynamics and its double-constraint modification in the spin-$\frac{1}{2}$ triangular-prism Heisenberg antiferromagnet

Shoji Yamamoto and Jun Ohara
*Department of Physics, Hokkaido University, Sapporo 060-0810, Japan*
(Dated: July 9, 2025)

## S1. SPIN WAVES IN NONCOLLINEAR ANTIFERROMAGNETS AND THEIR MODIFICATION

### S1.1. Bosonic Hamiltonian

We define the nearest-neighbor antiferromagnetic Heisenberg model on the equilateral triangular prism (three-legged ladder with the periodic boundary condition in the rung direction) of $L \equiv 3 \times N$ lattice sites [Fig. 1(a)],

$$\mathcal{H} = \sum_{l=1}^{L} \sum_{\sigma=\parallel,\perp} J_\sigma \boldsymbol{S}_{\boldsymbol{r}_l} \cdot \boldsymbol{S}_{\boldsymbol{r}_l+\boldsymbol{\delta}_\sigma}, \tag{S1}$$

where $\boldsymbol{S}_{\boldsymbol{r}_l}$ and $\boldsymbol{S}_{\boldsymbol{r}_l+\boldsymbol{\delta}_\sigma}$ are the vector spin operators of magnitude $S$ attached to the nearest-neighbor sites at $\boldsymbol{r}_l$ and $\boldsymbol{r}_l+\boldsymbol{\delta}_\sigma$, respectively, with $\boldsymbol{\delta}_\sigma$ pointing to a nearest-neighbor site to any site $\boldsymbol{r}_l$ in the leg ($\sigma=\parallel$) or rung ($\sigma=\perp$) direction. Note that $\boldsymbol{\delta}_\perp$, as well as $\boldsymbol{\delta}_\parallel$, no longer depends on the site index $l$ when unfolding the prism into a two-dimensional plane [Fig. 1(a)] and then $\boldsymbol{r}_l$ reads, say, $n_\parallel\boldsymbol{\delta}_\parallel + n_\perp\boldsymbol{\delta}_\perp = a(n_\parallel, n_\perp, 0)$ with integers $n_\parallel = 0, 1, \cdots, N$ and $n_\perp = 0, 1, 2$. Henceforth we set $J_\parallel$ and $J_\perp$ both equal to $J\,(>0)$ and accordingly suppose $|\boldsymbol{\delta}_\parallel| = |\boldsymbol{\delta}_\perp| = a$. Then the classical ground state of (S1) is designated by the ordering vector $(q^z, q^x, q^y) = \frac{\pi}{a}\left(1, \frac{2}{3}, 0\right)$. As long as $q^y = 0$, we use a short-hand notation in the two-dimensional reciprocal space such as

$$\boldsymbol{Q}_{\Gamma,\Gamma} = (Q^z_\Gamma, Q^x_\Gamma) \equiv \frac{\pi}{a}(0,0), \;\; \boldsymbol{Q}_{\mathrm{X,K}} = (Q^z_\mathrm{X}, Q^x_\mathrm{K}) \equiv \frac{\pi}{a}\left(1, \frac{2}{3}\right). \tag{1}$$

It is useful to define the rotating frame $(\tilde{z}, \tilde{x}, \tilde{y})$ with its $\tilde{z}$ axis pointing along each local spin direction in the classical ground state. The spin components in the coordinate system at rest and the rotating one are related with each other as

$$\begin{bmatrix} S^z_{\boldsymbol{r}_l} \\ S^x_{\boldsymbol{r}_l} \\ S^y_{\boldsymbol{r}_l} \end{bmatrix} = \begin{bmatrix} \cos \boldsymbol{Q}_{\mathrm{X,K}} \cdot \boldsymbol{r}_l & -\sin \boldsymbol{Q}_{\mathrm{X,K}} \cdot \boldsymbol{r}_l & 0 \\ \sin \boldsymbol{Q}_{\mathrm{X,K}} \cdot \boldsymbol{r}_l & \cos \boldsymbol{Q}_{\mathrm{X,K}} \cdot \boldsymbol{r}_l & 0 \\ 0 & 0 & 1 \end{bmatrix} \begin{bmatrix} S^{\tilde{z}}_{\boldsymbol{r}_l} \\ S^{\tilde{x}}_{\boldsymbol{r}_l} \\ S^{\tilde{y}}_{\boldsymbol{r}_l} \end{bmatrix}, \tag{2}$$

Let us introduce Holstein-Primakoff bosons in the rotating frame as

$$\begin{aligned} & S^{\tilde{z}}_{\boldsymbol{r}_l} = S - a^\dagger_{\boldsymbol{r}_l} a_{\boldsymbol{r}_l}, \\ & S^{\tilde{x}}_{\boldsymbol{r}_l} + iS^{\tilde{y}}_{\boldsymbol{r}_l} \equiv S^{\tilde{+}}_{\boldsymbol{r}_l} = \sqrt{2S}\,\mathcal{R}_{\boldsymbol{r}_l}(S)\, a_{\boldsymbol{r}_l}; \\ & S^{\tilde{x}}_{\boldsymbol{r}_l} - iS^{\tilde{y}}_{\boldsymbol{r}_l} \equiv S^{\tilde{-}}_{\boldsymbol{r}_l} = \sqrt{2S}\, a^\dagger_{\boldsymbol{r}_l} \mathcal{R}_{\boldsymbol{r}_l}(S), \\ & \mathcal{R}_{\boldsymbol{r}_l}(S) \equiv \sqrt{1 - \frac{a^\dagger_{\boldsymbol{r}_l} a_{\boldsymbol{r}_l}}{2S}} = 1 - \sum_{l=1}^{\infty} \frac{(2l-3)!!}{l!} \left( \frac{a^\dagger_{\boldsymbol{r}_l} a_{\boldsymbol{r}_l}}{4S} \right)^l \end{aligned} \tag{3}$$

to obtain a spin-wave (SW) Hamiltonian,

$$\mathcal{H} = J \sum_{l=1}^{L} \sum_{\sigma=\parallel,\perp} \boldsymbol{S}_{\boldsymbol{r}_l} \cdot \boldsymbol{S}_{\boldsymbol{r}_l+\boldsymbol{\delta}_\sigma} = \sum_{m=0}^{4} \mathcal{H}^{(\frac{m}{2})} + O\left(S^{-\frac{1}{2}}\right), \tag{S2}$$

where $\mathcal{H}^{(\frac{m}{2})}$, on the order of $S^{\frac{m}{2}}$, read

$$\mathcal{H}^{(2)} = -\frac{3}{2} J S^2 L, \tag{S3}$$

$$\mathcal{H}^{(\frac{3}{2})} = 0, \tag{S4}$$

$$\begin{aligned} \mathcal{H}^{(1)} = -JS \sum_{l=1}^{L} \sum_{\sigma=\parallel,\perp} \Bigg[ & \left( a^\dagger_{\boldsymbol{r}_l} a_{\boldsymbol{r}_l} + a^\dagger_{\boldsymbol{r}_l+\boldsymbol{\delta}_\sigma} a_{\boldsymbol{r}_l+\boldsymbol{\delta}_\sigma} \right) \cos \boldsymbol{Q}_{\mathrm{X,K}} \cdot \boldsymbol{\delta}_\sigma \\ & - \frac{\cos \boldsymbol{Q}_{\mathrm{X,K}} \cdot \boldsymbol{\delta}_\sigma - 1}{2} \left( a^\dagger_{\boldsymbol{r}_l} a^\dagger_{\boldsymbol{r}_l+\boldsymbol{\delta}_\sigma} + a_{\boldsymbol{r}_l} a_{\boldsymbol{r}_l+\boldsymbol{\delta}_\sigma} \right) \\ & - \frac{\cos \boldsymbol{Q}_{\mathrm{X,K}} \cdot \boldsymbol{\delta}_\sigma + 1}{2} \left( a^\dagger_{\boldsymbol{r}_l} a_{\boldsymbol{r}_l+\boldsymbol{\delta}_\sigma} + a^\dagger_{\boldsymbol{r}_l+\boldsymbol{\delta}_\sigma} a_{\boldsymbol{r}_l} \right) \Bigg] \end{aligned} \tag{S5}$$

$$\begin{aligned} \mathcal{H}^{(\frac{1}{2})} = J \sqrt{\frac{S}{2}} \sum_{l=1}^{L} \sum_{\sigma=\parallel,\perp} \Big[ & a^\dagger_{\boldsymbol{r}_l} a_{\boldsymbol{r}_l} \left( a^\dagger_{\boldsymbol{r}_l+\boldsymbol{\delta}_\sigma} + a_{\boldsymbol{r}_l+\boldsymbol{\delta}_\sigma} \right) \\ & - \left( a^\dagger_{\boldsymbol{r}_l} + a_{\boldsymbol{r}_l} \right) a^\dagger_{\boldsymbol{r}_l+\boldsymbol{\delta}_\sigma} a_{\boldsymbol{r}_l+\boldsymbol{\delta}_\sigma} \Big] \sin \boldsymbol{Q}_{\mathrm{X,K}} \cdot \boldsymbol{\delta}_\sigma, \end{aligned} \tag{S6}$$

$$\begin{aligned} \mathcal{H}^{(0)} = J \sum_{l=1}^{L} \sum_{\sigma=\parallel,\perp} \Bigg\{ & a^\dagger_{\boldsymbol{r}_l} a_{\boldsymbol{r}_l} a^\dagger_{\boldsymbol{r}_l+\boldsymbol{\delta}_\sigma} a_{\boldsymbol{r}_l+\boldsymbol{\delta}_\sigma} \cos \boldsymbol{Q}_{\mathrm{X,K}} \cdot \boldsymbol{\delta}_\sigma \\ & - \frac{\cos \boldsymbol{Q}_{\mathrm{X,K}} \cdot \boldsymbol{\delta}_\sigma - 1}{8} \Big[ a^\dagger_{\boldsymbol{r}_l} a^\dagger_{\boldsymbol{r}_l+\boldsymbol{\delta}_\sigma} \left( a^\dagger_{\boldsymbol{r}_l} a_{\boldsymbol{r}_l} + a^\dagger_{\boldsymbol{r}_l+\boldsymbol{\delta}_\sigma} a_{\boldsymbol{r}_l+\boldsymbol{\delta}_\sigma} \right) \\ & \qquad + \left( a^\dagger_{\boldsymbol{r}_l} a_{\boldsymbol{r}_l} + a^\dagger_{\boldsymbol{r}_l+\boldsymbol{\delta}_\sigma} a_{\boldsymbol{r}_l+\boldsymbol{\delta}_\sigma} \right) a_{\boldsymbol{r}_l} a_{\boldsymbol{r}_l+\boldsymbol{\delta}_\sigma} \Big] \\ & - \frac{\cos \boldsymbol{Q}_{\mathrm{X,K}} \cdot \boldsymbol{\delta}_\sigma + 1}{8} \Big[ a^\dagger_{\boldsymbol{r}_l} \left( a^\dagger_{\boldsymbol{r}_l} a_{\boldsymbol{r}_l} + a^\dagger_{\boldsymbol{r}_l+\boldsymbol{\delta}_\sigma} a_{\boldsymbol{r}_l+\boldsymbol{\delta}_\sigma} \right) a_{\boldsymbol{r}_l+\boldsymbol{\delta}_\sigma} \\ & \qquad + a^\dagger_{\boldsymbol{r}_l+\boldsymbol{\delta}_\sigma} \left( a^\dagger_{\boldsymbol{r}_l} a_{\boldsymbol{r}_l} + a^\dagger_{\boldsymbol{r}_l+\boldsymbol{\delta}_\sigma} a_{\boldsymbol{r}_l+\boldsymbol{\delta}_\sigma} \right) a_{\boldsymbol{r}_l} \Big] \Bigg\}. \end{aligned} \tag{S7}$$

We divide the conventional SW (CSW) Hamiltonian into the harmonic part $\mathcal{H}_\mathrm{harm} \equiv \mathcal{H}^{(2)} + \mathcal{H}^{(1)}$ to yield linear SWs (LSWs) and higher-order anharmonicities $\mathcal{V} \equiv \mathcal{H}^{(\frac{1}{2})} + \mathcal{H}^{(0)}$ consisting of cubic and quartic terms. We treat $\mathcal{V}$ in two ways, variationally on one hand, which is usual with collinear magnets, and perturbatively on the other hand, which is indispensable for noncollinear magnets, to obtain what we distinguishably call interacting SWs (ISWs) and perturbed SWs (PSWs), respectively. Starting from diagonalizing $\mathcal{H}_\mathrm{harm}$ to obtain conventional LSWs (CLSWs), we consider various manners of modifying them and further bringing them into interaction. We introduce a wavevector running over the first Brillouin

zone [Fig. 1(b)],

$$\boldsymbol{k}_{\nu,\sigma} \equiv (k^z_\nu, k^x_\sigma) = \frac{\pi}{a}\left(\frac{2\nu}{N} - 1, \frac{2}{3}\sigma\right), \tag{S8}$$

to define Fourier transforms of spin operators and Holstein-Primakoff bosons,

$$S^\lambda_{\boldsymbol{k}_{\nu,\sigma}} = \sum_{l=1}^{L} \frac{e^{i\boldsymbol{k}_{\nu,\sigma}\cdot\boldsymbol{r}_l}}{\sqrt{L}} S^\lambda_{\boldsymbol{r}_l},\ S^\lambda_{\boldsymbol{r}_l} = \sum_{\sigma=0,\pm}\sum_{\nu=1}^{N} \frac{e^{-i\boldsymbol{k}_{\nu,\sigma}\cdot\boldsymbol{r}_l}}{\sqrt{L}} S^\lambda_{\boldsymbol{k}_{\nu,\sigma}}, \tag{S9}$$

$$a^\dagger_{\boldsymbol{k}_{\nu,\sigma}} = \sum_{l=1}^{L} \frac{e^{i\boldsymbol{k}_{\nu,\sigma}\cdot\boldsymbol{r}_l}}{\sqrt{L}} a^\dagger_{\boldsymbol{r}_l},\ a^\dagger_{\boldsymbol{r}_l} = \sum_{\sigma=0,\pm}\sum_{\nu=1}^{N} \frac{e^{-i\boldsymbol{k}_{\nu,\sigma}\cdot\boldsymbol{r}_l}}{\sqrt{L}} a^\dagger_{\boldsymbol{k}_{\nu,\sigma}}. \tag{S10}$$

At each momentum, a Bogoliubov quasiparticle is created by

$$\alpha^\dagger_{\boldsymbol{k}_{\nu,\sigma}} = u_{\boldsymbol{k}_{\nu,\sigma}} a^\dagger_{\boldsymbol{k}_{\nu,\sigma}} - v_{\boldsymbol{k}_{\nu,\sigma}} a_{-\boldsymbol{k}_{\nu,\sigma}} \tag{S11}$$

with $u_{\boldsymbol{k}_{\nu,\sigma}}$ and $v_{\boldsymbol{k}_{\nu,\sigma}}$ diagonalizing $\mathcal{H}_{\rm harm}$ or any modified-SW (MSW) Hamiltonian in question. Here we perform all calculations at $T = 0$.

### S1.2. Harmonic spin waves

The harmonic Hamiltonian is diagonalized as

$$\mathcal{H}_{\rm harm} = \sum_{m=1}^{2} E^{(m)} + \sum_{\sigma=0,\pm}\sum_{\nu=1}^{N} \varepsilon_{\boldsymbol{k}_{\nu,\sigma}} \alpha^\dagger_{\boldsymbol{k}_{\nu,\sigma}} \alpha_{\boldsymbol{k}_{\nu,\sigma}}; \tag{4}$$

$$E^{(2)} = -\frac{3}{2}LJS^2,\ E^{(1)} = -\frac{3}{2}LJS + \sum_{\sigma=0,\pm}\sum_{\nu=1}^{N}\frac{\varepsilon_{\boldsymbol{k}_{\nu,\sigma}}}{2},$$
$$\varepsilon_{(k^z_\nu,k^x_0)} = JS\sqrt{2(1-\cos ak^z_\nu)(5+2\cos ak^z_\nu)},$$
$$\varepsilon_{(k^z_\nu,k^x_\pm)} = JS\sqrt{2(1+\cos ak^z_\nu)\left(\frac{7}{2} - 2\cos ak^z_\nu\right)} \tag{5}$$

via the Bogoliubov transformation

$$u_{(k^z_\nu,k^x_0)} = \sqrt{\frac{2\varepsilon_{(k^z_\nu,k^x_0)} + 7JS}{4\varepsilon_{(k^z_\nu,k^x_0)}}},$$
$$v_{(k^z_\nu,k^x_0)} = \frac{JS\ (4\cos ak^z_\nu + 3)}{\sqrt{4\varepsilon_{(k^z_\nu,k^x_0)}\left(2\varepsilon_{(k^z_\nu,k^x_0)} + 7JS\right)}},$$
$$u_{(k^z_\nu,k^x_\pm)} = \sqrt{\frac{4\varepsilon_{(k^z_\nu,k^x_\pm)} + 11JS}{8\varepsilon_{(k^z_\nu,k^x_\pm)}}},$$
$$v_{(k^z_\nu,k^x_\pm)} = \frac{JS\ (8\cos ak^z_\nu - 3)}{\sqrt{8\varepsilon_{(k^z_\nu,k^x_\pm)}\left(4\varepsilon_{(k^z_\nu,k^x_\pm)} + 11JS\right)}}. \tag{S12}$$

Local spin expectation values in the CLSW vacuum state are given by

$$\langle S^{\tilde z}_{\boldsymbol{r}_l}\rangle_0 = S + 1 - \frac{JS}{24\pi}\int_{-\frac{\pi}{a}}^{\frac{\pi}{a}}\left(\frac{9}{\varepsilon_{(k^z,k^x_0)}} + \frac{11}{\varepsilon_{(k^z,k^x_\pm)}}\right)dk^z,\ \langle S^{\tilde x}_{\boldsymbol{r}_l}\rangle_0 = 0,\ \langle S^{\tilde y}_{\boldsymbol{r}_l}\rangle_0 = 0. \tag{S13}$$

The static structure factors are defined in terms of spatial spin fluctuations $\delta S^\lambda_{\boldsymbol{r}_l} \equiv S^\lambda_{\boldsymbol{r}_l} - \langle S^\lambda_{\boldsymbol{r}_l}\rangle_0$ as

$$S^{\lambda\lambda'}(\boldsymbol{q}) \equiv \sum_{l,l'=1}^{L}\frac{e^{i\boldsymbol{q}\cdot(\boldsymbol{r}_l-\boldsymbol{r}_{l'})}}{L}\langle\delta S^\lambda_{\boldsymbol{r}_l}\delta S^{\lambda'}_{\boldsymbol{r}_{l'}}\rangle_0 = \sum_{l,l'=1}^{L}\frac{e^{i\boldsymbol{q}\cdot(\boldsymbol{r}_l-\boldsymbol{r}_{l'})}}{L}\left(\langle S^\lambda_{\boldsymbol{r}_l}S^{\lambda'}_{\boldsymbol{r}_{l'}}\rangle_0 - \langle S^\lambda_{\boldsymbol{r}_l}\rangle_0\langle S^{\lambda'}_{\boldsymbol{r}_{l'}}\rangle_0\right) \tag{S14}$$

and written in the rotating frame as

$$S^{\tilde z\tilde z}(\boldsymbol{q}) = \frac{(JS)^2}{96\pi}\int_{-\frac{\pi}{a}}^{\frac{\pi}{a}}\left\{\frac{42 + 7\cos aq^x + (3+4\cos ak^z)\left[3\cos aq^x + 4\cos a(k^z+q^z)\right]}{\varepsilon_{(k^z,k^x_0)}\varepsilon_{(k^z+q^z,k^x_0+q^x)}}\right.$$
$$\left. + \frac{132 - 11\cos aq^x + (6 - 16\cos ak^z)\left[3\cos aq^x - 8\cos a(k^z+q^z)\right]}{\varepsilon_{(k^z,k^x_\pm)}\varepsilon_{(k^z+q^z,k^x_\pm+q^x)}}\right\}dk^z - \frac{1}{4},$$
$$S^{\tilde x\tilde x}(\boldsymbol{q}) = \frac{JS(3+2\cos aq^x+2\cos aq^z)}{\varepsilon_{(q^z,q^x)}}\left[\frac{S}{2} + \frac{1}{4} - \frac{JS}{48\pi}\int_{-\frac{\pi}{a}}^{\frac{\pi}{a}}\left(\frac{13+8\cos ak^z}{\varepsilon_{(k^z,k^x_0)}} + \frac{5+16\cos ak^z}{\varepsilon_{(k^z,k^x_\pm)}}\right)dk^z\right] + O(S^{-1}),$$
$$S^{\tilde y\tilde y}(\boldsymbol{q}) = \frac{JS(6-\cos aq^x-4\cos aq^z)}{2\varepsilon_{(q^z,q^x)}}\left[\frac{S}{2} + \frac{1}{4} - \frac{JS}{48\pi}\int_{-\frac{\pi}{a}}^{\frac{\pi}{a}}\left(\frac{1-4\cos ak^z}{\varepsilon_{(k^z,k^x_0)}} + \frac{17-16\cos ak^z}{\varepsilon_{(k^z,k^x_\pm)}}\right)dk^z\right] + O(S^{-1}),$$
$$S^{\tilde z\tilde x}(\boldsymbol{q}) = \left[S^{\tilde x\tilde z}(\boldsymbol{q})\right]^* = 0,\ S^{\tilde y\tilde z}(\boldsymbol{q}) = \left[S^{\tilde z\tilde y}(\boldsymbol{q})\right]^* = 0,\ S^{\tilde x\tilde y}(\boldsymbol{q}) = \left[S^{\tilde y\tilde x}(\boldsymbol{q})\right]^* = \frac{1}{4i}\left[-\frac{S}{2} - \frac{1}{4} + \frac{JS(6+\cos aq^x)}{2\varepsilon_{(q^z,q^x)}}\right.$$
$$\left.\times\frac{JS}{384\pi}\int_{-\frac{\pi}{a}}^{\frac{\pi}{a}}\left(\frac{3+4\cos ak^z}{\varepsilon_{(k^z,k^x_0)}} - \frac{3-8\cos ak^z}{\varepsilon_{(k^z,k^x_\pm)}}\right)dk^z + \frac{JS}{384\pi}\int_{-\frac{\pi}{a}}^{\frac{\pi}{a}}\left(\frac{65+12\cos ak^z}{\varepsilon_{(k^z,k^x_0)}} + \frac{79+24\cos ak^z}{\varepsilon_{(k^z,k^x_\pm)}}\right)dk^z\right] + O(S^{-1}). \tag{S15}$$

Having in mind that

$$S^z_{\boldsymbol{q}} = \frac{1}{2}\sum_{\tau=\pm}\left(S^{\tilde{z}}_{\tau\boldsymbol{Q}_{\mathrm{X,K}}+\boldsymbol{q}} - i\tau S^{\tilde{x}}_{\tau\boldsymbol{Q}_{\mathrm{X,K}}+\boldsymbol{q}}\right),\ S^x_{\boldsymbol{q}} = \frac{1}{2}\sum_{\tau=\pm}\left(S^{\tilde{x}}_{\tau\boldsymbol{Q}_{\mathrm{X,K}}+\boldsymbol{q}} + i\tau S^{\tilde{z}}_{\tau\boldsymbol{Q}_{\mathrm{X,K}}+\boldsymbol{q}}\right),\ S^y_{\boldsymbol{q}} = S^{\tilde{y}}_{\boldsymbol{q}} \tag{S16}$$

together with $\left\langle \delta S^{\lambda}_{\boldsymbol{q}} \delta S^{\lambda'}_{-\boldsymbol{q}'}\right\rangle_0 = \delta_{\boldsymbol{q}\boldsymbol{q}'} S^{\lambda\lambda'}(\boldsymbol{q})$, we can readily construct the structure factors in the laboratory frame from (S15),

$$S^{zz}(\boldsymbol{q}) = S^{xx}(\boldsymbol{q}) = \frac{1}{4}\sum_{\tau=\pm}\left\{S^{\tilde{z}\tilde{z}}(\tau\boldsymbol{Q}_{\mathrm{X,K}}+\boldsymbol{q}) + S^{\tilde{x}\tilde{x}}(\tau\boldsymbol{Q}_{\mathrm{X,K}}+\boldsymbol{q}) + i\tau\left[S^{\tilde{z}\tilde{x}}(\tau\boldsymbol{Q}_{\mathrm{X,K}}+\boldsymbol{q}) - S^{\tilde{x}\tilde{z}}(\tau\boldsymbol{Q}_{\mathrm{X,K}}+\boldsymbol{q})\right]\right\},\ S^{yy}(\boldsymbol{q}) = S^{\tilde{y}\tilde{y}}(\boldsymbol{q}). \tag{S17}$$

Since the CLSW spectrum (5) contain fictitious soft modes of linear dispersion, one-dimensional integrals in (S13) and (S15) logarithmically diverge, not to mention any such calculations in the laboratory frame.

### S1.3. Single-constraint modification

MSWs constrained to keep their total staggered magnetization zero, which were originally designed for square-lattice antiferromagnets [1–4] and are good at describing collinear antiferromagnets [5, 6] in general, can be applied to non-collinear antiferromagnets [7] as well. The single-constraint (SC)-modified-LSW (MLSW) Hamiltonian is diagonalized as

$$\begin{aligned}
&\mathcal{H}_{\mathrm{harm}} + \sum_{l=1}^{L}\mu_l(S - a^{\dagger}_{\boldsymbol{r}_l}a_{\boldsymbol{r}_l}) \equiv \widetilde{\mathcal{H}}^{\mathrm{SC}}_{\mathrm{harm}} \\
&= \sum_{m=1}^{2}E^{(m)} + \mu L\left(S+\frac{1}{2}\right) + \sum_{\sigma=0,\pm}\sum_{\nu=1}^{N}\tilde{\varepsilon}^{\mathrm{SC}}_{\boldsymbol{k}_{\nu,\sigma}}\alpha^{\dagger}_{\boldsymbol{k}_{\nu,\sigma}}\alpha_{\boldsymbol{k}_{\nu,\sigma}}; \qquad (6)\\
&E^{(2)} = -\frac{3}{2}LJS^2,\ E^{(1)} = -\frac{3}{2}LJS + \sum_{\sigma=0,\pm}\sum_{\nu=1}^{N}\frac{\tilde{\varepsilon}^{\mathrm{SC}}_{\boldsymbol{k}_{\nu,\sigma}}}{2}, \\
&\frac{\tilde{\varepsilon}^{\mathrm{SC}}_{(k^z_\nu,k^x_0)}}{JS} = \sqrt{2\left(1-\cos ak^z_\nu - \frac{\mu}{2JS}\right)\left(5+2\cos ak^z_\nu - \frac{\mu}{JS}\right)}, \\
&\frac{\tilde{\varepsilon}^{\mathrm{SC}}_{(k^z_\nu,k^x_\pm)}}{JS} = \sqrt{2\left(1+\cos ak^z_\nu - \frac{\mu}{2JS}\right)\left(\frac{7}{2}-2\cos ak^z_\nu - \frac{\mu}{JS}\right)} \qquad (7)
\end{aligned}$$

via the Bogoliubov transformation

$$\begin{aligned}
u_{(k^z_\nu,k^x_0)} &= \sqrt{\frac{2\tilde{\varepsilon}^{\mathrm{SC}}_{(k^z_\nu,k^x_0)} + 7JS - 2\mu}{4\tilde{\varepsilon}^{\mathrm{SC}}_{(k^z_\nu,k^x_0)}}}, \\
v_{(k^z_\nu,k^x_0)} &= \frac{JS\,(4\cos ak^z_\nu + 3)}{\sqrt{4\tilde{\varepsilon}^{\mathrm{SC}}_{(k^z_\nu,k^x_0)}\left(2\tilde{\varepsilon}^{\mathrm{SC}}_{(k^z_\nu,k^x_0)} + 7JS - 2\mu\right)}}, \\
u_{(k^z_\nu,k^x_\pm)} &= \sqrt{\frac{4\tilde{\varepsilon}^{\mathrm{SC}}_{(k^z_\nu,k^x_\pm)} + 11JS - 4\mu}{8\tilde{\varepsilon}^{\mathrm{SC}}_{(k^z_\nu,k^x_\pm)}}}, \\
v_{(k^z_\nu,k^x_\pm)} &= \frac{JS\,(8\cos ak^z_\nu - 3)}{\sqrt{8\tilde{\varepsilon}^{\mathrm{SC}}_{(k^z_\nu,k^x_\pm)}\left(4\tilde{\varepsilon}^{\mathrm{SC}}_{(k^z_\nu,k^x_\pm)} + 11JS - 4\mu\right)}}
\end{aligned} \tag{S18}$$

on condition that

$$\langle S^{\tilde{z}}_{\boldsymbol{r}_l}\rangle^{\mathrm{SC}}_0 = S - \langle a^{\dagger}_{\boldsymbol{r}_l}a_{\boldsymbol{r}_l}\rangle^{\mathrm{SC}}_0 = 0 \tag{S19}$$

with $\langle\cdots\rangle^{\mathrm{SC}}_0$ denoting a quantum average in the SC-MLSW ground state.

We can bring such MLSWs into interaction in a variational manner [8, 9]. Denoting some quadratic terms by

$$\begin{aligned}
&\mathcal{A} \equiv a^{\dagger}_{\boldsymbol{r}_l}a_{\boldsymbol{r}_l},\ \mathcal{B}_\sigma \equiv \frac{a^{\dagger}_{\boldsymbol{r}_l}a^{\dagger}_{\boldsymbol{r}_l+\boldsymbol{\delta}_\sigma} + a_{\boldsymbol{r}_l}a_{\boldsymbol{r}_l+\boldsymbol{\delta}_\sigma}}{2}, \\
&C \equiv \frac{a^{\dagger}_{\boldsymbol{r}_l}a^{\dagger}_{\boldsymbol{r}_l} + a_{\boldsymbol{r}_l}a_{\boldsymbol{r}_l}}{2},\ \mathcal{D}_\sigma \equiv \frac{a^{\dagger}_{\boldsymbol{r}_l}a_{\boldsymbol{r}_l+\boldsymbol{\delta}_\sigma} + a^{\dagger}_{\boldsymbol{r}_l+\boldsymbol{\delta}_\sigma}a_{\boldsymbol{r}_l}}{2}
\end{aligned} \tag{S20}$$

and their thermal averages at temperature $T$ with respect to a certain MSW Hamiltonian by $\langle\cdots\rangle_T$, we apply the Hartree-Fock decomposition to the $O(S^0)$ quartic interaction (S7)

$$\begin{aligned}
\mathcal{H}^{(0)} \simeq J\sum_{l=1}^{L}\sum_{\sigma=\parallel,\perp}\Bigg\{&\left[\left(\langle\mathcal{A}\rangle_T - \frac{\langle\mathcal{B}_\sigma\rangle_T + \langle\mathcal{D}_\sigma\rangle_T}{2}\right)\cos\boldsymbol{Q}_{\mathrm{X,K}}\cdot\boldsymbol{\delta}_\sigma + \frac{\langle\mathcal{B}_\sigma\rangle_T - \langle\mathcal{D}_\sigma\rangle_T}{2}\right]\left(a^{\dagger}_{\boldsymbol{r}_l}a_{\boldsymbol{r}_l} + a^{\dagger}_{\boldsymbol{r}_l+\boldsymbol{\delta}_\sigma}a_{\boldsymbol{r}_l+\boldsymbol{\delta}_\sigma}\right) \\
&+\left[\left(\langle\mathcal{B}_\sigma\rangle_T - \frac{2\langle\mathcal{A}\rangle_T + \langle C\rangle_T}{4}\right)\cos\boldsymbol{Q}_{\mathrm{X,K}}\cdot\boldsymbol{\delta}_\sigma + \frac{2\langle\mathcal{A}\rangle_T - \langle C\rangle_T}{4}\right]\left(a^{\dagger}_{\boldsymbol{r}_l}a^{\dagger}_{\boldsymbol{r}_l+\boldsymbol{\delta}_\sigma} + a_{\boldsymbol{r}_l}a_{\boldsymbol{r}_l+\boldsymbol{\delta}_\sigma}\right) \\
&+\left[\left(\langle\mathcal{D}_\sigma\rangle_T - \frac{2\langle\mathcal{A}\rangle_T + \langle C\rangle_T}{4}\right)\cos\boldsymbol{Q}_{\mathrm{X,K}}\cdot\boldsymbol{\delta}_\sigma - \frac{2\langle\mathcal{A}\rangle_T - \langle C\rangle_T}{4}\right]\left(a^{\dagger}_{\boldsymbol{r}_l}a_{\boldsymbol{r}_l+\boldsymbol{\delta}_\sigma} + a^{\dagger}_{\boldsymbol{r}_l+\boldsymbol{\delta}_\sigma}a_{\boldsymbol{r}_l}\right) \\
&-\left[\frac{\langle\mathcal{B}_\sigma\rangle_T + \langle\mathcal{D}_\sigma\rangle_T}{8}\cos\boldsymbol{Q}_{\mathrm{X,K}}\cdot\boldsymbol{\delta}_\sigma + \frac{\langle\mathcal{B}_\sigma\rangle_T - \langle\mathcal{D}_\sigma\rangle_T}{8}\right]\left(a^{\dagger}_{\boldsymbol{r}_l}a^{\dagger}_{\boldsymbol{r}_l} + a^{\dagger}_{\boldsymbol{r}_l+\boldsymbol{\delta}_\sigma}a^{\dagger}_{\boldsymbol{r}_l+\boldsymbol{\delta}_\sigma} + a_{\boldsymbol{r}_l}a_{\boldsymbol{r}_l} + a_{\boldsymbol{r}_l+\boldsymbol{\delta}_\sigma}a_{\boldsymbol{r}_l+\boldsymbol{\delta}_\sigma}\right) \\
&-\left[(\langle\mathcal{A}\rangle_T)^2 + (\langle\mathcal{B}_\sigma\rangle_T)^2 + (\langle\mathcal{D}_\sigma\rangle_T)^2 - (2\langle\mathcal{A}\rangle_T + \langle C\rangle_T)\frac{\langle\mathcal{B}_\sigma\rangle_T + \langle\mathcal{D}_\sigma\rangle_T}{2}\right]\cos\boldsymbol{Q}_{\mathrm{X,K}}\cdot\boldsymbol{\delta}_\sigma \\
&-(2\langle\mathcal{A}\rangle_T - \langle C\rangle_T)\frac{\langle\mathcal{B}_\sigma\rangle_T - \langle\mathcal{D}_\sigma\rangle_T}{2}\Bigg\} \equiv \mathcal{H}^{(0)}_{\mathrm{quad}}
\end{aligned} \tag{S21}$$

to have the tractable SW Hamiltonian $\mathcal{H}_{\rm quad} = \mathcal{H}_{\rm harm} + \mathcal{H}^{(0)}_{\rm quad}$. Its SC-MSW extension, i.e., the SC-modified Hartree-Fock-decomposition-based-ISW (SC-MHFISW) Hamiltonian, where we suppose $\langle\cdots\rangle_T$ in (S21) to be $\langle\cdots\rangle'^{\rm SC}_T$, is diagonalized as

$$\mathcal{H}_{\rm quad} + \sum_{l=1}^{L}\mu_l(S - a^\dagger_{\boldsymbol{r}_l}a_{\boldsymbol{r}_l}) \equiv \widetilde{\mathcal{H}}'^{\rm SC} = \sum_{m=0}^{2}E^{(m)} + \mu L\left(S+\frac{1}{2}\right) + \sum_{\sigma=0,\pm}\sum_{\nu=1}^{N}\tilde{\varepsilon}'^{\rm SC}_{\boldsymbol{k}_{\nu,\sigma}}\alpha^\dagger_{\boldsymbol{k}_{\nu,\sigma}}\alpha_{\boldsymbol{k}_{\nu,\sigma}}; \tag{S22}$$

$$E^{(2)} = -\frac{3}{2}LJS^2,\ E^{(1)} = -\frac{3}{2}LJS + \sum_{\sigma=0,\pm}\sum_{\nu=1}^{N}\frac{\tilde{\varepsilon}'^{\rm SC}_{\boldsymbol{k}_{\nu,\sigma}}}{2},\ E^{(0)} = \langle\mathcal{H}^{(0)}\rangle'^{\rm SC}_T = -JL$$
$$\times\sum_{\sigma=\parallel,\perp}\left\{\left[\left(\langle\mathcal{A}\rangle'^{\rm SC}_T\right)^2 + \left(\langle\mathcal{B}_\sigma\rangle'^{\rm SC}_T\right)^2 + \left(\langle\mathcal{D}_\sigma\rangle'^{\rm SC}_T\right)^2 - \left(2\langle\mathcal{A}\rangle'^{\rm SC}_T + \langle C\rangle'^{\rm SC}_T\right)\frac{\langle\mathcal{B}_\sigma\rangle'^{\rm SC}_T + \langle\mathcal{D}_\sigma\rangle'^{\rm SC}_T}{2}\right]\cos\boldsymbol{Q}_{\rm X,K}\cdot\boldsymbol{\delta}_\sigma\right.$$
$$\left. - \left(2\langle\mathcal{A}\rangle'^{\rm SC}_T - \langle C\rangle'^{\rm SC}_T\right)\frac{\langle\mathcal{B}_\sigma\rangle'^{\rm SC}_T - \langle\mathcal{D}_\sigma\rangle'^{\rm SC}_T}{2} - \left(\frac{\langle\mathcal{A}\rangle'^{\rm SC}_T}{2} - \frac{\langle\mathcal{B}_\sigma\rangle'^{\rm SC}_T + \langle\mathcal{D}_\sigma\rangle'^{\rm SC}_T}{4}\right)\cos\boldsymbol{Q}_{\rm X,K}\cdot\boldsymbol{\delta}_\sigma - \frac{\langle\mathcal{B}_\sigma\rangle'^{\rm SC}_T - \langle\mathcal{D}_\sigma\rangle'^{\rm SC}_T}{4}\right\}, \tag{S23}$$

$$\frac{\tilde{\varepsilon}'^{\rm SC}_{(k^z_\nu,k^x_0)}}{JS} = \sqrt{2\left[1+\frac{F_0-G_0}{2} - \left(1-\frac{F'_0-G'_0}{2}\right)\cos ak^z_\nu - \frac{\mu}{2JS}\right]\left[5+F_0+G_0+\left(2+F'_0+G'_0\right)\cos ak^z_\nu - \frac{\mu}{JS}\right]},$$
$$\frac{\tilde{\varepsilon}'^{\rm SC}_{(k^z_\nu,k^x_\pm)}}{JS} = \sqrt{2\left[1+\frac{F_\pm-G_\pm}{2} + \left(1+\frac{F'_\pm-G'_\pm}{2}\right)\cos ak^z_\nu - \frac{\mu}{2JS}\right]\left[\frac{7}{2}+F_\pm+G_\pm-(2-F'_\pm-G'_\pm)\cos ak^z_\nu - \frac{\mu}{JS}\right]}, \tag{S24}$$

$$F_0 = -\frac{7\langle\mathcal{A}\rangle'^{\rm SC}_T}{2S} + \frac{3\langle C\rangle'^{\rm SC}_T}{4S} + \frac{3\langle\mathcal{B}_\perp\rangle'^{\rm SC}_T}{2S} + \frac{2\langle\mathcal{B}_\parallel\rangle'^{\rm SC}_T}{S} - \frac{3\langle\mathcal{D}_\perp\rangle'^{\rm SC}_T}{2S},\ F'_0 = \frac{\langle C\rangle'^{\rm SC}_T - 2\langle\mathcal{D}_\parallel\rangle'^{\rm SC}_T}{S},$$
$$G_0 = \frac{3\langle\mathcal{A}\rangle'^{\rm SC}_T}{2S} - \frac{\langle\mathcal{B}_\perp\rangle'^{\rm SC}_T}{S} - \frac{\langle C\rangle'^{\rm SC}_T}{2S} + \frac{3\langle\mathcal{D}_\perp\rangle'^{\rm SC}_T}{4S} + \frac{\langle\mathcal{D}_\parallel\rangle'^{\rm SC}_T}{S},\ G'_0 = \frac{2\left(\langle\mathcal{A}\rangle'^{\rm SC}_T - \langle\mathcal{B}_\parallel\rangle'^{\rm SC}_T\right)}{S},$$
$$F_\pm = -\frac{11\langle\mathcal{A}\rangle'^{\rm SC}_T}{4S} + \frac{3\langle\mathcal{B}_\perp\rangle'^{\rm SC}_T}{2S} + \frac{2\langle\mathcal{B}_\parallel\rangle'^{\rm SC}_T}{S} - \frac{3\langle C\rangle'^{\rm SC}_T}{8S},\ F'_\pm = \frac{2\left(\langle C\rangle'^{\rm SC}_T - \langle\mathcal{D}_\parallel\rangle'^{\rm SC}_T\right)}{S},$$
$$G_\pm = -\frac{3\langle\mathcal{A}\rangle'^{\rm SC}_T}{4S} + \frac{\langle\mathcal{B}_\perp\rangle'^{\rm SC}_T}{2S} + \frac{\langle C\rangle'^{\rm SC}_T}{8S} + \frac{3\langle\mathcal{D}_\perp\rangle'^{\rm SC}_T}{4S} + \frac{\langle\mathcal{D}_\parallel\rangle'^{\rm SC}_T}{S},\ G'_\pm = \frac{2\left(\langle\mathcal{A}\rangle'^{\rm SC}_T - \langle\mathcal{B}_\parallel\rangle'^{\rm SC}_T\right)}{S} \tag{S25}$$

via the Bogoliubov transformation

$$u_{(k^z_\nu,k^x_0)} = \sqrt{\frac{2\tilde{\varepsilon}'^{\rm SC}_{(k^z_\nu,k^x_0)} + JS\left(7+2F_0+2F'_0\cos ak^z_\nu\right) - 2\mu}{4\tilde{\varepsilon}'^{\rm SC}_{(k^z_\nu,k^x_0)}}},$$
$$v_{(k^z_\nu,k^x_0)} = \frac{JS\left(4\cos ak^z_\nu - 2G'_0\cos ak^z_\nu + 3 - 2G_0\right)}{\sqrt{4\tilde{\varepsilon}'^{\rm SC}_{(k^z_\nu,k^x_0)}\left[2\tilde{\varepsilon}'^{\rm SC}_{(k^z_\nu,k^x_0)} + JS\left(7+2F_0+2F'_0\cos ak^z_\nu\right) - 2\mu\right]}},$$
$$u_{(k^z_\nu,k^x_\pm)} = \sqrt{\frac{4\tilde{\varepsilon}'^{\rm SC}_{(k^z_\nu,k^x_\pm)} + JS\left(11+4F_0+4F'_0\cos ak^z_\nu\right) - 4\mu}{8\tilde{\varepsilon}'^{\rm SC}_{(k^z_\nu,k^x_\pm)}}},$$
$$v_{(k^z_\nu,k^x_\pm)} = \frac{JS\left(8\cos ak^z_\nu - 4G'_0\cos ak^z_\nu + 3 - 2G_0\right)}{\sqrt{8\tilde{\varepsilon}'^{\rm SC}_{(k^z_\nu,k^x_\pm)}\left[4\tilde{\varepsilon}'^{\rm SC}_{(k^z_\nu,k^x_\pm)} + JS\left(11+4F_0+4F'_0\cos ak^z_\nu\right) - 4\mu\right]}} \tag{S26}$$

on condition that

$$S - \langle\mathcal{A}\rangle'^{\rm SC}_T = S - \langle a^\dagger_{\boldsymbol{r}_l}a_{\boldsymbol{r}_l}\rangle'^{\rm SC}_T = 0 \tag{S27}$$

with $\langle\cdots\rangle_T'^{\rm SC}$ denoting a thermal average at temperature $T$ with respect to $\widetilde{\mathcal{H}}'^{\rm SC}$. In terms of the thermal distribution function

$$\langle\alpha^\dagger_{\boldsymbol{k}_{\nu,\sigma}}\alpha_{\boldsymbol{k}_{\nu,\sigma}}\rangle_T'^{\rm SC}=\frac{{\rm Tr}\left[e^{-\tilde{\varepsilon}'^{\rm SC}_{\boldsymbol{k}_{\nu,\sigma}}\alpha^\dagger_{\boldsymbol{k}_{\nu,\sigma}}\alpha_{\boldsymbol{k}_{\nu,\sigma}}/k_{\rm B}T}\alpha^\dagger_{\boldsymbol{k}_{\nu,\sigma}}\alpha_{\boldsymbol{k}_{\nu,\sigma}}\right]}{{\rm Tr}\left[e^{-\tilde{\varepsilon}'^{\rm SC}_{\boldsymbol{k}_{\nu,\sigma}}\alpha^\dagger_{\boldsymbol{k}_{\nu,\sigma}}\alpha_{\boldsymbol{k}_{\nu,\sigma}}/k_{\rm B}T}\right]}=\frac{1}{e^{\tilde{\varepsilon}'^{\rm SC}_{\boldsymbol{k}_{\nu,\sigma}}/k_{\rm B}T}-1}\equiv\tilde{n}'^{\rm SC}_{\boldsymbol{k}_{\nu,\sigma}},\tag{S28}$$

such self-consistent fields as to diagonalize $\widetilde{\mathcal{H}}'^{\rm SC}$ are expressed as

$$\begin{aligned}
\langle\mathcal{A}\rangle_T'^{\rm SC}&=\frac{JS}{N}\sum_{\nu=1}^{N}\left[\frac{7+2F_0+2F_0'\cos ak_\nu^z-2\mu/JS}{\tilde{\varepsilon}'^{\rm SC}_{(k_\nu^z,k_0^x)}}\left(\tilde{n}'^{\rm SC}_{(k_\nu^z,k_0^x)}+\frac{1}{2}\right)+\frac{11+4F_\pm+4F_\pm'\cos ak_\nu^z-4\mu/JS}{\tilde{\varepsilon}'^{\rm SC}_{(k_\nu^z,k_\pm^x)}}\left(\tilde{n}'^{\rm SC}_{(k_\nu^z,k_\pm^x)}+\frac{1}{2}\right)-\frac{1}{2JS}\right],\\
\langle\mathcal{B}_\sigma\rangle_T'^{\rm SC}&=\frac{JS}{N}\sum_{\nu=1}^{N}\left[\frac{-3+2G_0-2(2-G_0')\cos ak_\nu^z}{\tilde{\varepsilon}'^{\rm SC}_{(k_\nu^z,k_0^x)}}\left(\tilde{n}'^{\rm SC}_{(k_\nu^z,k_0^x)}+\frac{1}{2}\right)\cos a(k_\nu^z\delta_{\sigma,\parallel}+k_0^x\delta_{\sigma,\perp})+\frac{3+4G_0-4(2-G_0')\cos ak_\nu^z}{\tilde{\varepsilon}'^{\rm SC}_{(k_\nu^z,k_\pm^x)}}\right.\\
&\qquad\left.\times\left(\tilde{n}'^{\rm SC}_{(k_\nu^z,k_\pm^x)}+\frac{1}{2}\right)\cos a(k_\nu^z\delta_{\sigma,\parallel}+k_\pm^x\delta_{\sigma,\perp})\right],\\
\langle\mathcal{C}\rangle_T'^{\rm SC}&=\frac{JS}{N}\sum_{\nu=1}^{N}\left[\frac{-3+2G_0-2(2-G_0')\cos ak_\nu^z}{\tilde{\varepsilon}'^{\rm SC}_{(k_\nu^z,k_0^x)}}\left(\tilde{n}'^{\rm SC}_{(k_\nu^z,k_0^x)}+\frac{1}{2}\right)+\frac{3+4G_0-4(2-G_0')\cos ak_\nu^z}{\tilde{\varepsilon}'^{\rm SC}_{(k_\nu^z,k_\pm^x)}}\left(\tilde{n}'^{\rm SC}_{(k_\nu^z,k_\pm^x)}+\frac{1}{2}\right)\right],\\
\langle\mathcal{D}_\sigma\rangle_T'^{\rm SC}&=\frac{JS}{N}\sum_{\nu=1}^{N}\left[\frac{7+2F_0+2F_0'\cos ak_\nu^z-2\mu/JS}{\tilde{\varepsilon}'^{\rm SC}_{(k_\nu^z,k_0^x)}}\left(\tilde{n}'^{\rm SC}_{(k_\nu^z,k_0^x)}+\frac{1}{2}\right)\cos a(k_\nu^z\delta_{\sigma,\parallel}+k_0^x\delta_{\sigma,\perp})+\frac{11+4F_\pm+4F_\pm'\cos ak_\nu^z-4\mu/JS}{\tilde{\varepsilon}'^{\rm SC}_{(k_\nu^z,k_\pm^x)}}\right.\\
&\qquad\left.\times\left(\tilde{n}'^{\rm SC}_{(k_\nu^z,k_\pm^x)}+\frac{1}{2}\right)\cos a(k_\nu^z\delta_{\sigma,\parallel}+k_\pm^x\delta_{\sigma,\perp})-\frac{\cos a(k_\nu^z\delta_{\sigma,\parallel}+k_0^x\delta_{\sigma,\perp})+2\cos a(k_\nu^z\delta_{\sigma,\parallel}+k_\pm^x\delta_{\sigma,\perp})}{2JS}\right].
\end{aligned}\tag{S29}$$

At $T=0$, MHFISWs are no different from modified Wick-decomposition-based-interacting SWs (MWDISWs) [8, 9].

### S1.4. Double-constraint modification

SC MSWs in noncollinear antiferromagnets, whether MLSWs [Figs. 2(a1) and 2(a2)] or MWDISWs [Figs. 2(a1″) and 2(a2″)], are no longer so successful as those in collinear antiferromagnets [1, 9]. Before pointing out that they are in total ignorance of cubic anharmonicities, we may need to solve a more fundamental problem with them [7]. The Holstein-Primakoff-boson representation in the local spin reference frame (3) gives the correct spin magnitude but breaks the original spin rotational symmetry,

$$\begin{aligned}
\langle S^{\tilde{x}}_{\boldsymbol{r}_l}S^{\tilde{x}}_{\boldsymbol{r}_l}\rangle_T&=S\left(\frac{1}{2}+\langle\mathcal{A}\rangle_T+\langle\mathcal{C}\rangle_T\right)\\
&\quad-\left(\langle\mathcal{A}\rangle_T+\frac{\langle\mathcal{C}\rangle_T}{2}\right)\left(\frac{1}{2}+\langle\mathcal{A}\rangle_T+\langle\mathcal{C}\rangle_T\right)+O(S^{-1}),\\
\langle S^{\tilde{y}}_{\boldsymbol{r}_l}S^{\tilde{y}}_{\boldsymbol{r}_l}\rangle_T&=S\left(\frac{1}{2}+\langle\mathcal{A}\rangle_T-\langle\mathcal{C}\rangle_T\right)\\
&\quad-\left(\langle\mathcal{A}\rangle_T-\frac{\langle\mathcal{C}\rangle_T}{2}\right)\left(\frac{1}{2}+\langle\mathcal{A}\rangle_T-\langle\mathcal{C}\rangle_T\right)+O(S^{-1}),\\
\langle S^{\tilde{z}}_{\boldsymbol{r}_l}S^{\tilde{z}}_{\boldsymbol{r}_l}\rangle_T&=S^2-2S\langle\mathcal{A}\rangle_T+\langle\mathcal{A}\rangle_T+2\langle\mathcal{A}\rangle_T^2+\langle\mathcal{C}\rangle_T^2;\\
\sum_{\lambda=\tilde{x},\tilde{y},\tilde{z}}\langle S^\lambda_{\boldsymbol{r}_l}S^\lambda_{\boldsymbol{r}_l}\rangle_T&=\sum_{\lambda=x,y,z}\langle S^\lambda_{\boldsymbol{r}_l}S^\lambda_{\boldsymbol{r}_l}\rangle_T=S(S+1).
\end{aligned}\tag{S30}$$

For collinear antiferromagnets, $\langle\mathcal{C}\rangle_T$ spontaneously vanishes to retain a U(1) symmetry of each local spin operator in the rotating frame as well as the global U(1) symmetry related to the conservation of the total uniform magnetization

$$\sum_{l=1}^{L}S^z_{\boldsymbol{r}_l}=\sum_{l=1}^{L}\left(S^{\tilde{z}}_{\boldsymbol{r}_l}\cos\boldsymbol{Q}_{\rm X,K}\cdot\boldsymbol{r}_l-S^{\tilde{x}}_{\boldsymbol{r}_l}\sin\boldsymbol{Q}_{\rm X,K}\cdot\boldsymbol{r}_l\right).\tag{S31}$$

For noncollinear antiferromagnets, any bosonic Hamiltonian, even $\mathcal{H}_{\rm harm}$, no longer commutes with $\sum_{l=1}^{L}S^z_{\boldsymbol{r}_l}$, yet we should expect each spin operator to possess rotational symmetry about its local quantization axis $\tilde{z}$, which is met by demanding that $\langle S^{\tilde{x}}_{\boldsymbol{r}_l}S^{\tilde{x}}_{\boldsymbol{r}_l}\rangle_T=\langle S^{\tilde{y}}_{\boldsymbol{r}_l}S^{\tilde{y}}_{\boldsymbol{r}_l}\rangle_T$, i.e.,

$$\langle\mathcal{C}\rangle_T=\frac{\langle a^\dagger_{\boldsymbol{r}_l}a^\dagger_{\boldsymbol{r}_l}+a_{\boldsymbol{r}_l}a_{\boldsymbol{r}_l}\rangle_T}{2}=0.\tag{S32}$$

Constraining SC MSWs to (S32) as they are, i.e., together with (S19) or (S27), however, causes to increase their otherwise stable ground-state energy (cf. Fig. S1). In order to solve this composite problem, we diagonalize the LSW Hamiltonian subject to a double-constraint (DC) condition. Namely, the DC-MLSW Hamiltonian is diagonalized as

$$\begin{aligned}
&\mathcal{H}_{\rm harm}+\sum_{l=1}^{L}\left[\mu_l\left(S-\delta-a^\dagger_{\boldsymbol{r}_l}a_{\boldsymbol{r}_l}\right)+\eta_l\frac{a^\dagger_{\boldsymbol{r}_l}a^\dagger_{\boldsymbol{r}_l}+a_{\boldsymbol{r}_l}a_{\boldsymbol{r}_l}}{2}\right]\equiv\widetilde{\mathcal{H}}^{\rm DC}_{\rm harm}\\
&=\sum_{m=1}^{2}E^{(m)}+\mu L\left(S-\delta+\frac{1}{2}\right)+\sum_{\sigma=0,\pm}\sum_{\nu=1}^{N}\tilde{\varepsilon}^{\rm DC}_{\boldsymbol{k}_{\nu,\sigma}}\alpha^\dagger_{\boldsymbol{k}_{\nu,\sigma}}\alpha_{\boldsymbol{k}_{\nu,\sigma}};
\end{aligned}\tag{8}$$

$$E^{(2)} = -\frac{3}{2}LJS^2,\ E^{(1)} = -\frac{3}{2}LJS + \sum_{\sigma=0,\pm}\sum_{\nu=1}^{N}\frac{\tilde{\varepsilon}^{\rm DC}_{\boldsymbol{k}_{\nu,\sigma}}}{2},$$
$$\frac{\tilde{\varepsilon}^{\rm DC}_{(k^z_\nu,k^x_0)}}{JS} = \sqrt{2\left(1-\cos ak^z_\nu - \frac{\mu-\eta}{2JS}\right)\left(5+2\cos ak^z_\nu - \frac{\mu+\eta}{JS}\right)},$$
$$\frac{\tilde{\varepsilon}^{\rm DC}_{(k^z_\nu,k^x_\pm)}}{JS} = \sqrt{2\left(1+\cos ak^z_\nu - \frac{\mu+\eta}{2JS}\right)\left(\frac{7}{2}-2\cos ak^z_\nu - \frac{\mu-\eta}{JS}\right)} \tag{9}$$

via the Bogoliubov transformation

$$u_{(k^z_\nu,k^x_0)} = \sqrt{\frac{2\tilde{\varepsilon}^{\rm DC}_{(k^z_\nu,k^x_0)} + 7JS - 2\mu}{4\tilde{\varepsilon}^{\rm DC}_{(k^z_\nu,k^x_0)}}},$$
$$v_{(k^z_\nu,k^x_0)} = \frac{JS\,(4\cos ak^z_\nu + 3) - 2\eta}{\sqrt{4\tilde{\varepsilon}^{\rm DC}_{(k^z_\nu,k^x_0)}\left(2\tilde{\varepsilon}^{\rm DC}_{(k^z_\nu,k^x_0)} + 7JS - 2\mu\right)}},$$
$$u_{(k^z_\nu,k^x_\pm)} = \sqrt{\frac{4\tilde{\varepsilon}^{\rm DC}_{(k^z_\nu,k^x_\pm)} + 11JS - 4\mu}{8\tilde{\varepsilon}^{\rm DC}_{(k^z_\nu,k^x_\pm)}}},$$
$$v_{(k^z_\nu,k^x_\pm)} = \frac{JS\,(8\cos ak^z_\nu - 3) - 4\eta}{\sqrt{8\tilde{\varepsilon}^{\rm DC}_{(k^z_\nu,k^x_\pm)}\left(4\tilde{\varepsilon}^{\rm DC}_{(k^z_\nu,k^x_\pm)} + 11JS - 4\mu\right)}} \tag{S33}$$

on condition that

$$S - \langle a^\dagger_{\boldsymbol{r}_l}a_{\boldsymbol{r}_l}\rangle^{\rm DC}_0 = \delta,\ \langle a^\dagger_{\boldsymbol{r}_l}a^\dagger_{\boldsymbol{r}_l} + a_{\boldsymbol{r}_l}a_{\boldsymbol{r}_l}\rangle^{\rm DC}_0 = 0 \tag{S34}$$

with $\delta$ serving to optimize the ground-state energy and $\langle\cdots\rangle^{\rm DC}_0$ denoting a quantum average in the thus-obtained DC-MLSW ground state. By tuning $\delta$, we can retain the local U(1) symmetry with the SC-MLSW ground-state energy remaining almost the same, as will be demonstrated later in Sect. S3.

## S2. GREEN'S FUNCTION FORMALISM

Let us introduce Feynman's time-ordered Greens functions of Bogoliubov quasiparticles and spin operators,

$$G^{\sigma\sigma'}(\boldsymbol{k};\omega+i\epsilon) \equiv -i\int_{-\infty}^{\infty}\left\langle \mathcal{T}\,\alpha^{\sigma}_{-\sigma\boldsymbol{k}}(t)\alpha^{\sigma'}_{\sigma'\boldsymbol{k}}\right\rangle e^{i[\omega+i\epsilon\sigma(t)]t}dt, \tag{S35}$$
$$\mathcal{G}^{\lambda\lambda'}(\boldsymbol{q};\omega+i\epsilon) \equiv -i\int_{-\infty}^{\infty}\left\langle \mathcal{T}\delta S^{\lambda}_{\boldsymbol{q}}(t)\delta S^{\lambda'}_{-\boldsymbol{q}}\right\rangle e^{i[\omega+i\epsilon\sigma(t)]t}dt, \tag{S36}$$

where $\mathcal{P}(t) \equiv e^{i\widetilde{\mathcal{H}}t/\hbar}\mathcal{P}e^{-i\widetilde{\mathcal{H}}t/\hbar}$ and $\langle Q\rangle$ represent time evolution driven by $\widetilde{\mathcal{H}}$ and a quantum average in the ground state of $\widetilde{\mathcal{H}}$, respectively, with $\widetilde{\mathcal{H}}$ being a modified PSW (MPSW) Hamiltonian, $\widetilde{\mathcal{H}}^{\rm SC}_{\rm harm} + \mathcal{V}$ or $\widetilde{\mathcal{H}}^{\rm DC}_{\rm harm} + \mathcal{V}$, while $\alpha^-_{\boldsymbol{k}} \equiv \alpha_{\boldsymbol{k}}$ and $\alpha^+_{\boldsymbol{k}} \equiv \alpha^\dagger_{\boldsymbol{k}}$ are the annihilation and creation operators, respectively, for the corresponding harmonic Hamiltonian $\widetilde{\mathcal{H}}^{\rm SC}_{\rm harm}$ or $\widetilde{\mathcal{H}}^{\rm DC}_{\rm harm}$. $\mathcal{T}$ and $\epsilon$ shall signify time ordering operation and a positive infinitesimal value, respectively, with $\sigma(t) = 2\theta(t) - 1$. Let $\widetilde{E}_n$ and $|n\rangle$ be the eigenvalues and eigenstates of $\mathcal{H}$, $\widetilde{\mathcal{H}}|n\rangle = \widetilde{E}_n|n\rangle$ $\left(\widetilde{E}_0 \le \widetilde{E}_1 \le \widetilde{E}_2 \le \cdots\right)$. We shall express Green's functions of different types in terms of a Lehmann representation [10, 11] in the purpose of finding an identity among them. When we consider bare magnon Green's functions replacing $\widetilde{\mathcal{H}}$ by its harmonic part $\widetilde{\mathcal{H}}_{\rm harm}$, we use $G_0$, $\mathcal{G}_0$, $\mathcal{P}(t)^{\rm harm} \equiv e^{i\widetilde{\mathcal{H}}_{\rm harm}t/\hbar}\mathcal{P}e^{-i\widetilde{\mathcal{H}}_{\rm harm}t/\hbar}$, and $\langle Q\rangle_0$ instead of $G$, $\mathcal{G}$, $\mathcal{P}(t)$, and $\langle Q\rangle$, respectively, where we let $\tilde{\varepsilon}_{\boldsymbol{k}_{\nu,\sigma}}$ be either $\tilde{\varepsilon}^{\rm SC}_{\boldsymbol{k}_{\nu,\sigma}}$ (7) or $\tilde{\varepsilon}^{\rm DC}_{\boldsymbol{k}_{\nu,\sigma}}$ (9). Note that the anomalous bare Green's functions $G^{++}_0$ and $G^{--}_0$ are trivially zero.

### S2.1. Spectral function $A(\boldsymbol{k},\omega)$

The ground-state spectral function $A(\boldsymbol{k},\omega)$ is calculated via the magnon Green's function (S35), which is readily obtainable in the harmonic approximation as

$$G^{-+}_0(\boldsymbol{k};\omega+i\epsilon) = -i\int_{-\infty}^{\infty}\left\langle \mathcal{T}\alpha_{\boldsymbol{k}}(t)^{\rm harm}\alpha^\dagger_{\boldsymbol{k}}\right\rangle_0 e^{i[\omega+i\epsilon\sigma(t)]t}dt = -i\int_0^{\infty}\left\langle \alpha_{\boldsymbol{k}}\alpha^\dagger_{\boldsymbol{k}}\right\rangle_0 e^{i(\omega-\tilde{\varepsilon}_{\boldsymbol{k}}/\hbar+i\epsilon)t}dt = \frac{\hbar}{\hbar\omega - \tilde{\varepsilon}_{\boldsymbol{k}} + i\hbar\epsilon} \tag{S37}$$

and generally written in the interaction picture as [11]

$$G^{-+}(\boldsymbol{k};\omega+i\epsilon) = G^{-+}_0(\boldsymbol{k};\omega+i\epsilon) - i\sum_{l=1}^{\infty}\frac{(-i)^l}{l!\hbar^l}\int_{-\infty}^{\infty}dt_1\cdots\int_{-\infty}^{\infty}dt_l\int_{-\infty}^{\infty}\left\langle \mathcal{T}\mathcal{V}(t_1)^{\rm harm}\cdots\mathcal{V}(t_l)^{\rm harm}\alpha_{\boldsymbol{k}}(t)^{\rm harm}\alpha^\dagger_{\boldsymbol{k}}\right\rangle_0 e^{i[\omega+i\epsilon\sigma(t)]t}dt. \tag{S38}$$

Calculation of (S38) starts with expressing $\mathcal{V}$ as well as $\widetilde{\mathcal{H}}_{\rm harm}$ in terms of Bogoliubov bosons,

$$\mathcal{H}^{(\frac{1}{2})} = \sum_{\sigma=0,\pm}\sum_{\nu=1}^{N}\sum_{\sigma'=0,\pm}\sum_{\nu'=1}^{N}\Big[\Lambda_{++-}(\boldsymbol{k}_{\nu,\sigma},\boldsymbol{k}_{\nu',\sigma'}-\boldsymbol{k}_{\nu,\sigma},\boldsymbol{k}_{\nu',\sigma'})\,\alpha^\dagger_{\boldsymbol{k}_{\nu,\sigma}}\alpha^\dagger_{\boldsymbol{k}_{\nu',\sigma'}-\boldsymbol{k}_{\nu,\sigma}}\alpha_{\boldsymbol{k}_{\nu',\sigma'}}$$
$$+\Lambda_{+++}(\boldsymbol{k}_{\nu,\sigma},-\boldsymbol{k}_{\nu',\sigma'}-\boldsymbol{k}_{\nu,\sigma},\boldsymbol{k}_{\nu',\sigma'})\,\alpha^\dagger_{\boldsymbol{k}_{\nu,\sigma}}\alpha^\dagger_{-\boldsymbol{k}_{\nu,\sigma}-\boldsymbol{k}_{\nu',\sigma'}}\alpha^\dagger_{\boldsymbol{k}_{\nu',\sigma'}} + \text{H.c.}\Big], \tag{S39}$$

$$\mathcal{H}^{(0)} = \delta E_1^{(0)} + \sum_{\sigma=0,\pm}\sum_{\nu=1}^{N}\left\{\Lambda_{+-}\left(\boldsymbol{k}_{\nu,\sigma},\boldsymbol{k}_{\nu,\sigma}\right)\alpha^{\dagger}_{\boldsymbol{k}_{\nu,\sigma}}\alpha_{\boldsymbol{k}_{\nu,\sigma}} + \left[\Lambda_{++}\left(\boldsymbol{k}_{\nu,\sigma},-\boldsymbol{k}_{\nu,\sigma}\right)\alpha^{\dagger}_{\boldsymbol{k}_{\nu,\sigma}}\alpha^{\dagger}_{-\boldsymbol{k}_{\nu,\sigma}} + \text{H.c.}\right]\right\}$$
$$+ \sum_{\sigma=0,\pm}\sum_{\nu=1}^{N}\sum_{\sigma'=0,\pm}\sum_{\nu'=1}^{N}\sum_{\sigma''=0,\pm}\sum_{\nu''=1}^{N}\left\{\Lambda_{++--}\left(\boldsymbol{k}_{\nu,\sigma},\boldsymbol{k}_{\nu',\sigma'},\boldsymbol{k}_{\nu,\sigma}+\boldsymbol{k}_{\nu'',\sigma''},\boldsymbol{k}_{\nu',\sigma'}-\boldsymbol{k}_{\nu'',\sigma''}\right)\alpha^{\dagger}_{\boldsymbol{k}_{\nu,\sigma}}\alpha^{\dagger}_{\boldsymbol{k}_{\nu',\sigma'}}\alpha_{\boldsymbol{k}_{\nu,\sigma}+\boldsymbol{k}_{\nu'',\sigma''}}\alpha_{\boldsymbol{k}_{\nu',\sigma'}-\boldsymbol{k}_{\nu'',\sigma''}}\right.$$
$$+\left[\Lambda_{+++-}\left(\boldsymbol{k}_{\nu,\sigma},\boldsymbol{k}_{\nu',\sigma'},-\boldsymbol{k}_{\nu,\sigma}+\boldsymbol{k}_{\nu'',\sigma''},\boldsymbol{k}_{\nu',\sigma'}+\boldsymbol{k}_{\nu'',\sigma''}\right)\alpha^{\dagger}_{\boldsymbol{k}_{\nu,\sigma}}\alpha^{\dagger}_{\boldsymbol{k}_{\nu',\sigma'}}\alpha^{\dagger}_{-\boldsymbol{k}_{\nu,\sigma}+\boldsymbol{k}_{\nu'',\sigma''}}\alpha_{\boldsymbol{k}_{\nu',\sigma'}+\boldsymbol{k}_{\nu'',\sigma''}}\right.$$
$$\left.\left.+\Lambda_{++++}\left(\boldsymbol{k}_{\nu,\sigma},\boldsymbol{k}_{\nu',\sigma'},-\boldsymbol{k}_{\nu,\sigma}-\boldsymbol{k}_{\nu'',\sigma''},-\boldsymbol{k}_{\nu',\sigma'}+\boldsymbol{k}_{\nu'',\sigma''}\right)\alpha^{\dagger}_{\boldsymbol{k}_{\nu,\sigma}}\alpha^{\dagger}_{\boldsymbol{k}_{\nu',\sigma'}}\alpha^{\dagger}_{-\boldsymbol{k}_{\nu,\sigma}-\boldsymbol{k}_{\nu'',\sigma''}}\alpha^{\dagger}_{-\boldsymbol{k}_{\nu',\sigma'}+\boldsymbol{k}_{\nu'',\sigma''}} + \text{H.c.}\right]\right\}, \quad \text{(S40)}$$

where the ground-state energy correction $\delta E_1^{(0)} \equiv \langle\mathcal{H}^{(0)}\rangle_0$ and vertex functions $\Lambda_{++-}$ and $\Lambda_{+++}$ in (S39) and $\Lambda_{+-}$, $\Lambda_{++}$, $\Lambda_{++--}$, $\Lambda_{+++-}$, and $\Lambda_{++++}$ in (S40) are all written in terms of the MLSW ground-state Bogoliubov parameters $u_{\boldsymbol{k}_{\nu,\sigma}}$ and $v_{\boldsymbol{k}_{\nu,\sigma}}$. By virtue of Wick's theorem [12], we can rewrite (S38) into a series in $G_0^{-+}$ and $\mathcal{V}$. In the spirit of the $1/S$ expansion, we renormalize the bare magnon Green's function by the lowest-order $O(S^0)$ corrections arising at $l=1$, to first order in $\mathcal{H}^{(0)}$, and at $l=2$, to second order in $\mathcal{H}^{(\frac{1}{2})}$,

$$G^{-+}(\boldsymbol{k};\omega+i\epsilon) = G_0^{-+}(\boldsymbol{k};\omega+i\epsilon) - \frac{1}{\hbar}\int_{-\infty}^{\infty}dt_1\int_{-\infty}^{\infty}\left\langle\mathcal{T}\mathcal{H}^{(0)}(t_1)^{\text{harm}}\alpha_{\boldsymbol{k}}(t)^{\text{harm}}\alpha^{\dagger}_{\boldsymbol{k}}\right\rangle_0 e^{i[\omega+i\epsilon\sigma(t)]t}dt + \frac{i}{2!\hbar^2}$$
$$\times\int_{-\infty}^{\infty}dt_1\int_{-\infty}^{\infty}dt_2\int_{-\infty}^{\infty}\left\langle\mathcal{T}\mathcal{H}^{(\frac{1}{2})}(t_1)^{\text{harm}}\mathcal{H}^{(\frac{1}{2})}(t_2)^{\text{harm}}\alpha_{\boldsymbol{k}}(t)^{\text{harm}}\alpha^{\dagger}_{\boldsymbol{k}}\right\rangle_0 e^{i[\omega+i\epsilon\sigma(t)]t}dt + \cdots$$
$$= G_0^{-+}(\boldsymbol{k};\omega+i\epsilon) + G_0^{-+}(\boldsymbol{k};\omega+i\epsilon)\,\frac{\Sigma_1^{(0)}(\boldsymbol{k})+\Sigma_2^{(0)}(\boldsymbol{k};\omega+i\epsilon)}{\hbar}G_0^{-+}(\boldsymbol{k};\omega+i\epsilon) + \cdots$$
$$\simeq G_0^{-+}(\boldsymbol{k};\omega+i\epsilon)\sum_{l=0}^{\infty}\left[\frac{\Sigma_1^{(0)}(\boldsymbol{k})+\Sigma_2^{(0)}(\boldsymbol{k};\omega+i\epsilon)}{\hbar}G_0^{-+}(\boldsymbol{k};\omega+i\epsilon)\right]^l = G_0^{-+}(\boldsymbol{k};\omega+i\epsilon)\left[1+\frac{\Sigma^{(0)}(\boldsymbol{k};\omega+i\epsilon)}{\hbar}G^{-+}(\boldsymbol{k};\omega+i\epsilon)\right], \quad \text{(S41)}$$

where the primary self-energies $\Sigma^{(0)}(\boldsymbol{k};\omega+i\epsilon) \equiv \Sigma_1^{(0)}(\boldsymbol{k}) + \Sigma_2^{(0)}(\boldsymbol{k};\omega+i\epsilon)$ are given by

$$\Sigma_1^{(0)}(\boldsymbol{k}) = \Lambda_{+-}(\boldsymbol{k},\boldsymbol{k}),\ \Sigma_2^{(0)}(\boldsymbol{k};\omega+i\epsilon) = \sum_{\sigma=0,\pm}\sum_{\nu=1}^{N}\frac{2|\Lambda_{++-}(\boldsymbol{k},\boldsymbol{k}_{\nu,\sigma}-\boldsymbol{k},\boldsymbol{k}_{\nu,\sigma})|^2}{\hbar\omega-\tilde{\varepsilon}_{\boldsymbol{k}_{\nu,\sigma}}-\tilde{\varepsilon}_{\boldsymbol{k}-\boldsymbol{k}_{\nu,\sigma}}+i\hbar\epsilon} - \sum_{\sigma=0,\pm}\sum_{\nu=1}^{N}\frac{18|\Lambda_{+++}(\boldsymbol{k},-\boldsymbol{k}_{\nu,\sigma}-\boldsymbol{k},\boldsymbol{k}_{\nu,\sigma})|^2}{\hbar\omega+\tilde{\varepsilon}_{\boldsymbol{k}_{\nu,\sigma}}+\tilde{\varepsilon}_{\boldsymbol{k}+\boldsymbol{k}_{\nu,\sigma}}+i\hbar\epsilon}. \quad \text{(S42)}$$

$\Sigma_1^{(0)}(\boldsymbol{k})$ has no frequency dependence and therefore no imaginary part, $\Sigma_1^{(0)}(\boldsymbol{k}) = \bar{\Sigma}_1^{(0)}(\boldsymbol{k})$. $\Sigma_2^{(0)}(\boldsymbol{k};\omega+i\epsilon)$ may have both real and imaginary parts, which we shall denote by $\bar{\Sigma}_2^{(0)}(\boldsymbol{k};\omega+i\epsilon)$ and $\bar{\bar{\Sigma}}_2^{(0)}(\boldsymbol{k};\omega+i\epsilon)$, respectively. The Dyson formulation (S41) gives

$$G^{-+}(\boldsymbol{k};\omega+i\epsilon) = \frac{1}{\left[G_0^{-+}(\boldsymbol{k};\omega+i\epsilon)\right]^{-1} - \Sigma^{(0)}(\boldsymbol{k};\omega+i\epsilon)/\hbar + i\epsilon} = \frac{\hbar}{\hbar\omega-\tilde{\varepsilon}_{\boldsymbol{k}}-\Sigma^{(0)}(\boldsymbol{k};\omega+i\epsilon)+i\hbar\epsilon}. \quad \text{(S43)}$$

The bare and renormalized spectral functions

$$A(\boldsymbol{k},\omega) = \begin{cases} -\frac{1}{\pi\hbar}\text{Im}\left[G_0^{-+}(\boldsymbol{k};\omega+i\epsilon)\right] = -\frac{1}{\pi}\text{Im}\frac{1}{\hbar\omega-\tilde{\varepsilon}_{\boldsymbol{k}}+i\hbar\epsilon} = \delta(\hbar\omega-\tilde{\varepsilon}_{\boldsymbol{k}}) & \text{(MLSW)} \\ -\frac{1}{\pi\hbar}\text{Im}\left[G^{-+}(\boldsymbol{k};\omega+i\epsilon)\right] = -\frac{1}{\pi}\text{Im}\frac{1}{\hbar\omega-\tilde{\varepsilon}_{\boldsymbol{k}}-\Sigma^{(0)}(\boldsymbol{k};\omega+i\epsilon)+i\hbar\epsilon} & \text{(MPSW)} \end{cases} \quad (10)$$

are calculated in the SC and DC schemes and explicitly compared with each other as well as with MLSW pair-excitation continua later in Sect. S3.

### S2.2. Dynamic spin structure factor $S(\boldsymbol{q},\omega)$

The dynamic spin structure factors at temperature $T$

$$S^{\lambda\lambda'}(\boldsymbol{q},\omega) \equiv \frac{1}{2\pi\hbar}\int_{-\infty}^{\infty}\frac{\text{Tr}\left\{e^{-\widetilde{\mathcal{H}}/k_BT}\left[\delta S^{\lambda}_{\boldsymbol{q}}(t)\delta S^{\lambda'}_{-\boldsymbol{q}}\right]\right\}}{\text{Tr}\left\{e^{-\widetilde{\mathcal{H}}/k_BT}\right\}}e^{i\omega t}dt = \sum_{l,l'=1}^{L}\frac{e^{i\boldsymbol{q}\cdot(\boldsymbol{r}_l-\boldsymbol{r}_{l'})}}{2\pi\hbar L}\int_{-\infty}^{\infty}\frac{\text{Tr}\left\{e^{-\widetilde{\mathcal{H}}/k_BT}\left[\delta S^{\lambda}_{\boldsymbol{r}_l}(t)\delta S^{\lambda'}_{\boldsymbol{r}_{l'}}\right]\right\}}{\text{Tr}\left\{e^{-\widetilde{\mathcal{H}}/k_BT}\right\}}e^{i\omega t}dt \quad \text{(S44)}$$

are calculated via the retarded Green's functions

$$\mathcal{R}^{\lambda\lambda'}(\boldsymbol{q};\omega+i\epsilon)\equiv -i\int_{-\infty}^{\infty}\frac{\mathrm{Tr}\left\{e^{-\widetilde{\mathcal{H}}/k_{\mathrm{B}}T}\left[\delta S^{\lambda}_{\boldsymbol{q}}(t),\delta S^{\lambda'}_{-\boldsymbol{q}}\right]\right\}}{\mathrm{Tr}\left\{e^{-\widetilde{\mathcal{H}}/k_{\mathrm{B}}T}\right\}}e^{i(\omega+i\epsilon)t}\theta(t)dt. \tag{S45}$$

The fluctuation-dissipation theorem says that [13]

$$S^{\lambda\lambda'}(\boldsymbol{q},\omega)=-\frac{1}{\pi\hbar}\frac{1}{1-e^{-\hbar\omega/k_{\mathrm{B}}T}}\mathrm{Im}\left[\mathcal{R}^{\lambda\lambda'}(\boldsymbol{q};\omega+i\epsilon)\right]\overset{T\to 0}{\longrightarrow}\begin{cases}-\frac{1}{\pi\hbar}\lim\limits_{T\to 0}\mathrm{Im}\left[\mathcal{R}^{\lambda\lambda'}(\boldsymbol{q};\omega+i\epsilon)\right] & (\omega>0)\\ 0 & (\omega<0)\end{cases}. \tag{S46}$$

In terms of a Lehmann representation, the retarded correlator (S45) reads

$$\lim_{T\to 0}\mathcal{R}^{\lambda\lambda'}(\boldsymbol{q};\omega+i\epsilon)=-i\int_{-\infty}^{\infty}\left\langle\left[\delta S^{\lambda}_{\boldsymbol{q}}(t),\delta S^{\lambda'}_{-\boldsymbol{q}}\right]\right\rangle e^{i(\omega+i\epsilon)t}\theta(t)dt=-\sum_{n=0}^{\infty}\left[\frac{\langle 0|\delta S^{\lambda}_{\boldsymbol{q}}|n\rangle\langle n|\delta S^{\lambda'}_{-\boldsymbol{q}}|0\rangle}{\omega-\left(\widetilde{E}_n-\widetilde{E}_0\right)/\hbar+i\epsilon}-\frac{\langle 0|\delta S^{\lambda'}_{-\boldsymbol{q}}|n\rangle\langle n|\delta S^{\lambda}_{\boldsymbol{q}}|0\rangle}{\omega+\left(\widetilde{E}_n-\widetilde{E}_0\right)/\hbar+i\epsilon}\right], \tag{S47}$$

while the usual Feynman correlator (S36) evaluates to

$$\mathcal{G}^{\lambda\lambda'}(\boldsymbol{q};\omega+i\epsilon)=-i\int_{-\infty}^{\infty}\left\langle\mathcal{T}\delta S^{\lambda}_{\boldsymbol{q}}(t)\delta S^{\lambda'}_{-\boldsymbol{q}}\right\rangle e^{i[\omega+i\epsilon\sigma(t)]t}dt=-\sum_{\kappa=0}^{\infty}\left[\frac{\langle 0|\delta S^{\lambda}_{\boldsymbol{q}}|n\rangle\langle n|\delta S^{\lambda'}_{-\boldsymbol{q}}|0\rangle}{\omega-\left(\widetilde{E}_n-\widetilde{E}_0\right)/\hbar+i\epsilon}-\frac{\langle 0|\delta S^{\lambda'}_{-\boldsymbol{q}}|n\rangle\langle n|\delta S^{\lambda}_{\boldsymbol{q}}|0\rangle}{\omega+\left(\widetilde{E}_n-\widetilde{E}_0\right)/\hbar-i\epsilon}\right]. \tag{S48}$$

Having in mind that

$$\frac{1}{\omega+\left(\widetilde{E}_n-\widetilde{E}_0\right)/\hbar\pm i\epsilon}=\frac{\mathcal{P}}{\omega+\left(\widetilde{E}_n-\widetilde{E}_0\right)/\hbar}\mp i\pi\delta\left(\omega+\frac{\widetilde{E}_n-\widetilde{E}_0}{\hbar}\right) \tag{S49}$$

with $\mathcal{P}$ denoting the principal value and $\omega+\left(\widetilde{E}_n-\widetilde{E}_0\right)/\hbar>0$ for $\omega>0$, we learn that

$$S^{\lambda\lambda'}(\boldsymbol{q},\omega)=-\frac{1}{\pi\hbar}\mathrm{Im}\left[\mathcal{G}^{\lambda\lambda'}(\boldsymbol{q};\omega+i\epsilon)\right]\ (T\to 0). \tag{S50}$$

Similar to (S17), we can construct the dynamic structure factors in the laboratory frame from those in the rotating frame,

$$\begin{aligned}S^{zz}(\boldsymbol{q},\omega)=S^{xx}(\boldsymbol{q},\omega)&=\frac{1}{4}\sum_{\tau=\pm}\left\{S^{\tilde{z}\tilde{z}}(\tau\boldsymbol{Q}_{\mathrm{X,K}}+\boldsymbol{q},\omega)+S^{\tilde{x}\tilde{x}}(\tau\boldsymbol{Q}_{\mathrm{X,K}}+\boldsymbol{q},\omega)+i\tau\left[S^{\tilde{z}\tilde{x}}(\tau\boldsymbol{Q}_{\mathrm{X,K}}+\boldsymbol{q},\omega)-S^{\tilde{x}\tilde{z}}(\tau\boldsymbol{Q}_{\mathrm{X,K}}+\boldsymbol{q},\omega)\right]\right\}\\&=-\frac{1}{4\pi\hbar}\sum_{\tau=\pm}\mathrm{Im}\left\{\mathcal{G}^{\tilde{z}\tilde{z}}(\tau\boldsymbol{Q}_{\mathrm{X,K}}+\boldsymbol{q};\omega+i\epsilon)+\mathcal{G}^{\tilde{x}\tilde{x}}(\tau\boldsymbol{Q}_{\mathrm{X,K}}+\boldsymbol{q};\omega+i\epsilon)+\tau\left[\mathcal{G}^{\tilde{z}\tilde{x}}(\tau\boldsymbol{Q}_{\mathrm{X,K}}+\boldsymbol{q};\omega+i\epsilon)-\mathcal{G}^{\tilde{x}\tilde{z}}(\tau\boldsymbol{Q}_{\mathrm{X,K}}+\boldsymbol{q};\omega+i\epsilon)\right]\right\}\\S^{yy}(\boldsymbol{q},\omega)=S^{\tilde{y}\tilde{y}}(\boldsymbol{q},\omega)&=-\frac{1}{\pi\hbar}\mathrm{Im}\left[\mathcal{G}^{\tilde{y}\tilde{y}}(\boldsymbol{q};\omega+i\epsilon)\right].\end{aligned} \tag{S51}$$

First we investigate leading transverse fluctuations in (S51). Let us approximate on-site cubic terms as

$$a^{\dagger}_{\boldsymbol{r}_l}a^{\dagger}_{\boldsymbol{r}_l}a_{\boldsymbol{r}_l}\simeq 2\langle\mathcal{A}\rangle_0 a^{\dagger}_{\boldsymbol{r}_l}+\langle C\rangle_0 a_{\boldsymbol{r}_l};\ \langle a^{\dagger}_{\boldsymbol{r}_l}a_{\boldsymbol{r}_l}\rangle_0\equiv\langle\mathcal{A}\rangle_0=\sum_{\sigma=0,\pm}\sum_{\nu=1}^{N}\frac{u^2_{\boldsymbol{k}_{\nu,\sigma}}+v^2_{\boldsymbol{k}_{\nu,\sigma}}-1}{2L},\ \langle a^{\dagger}_{\boldsymbol{r}_l}a^{\dagger}_{\boldsymbol{r}_l}\rangle_0\equiv\langle C\rangle_0=\sum_{\sigma=0,\pm}\sum_{\nu=1}^{N}\frac{u_{\boldsymbol{k}_{\nu,\sigma}}v_{\boldsymbol{k}_{\nu,\sigma}}}{L} \tag{S52}$$

to write the relevant spin operators as

$$S^{\tilde{x}}_{\boldsymbol{r}_l}=\sqrt{\frac{S}{2}}\left[1-\frac{2\langle\mathcal{A}\rangle_0+\langle C\rangle_0}{4S}\right]\left(a_{\boldsymbol{r}_l}+a^{\dagger}_{\boldsymbol{r}_l}\right)+O\left(S^{-\frac{3}{2}}\right),\ S^{\tilde{y}}_{\boldsymbol{r}_l}=-i\sqrt{\frac{S}{2}}\left[1-\frac{2\langle\mathcal{A}\rangle_0-\langle C\rangle_0}{4S}\right]\left(a_{\boldsymbol{r}_l}-a^{\dagger}_{\boldsymbol{r}_l}\right)+O\left(S^{-\frac{3}{2}}\right). \tag{S53}$$

Via the Fourier transformation (S9) and (S10), we can express spin Green's functions in terms of the magnon language,

$$\begin{aligned}\mathcal{G}^{\tilde{x}\tilde{x}}(\boldsymbol{k};\omega+i\epsilon)&=\frac{S}{2}\left[1-\frac{2\langle\mathcal{A}\rangle_0+\langle C\rangle_0}{4S}\right]^2(u_{\boldsymbol{k}}+v_{\boldsymbol{k}})^2\left[G^{-+}(\boldsymbol{k};\omega+i\epsilon)+G^{-+}(-\boldsymbol{k};-\omega-i\epsilon)+G^{++}(\boldsymbol{k};\omega+i\epsilon)+G^{--}(\boldsymbol{k};\omega+i\epsilon)\right]\\&\simeq\frac{S}{2}\left[1-\frac{2\langle\mathcal{A}\rangle_0+\langle C\rangle_0}{2S}\right](u_{\boldsymbol{k}}+v_{\boldsymbol{k}})^2G^{-+}(\boldsymbol{k};\omega+i\epsilon),\end{aligned} \tag{S54}$$

$$\mathcal{G}^{\tilde{y}\tilde{y}}(\boldsymbol{k};\omega+i\epsilon)=\frac{S}{2}\left[1-\frac{2\langle\mathcal{A}\rangle_0-\langle C\rangle_0}{4S}\right]^2(u_{\boldsymbol{k}}-v_{\boldsymbol{k}})^2\left[G^{-+}(\boldsymbol{k};\omega+i\epsilon)+G^{-+}(-\boldsymbol{k};-\omega-i\epsilon)-G^{++}(\boldsymbol{k};\omega+i\epsilon)-G^{--}(\boldsymbol{k};\omega+i\epsilon)\right]$$
$$\simeq\frac{S}{2}\left[1-\frac{2\langle\mathcal{A}\rangle_0-\langle C\rangle_0}{2S}\right](u_{\boldsymbol{k}}-v_{\boldsymbol{k}})^2\,G^{-+}(\boldsymbol{k};\omega+i\epsilon),\tag{S55}$$

where the terms $G^{-+}(-\boldsymbol{k},-\omega-i\epsilon)$ have no pole for $\omega>0$ and therefore no contribution to the dynamic structure factor, while compared to the normal Green's functions $G^{-+}(\boldsymbol{k};\omega+i\epsilon)$ of $O(S^{-1})$ [cf. (S43)], the anomalous Green's functions

$$G^{\sigma\sigma}(\boldsymbol{k};\omega+i\epsilon)=-i\sum_{l=1}^{\infty}\frac{(-i)^l}{l!\hbar^l}\int_{-\infty}^{\infty}dt_1\cdots\int_{-\infty}^{\infty}dt_l\int_{-\infty}^{\infty}\left\langle\mathcal{T}\mathcal{V}(t_1)^{\rm harm}\cdots\mathcal{V}(t_l)^{\rm harm}\alpha^{\sigma}_{-\sigma\boldsymbol{k}}(t)^{\rm harm}\alpha^{\sigma}_{\sigma\boldsymbol{k}}\right\rangle_0 e^{i[\omega+i\epsilon\sigma(t)]t}dt$$
$$=-\frac{1}{\hbar}\int_{-\infty}^{\infty}dt_1\int_{-\infty}^{\infty}\left\langle\mathcal{T}\mathcal{H}^{(0)}(t_1)^{\rm harm}\alpha^{\sigma}_{-\sigma\boldsymbol{k}}(t)^{\rm harm}\alpha^{\sigma}_{\sigma\boldsymbol{k}}\right\rangle_0 e^{i[\omega+i\epsilon\sigma(t)]t}dt+\frac{i}{2!\hbar^2}$$
$$\times\int_{-\infty}^{\infty}dt_1\int_{-\infty}^{\infty}dt_2\int_{-\infty}^{\infty}\left\langle\mathcal{T}\mathcal{H}^{(\frac{1}{2})}(t_1)^{\rm harm}\mathcal{H}^{(\frac{1}{2})}(t_2)^{\rm harm}\alpha^{\sigma}_{-\sigma\boldsymbol{k}}(t)^{\rm harm}\alpha^{\sigma}_{\sigma\boldsymbol{k}}\right\rangle_0 e^{i[\omega+i\epsilon\sigma(t)]t}dt+\cdots$$
$$\simeq G^{-+}(\boldsymbol{k};\omega+i\epsilon)\frac{\Sigma_1'^{(0)}(\boldsymbol{k})+\Sigma_2'^{(0)}(\boldsymbol{k};\omega+i\epsilon)}{\hbar}G^{-+}(-\boldsymbol{k};-\omega-i\epsilon);\tag{S56}$$

$$\Sigma_1'^{(0)}(\boldsymbol{k})\equiv\Lambda_{++}(\boldsymbol{k},-\boldsymbol{k}),\ \Sigma_2'^{(0)}(\boldsymbol{k};\omega+i\epsilon)\equiv 6\sum_{\sigma=0,\pm}\sum_{\nu=1}^{N}$$
$$\times\left[\frac{\Lambda_{+++}(-\boldsymbol{k},\boldsymbol{k}-\boldsymbol{k}_{\nu,\sigma},\boldsymbol{k}_{\nu,\sigma})\,\Lambda_{++-}(\boldsymbol{k}-\boldsymbol{k}_{\nu,\sigma},\boldsymbol{k}_{\nu,\sigma},\boldsymbol{k})^*}{\hbar\omega-\tilde{\varepsilon}_{\boldsymbol{k}_{\nu,\sigma}}-\tilde{\varepsilon}_{\boldsymbol{k}-\boldsymbol{k}_{\nu,\sigma}}+i\hbar\epsilon}-\frac{\Lambda_{+++}(\boldsymbol{k},-\boldsymbol{k}-\boldsymbol{k}_{\nu,\sigma},\boldsymbol{k}_{\nu,\sigma})\,\Lambda_{++-}(-\boldsymbol{k}-\boldsymbol{k}_{\nu,\sigma},\boldsymbol{k}_{\nu,\sigma},-\boldsymbol{k})^*}{\hbar\omega+\tilde{\varepsilon}_{\boldsymbol{k}_{\nu,\sigma}}+\tilde{\varepsilon}_{\boldsymbol{k}+\boldsymbol{k}_{\nu,\sigma}}+i\hbar\epsilon}\right],\tag{S57}$$

evaluate to $O(S^{-2})$ and are therefore discarded in the spirit of the $1/S$ expansion. $\Sigma_1'^{(0)}$, to first order in $\mathcal{H}^{(0)}$, and $\Sigma_2'^{(0)}$, to second order in $\mathcal{H}^{(\frac{1}{2})}$, both on the order of $S^0$, play a similar role to that played by the usual self-energies $\Sigma_1^{(0)}$ and $\Sigma_2^{(0)}$ but with a change in the number of quasiparticles.

Next we figure out leading longitudinal fluctuations in (S51). MLSWs contribute

$$\mathcal{G}_0^{\tilde{z}\tilde{z}}(\boldsymbol{k};\omega+i\epsilon)=-i\int_{-\infty}^{\infty}\left\langle\mathcal{T}\delta S^{\tilde{z}}_{\boldsymbol{k}}(t)^{\rm harm}\delta S^{\tilde{z}}_{-\boldsymbol{k}}\right\rangle_0 e^{i[\omega+i\epsilon\sigma(t)]t}dt=-\frac{i}{L}\sum_{\sigma=0,\pm}\sum_{\nu=1}^{N}\sum_{\sigma'=0,\pm}\sum_{\nu'=1}^{N}$$
$$\times\int_{-\infty}^{\infty}\Big\{v_{\boldsymbol{k}_{\nu,\sigma}}u_{\boldsymbol{k}_{\nu,\sigma}+\boldsymbol{k}}u_{\boldsymbol{k}_{\nu',\sigma'}}v_{\boldsymbol{k}_{\nu',\sigma'}-\boldsymbol{k}}\left\langle\mathcal{T}\alpha_{-\boldsymbol{k}_{\nu,\sigma}}(t)^{\rm harm}\alpha_{\boldsymbol{k}_{\nu,\sigma}+\boldsymbol{k}}(t)^{\rm harm}\alpha^{\dagger}_{\boldsymbol{k}_{\nu',\sigma'}}\alpha^{\dagger}_{-\boldsymbol{k}_{\nu',\sigma'}+\boldsymbol{k}}\right\rangle_0+v_{\boldsymbol{k}_{\nu,\sigma}}v_{\boldsymbol{k}_{\nu,\sigma}+\boldsymbol{k}}v_{\boldsymbol{k}_{\nu',\sigma'}}v_{\boldsymbol{k}_{\nu',\sigma'}-\boldsymbol{k}}$$
$$\times\left[\left\langle\mathcal{T}\alpha_{-\boldsymbol{k}_{\nu,\sigma}}(t)^{\rm harm}\alpha^{\dagger}_{\boldsymbol{k}_{\nu,\sigma}+\boldsymbol{k}}(t)^{\rm harm}\alpha_{\boldsymbol{k}_{\nu',\sigma'}}\alpha^{\dagger}_{-\boldsymbol{k}_{\nu',\sigma'}+\boldsymbol{k}}\right\rangle_0-\left\langle\mathcal{T}\alpha_{-\boldsymbol{k}_{\nu,\sigma}}(t)^{\rm harm}\alpha^{\dagger}_{\boldsymbol{k}_{\nu,\sigma}+\boldsymbol{k}}(t)^{\rm harm}\right\rangle_0\left\langle\mathcal{T}\alpha_{\boldsymbol{k}_{\nu',\sigma'}}\alpha^{\dagger}_{-\boldsymbol{k}_{\nu',\sigma'}+\boldsymbol{k}}\right\rangle_0\right]\Big\}e^{i[\omega+i\epsilon\sigma(t)]t}dt$$
$$=\frac{i}{L}\sum_{\sigma=0,\pm}\sum_{\nu=1}^{N}\int_{-\infty}^{\infty}d\omega'\Big\{v_{\boldsymbol{k}_{\nu,\sigma}}u_{\boldsymbol{k}_{\nu,\sigma}+\boldsymbol{k}}(u_{\boldsymbol{k}_{\nu,\sigma}}v_{\boldsymbol{k}_{\nu,\sigma}+\boldsymbol{k}}+v_{\boldsymbol{k}_{\nu,\sigma}}u_{\boldsymbol{k}_{\nu,\sigma}-\boldsymbol{k}})G_0^{-+}(-\boldsymbol{k}_{\nu,\sigma};\omega'+i\epsilon)G_0^{-+}(\boldsymbol{k}_{\nu,\sigma}+\boldsymbol{k};\omega-\omega'+i\epsilon)$$
$$+v^2_{\boldsymbol{k}_{\nu,\sigma}}v^2_{\boldsymbol{k}_{\nu,\sigma}+\boldsymbol{k}}G_0^{-+}(-\boldsymbol{k}_{\nu,\sigma};\omega'+i\epsilon)G_0^{-+}(\boldsymbol{k}_{\nu,\sigma}+\boldsymbol{k};\omega+\omega'+i\epsilon)\Big\}$$
$$=\frac{\hbar}{L}\sum_{\sigma=0,\pm}\sum_{\nu=1}^{N}\frac{v_{\boldsymbol{k}_{\nu,\sigma}}u_{\boldsymbol{k}_{\nu,\sigma}+\boldsymbol{k}}(u_{\boldsymbol{k}_{\nu,\sigma}}v_{\boldsymbol{k}_{\nu,\sigma}+\boldsymbol{k}}+v_{\boldsymbol{k}_{\nu,\sigma}}u_{\boldsymbol{k}_{\nu,\sigma}+\boldsymbol{k}})}{\hbar\omega-\tilde{\varepsilon}_{\boldsymbol{k}_{\nu,\sigma}}-\tilde{\varepsilon}_{\boldsymbol{k}_{\nu,\sigma}+\boldsymbol{k}}+i\hbar\epsilon}\tag{S58}$$

to them, which prove to be of $O(S^{-1})$, and MPSWs merely give them $O(S^{-2})$ corrections. Therefore, we calculate longitudinal contributions no further beyond (S58).

Finally we discuss mixed transverse-longitudinal fluctuations emergent in (S51). The corresponding correlators trivially vanish in the bare magnon ground state, $\mathcal{G}_0^{\tilde{z}\tilde{x}}(\boldsymbol{k};\omega+i\epsilon)=\mathcal{G}_0^{\tilde{x}\tilde{z}}(\boldsymbol{k};\omega+i\epsilon)=0$ [cf. (S15)]. Their first nonzero contribution arises to first order in $\mathcal{H}^{(\frac{1}{2})}$. Again utilizing the Hartree-Fock decomposition (S52) for expanding $S^{\tilde{x}}_{\boldsymbol{r}_l}$ in $1/S$, we have

$$\mathcal{G}^{\tilde{z}\tilde{x}}(\boldsymbol{k};\omega+i\epsilon)=-i\sum_{l=1}^{\infty}\frac{(-i)^l}{l!\hbar^l}\int_{-\infty}^{\infty}dt_1\cdots\int_{-\infty}^{\infty}dt_l\int_{-\infty}^{\infty}\left\langle\mathcal{T}\mathcal{V}(t_1)^{\rm harm}\cdots\mathcal{V}(t_l)^{\rm harm}\delta S^{\tilde{z}}_{\boldsymbol{k}}(t)^{\rm harm}\delta S^{\tilde{x}}_{-\boldsymbol{k}}\right\rangle_0 e^{i[\omega+i\epsilon\sigma(t)]t}dt$$
$$=-\frac{1}{\hbar}\int_{-\infty}^{\infty}dt_1\int_{-\infty}^{\infty}\left\langle\mathcal{T}\mathcal{H}^{(\frac{1}{2})}(t_1)^{\rm harm}\delta S^{\tilde{z}}_{\boldsymbol{k}}(t)^{\rm harm}\delta S^{\tilde{x}}_{-\boldsymbol{k}}\right\rangle_0 e^{i[\omega+i\epsilon\sigma(t)]t}dt+\cdots=-\mathcal{G}^{\tilde{x}\tilde{z}}(\boldsymbol{k};\omega+i\epsilon)$$
$$\simeq\sqrt{\frac{S}{2}}\left[1-\frac{2\langle\mathcal{A}\rangle_0+\langle C\rangle_0}{4S}\right](u_{\boldsymbol{k}}+v_{\boldsymbol{k}})\left[\Gamma_1'^{(-\frac{1}{2})}(\boldsymbol{k};\omega+i\epsilon)G^{-+}(\boldsymbol{k};\omega+i\epsilon)+\Gamma_1''^{(-\frac{1}{2})}(\boldsymbol{k};\omega+i\epsilon)G^{-+}(-\boldsymbol{k};-\omega-i\epsilon)\right];$$

$$\Gamma_1'^{(-\frac{1}{2})}(\boldsymbol{k};\omega+i\epsilon)\equiv\sum_{\sigma=0,\pm}\sum_{\nu=1}^{N}(u_{\boldsymbol{k}_{\nu,\sigma}}v_{\boldsymbol{k}_{\nu,\sigma}-\boldsymbol{k}}+v_{\boldsymbol{k}_{\nu,\sigma}}u_{\boldsymbol{k}_{\nu,\sigma}-\boldsymbol{k}})\left[\frac{i\Lambda_{++-}(-\boldsymbol{k}+\boldsymbol{k}_{\nu,\sigma},-\boldsymbol{k}_{\nu,\sigma},-\boldsymbol{k})}{\hbar\omega-\tilde{\varepsilon}_{\boldsymbol{k}_{\nu,\sigma}}-\tilde{\varepsilon}_{\boldsymbol{k}-\boldsymbol{k}_{\nu,\sigma}}+i\hbar\epsilon}+\frac{3i\Lambda_{+++}(-\boldsymbol{k},\boldsymbol{k}-\boldsymbol{k}_{\nu,\sigma},\boldsymbol{k}_{\nu,\sigma})}{\hbar\omega+\tilde{\varepsilon}_{\boldsymbol{k}_{\nu,\sigma}}+\tilde{\varepsilon}_{\boldsymbol{k}-\boldsymbol{k}_{\nu,\sigma}}+i\hbar\epsilon}\right],$$

$$\Gamma_1''^{(-\frac{1}{2})}(\boldsymbol{k};\omega+i\epsilon)\equiv-\sum_{\sigma=0,\pm}\sum_{\nu=1}^{N}(u_{\boldsymbol{k}_{\nu,\sigma}}v_{\boldsymbol{k}_{\nu,\sigma}-\boldsymbol{k}}+v_{\boldsymbol{k}_{\nu,\sigma}}u_{\boldsymbol{k}_{\nu,\sigma}-\boldsymbol{k}})\left[\frac{3i\Lambda_{+++}(\boldsymbol{k},-\boldsymbol{k}+\boldsymbol{k}_{\nu,\sigma},-\boldsymbol{k}_{\nu,\sigma})^*}{\hbar\omega-\tilde{\varepsilon}_{\boldsymbol{k}_{\nu,\sigma}}-\tilde{\varepsilon}_{\boldsymbol{k}-\boldsymbol{k}_{\nu,\sigma}}+i\hbar\epsilon}+\frac{i\Lambda_{++-}(\boldsymbol{k}-\boldsymbol{k}_{\nu,\sigma},\boldsymbol{k}_{\nu,\sigma},\boldsymbol{k})^*}{\hbar\omega+\tilde{\varepsilon}_{\boldsymbol{k}_{\nu,\sigma}}+\tilde{\varepsilon}_{\boldsymbol{k}-\boldsymbol{k}_{\nu,\sigma}}+i\hbar\epsilon}\right]. \quad \text{(S59)}$$

Such evaluated $\mathcal{G}^{\tilde{z}\tilde{x}}(\boldsymbol{k};\omega+i\epsilon)$ and $\mathcal{G}^{\tilde{x}\tilde{z}}(\boldsymbol{k};\omega+i\epsilon)$ turn out still extremely small in value. Indeed, they merely make an invisible contribution to the total dynamic structure factor $S(\boldsymbol{q},\omega)\equiv\sum_{\lambda=\mathrm{z},x,y}S^{\lambda\lambda}(\boldsymbol{q},\omega)$ shown in Fig. 2. $\Gamma_1'^{(-\frac{1}{2})}$ and $\Gamma_1''^{(-\frac{1}{2})}$, both to first order in $\mathcal{H}^{(\frac{1}{2})}$ and on the order of $S^{-\frac{1}{2}}$, bear some resemblance to $\Sigma_2'^{(0)}$ but are dimensionless in energy. For the triangular-lattice antiferromagnet, Mourigal *et al.* [13] demonstrate that the mixed transverse-longitudinal correlators (S59) do not affect the leading quasiparticle-like part of the spectrum but sometimes cause an unphysical overcompensation, and therefore conclude that they, as well as the anomalous Green's functions (S56), can be neglected.

Thus and thus, the MPSW-ground-state dynamic structure factor is evaluated as

$$\begin{aligned}
S(\boldsymbol{q},\omega)\equiv\sum_{\lambda=x,y,z}S^{\lambda\lambda}(\boldsymbol{q},\omega)&=-\frac{1}{2\pi\hbar}\sum_{\tau=\pm}\mathrm{Im}\left[\mathcal{G}_0^{\tilde{z}\tilde{z}}(\tau\boldsymbol{Q}_{\mathrm{X,K}}+\boldsymbol{q};\omega+i\epsilon)+\mathcal{G}^{\tilde{x}\tilde{x}}(\tau\boldsymbol{Q}_{\mathrm{X,K}}+\boldsymbol{q};\omega+i\epsilon)\right]\\
&\quad-\frac{1}{\pi\hbar}\mathrm{Im}\,\mathcal{G}^{\tilde{y}\tilde{y}}(\boldsymbol{q};\omega+i\epsilon)-\frac{1}{2\pi\hbar}\sum_{\tau=\pm}\tau\mathrm{Im}\left[\mathcal{G}^{\tilde{z}\tilde{x}}(\tau\boldsymbol{Q}_{\mathrm{X,K}}+\boldsymbol{q};\omega+i\epsilon)-\mathcal{G}^{\tilde{x}\tilde{z}}(\tau\boldsymbol{Q}_{\mathrm{X,K}}+\boldsymbol{q};\omega+i\epsilon)\right]\\
&=\frac{1}{2L}\sum_{\tau=\pm}\sum_{\sigma=0,\pm}\sum_{\nu=1}^{N}v_{\boldsymbol{k}_{\nu,\sigma}}u_{\boldsymbol{k}_{\nu,\sigma}+\tau\boldsymbol{Q}_{\mathrm{X,K}}+\boldsymbol{q}}(u_{\boldsymbol{k}_{\nu,\sigma}}v_{\boldsymbol{k}_{\nu,\sigma}+\tau\boldsymbol{Q}_{\mathrm{X,K}}+\boldsymbol{q}}+v_{\boldsymbol{k}_{\nu,\sigma}}u_{\boldsymbol{k}_{\nu,\sigma}+\tau\boldsymbol{Q}_{\mathrm{X,K}}+\boldsymbol{q}})\delta\left(\hbar\omega-\tilde{\varepsilon}_{\boldsymbol{k}_{\nu,\sigma}}-\tilde{\varepsilon}_{\boldsymbol{k}_{\nu,\sigma}+\tau\boldsymbol{Q}_{\mathrm{X,K}}+\boldsymbol{q}}\right)\\
&\quad-\frac{S}{4\pi}\left[1-\frac{2\langle\mathcal{A}\rangle_0+\langle C\rangle_0}{2S}\right]\sum_{\tau=\pm}(u_{\tau\boldsymbol{Q}_{\mathrm{X,K}}+\boldsymbol{q}}+v_{\tau\boldsymbol{Q}_{\mathrm{X,K}}+\boldsymbol{q}})^2\mathrm{Im}\frac{1}{\hbar\omega-\tilde{\varepsilon}_{\tau\boldsymbol{Q}_{\mathrm{X,K}}+\boldsymbol{q}}-\Sigma^{(0)}(\tau\boldsymbol{Q}_{\mathrm{X,K}}+\boldsymbol{q};\omega+i\epsilon)+i\hbar\epsilon}\\
&\quad-\frac{S}{2\pi}\left[1-\frac{2\langle\mathcal{A}\rangle_0-\langle C\rangle_0}{2S}\right](u_{\boldsymbol{q}}-v_{\boldsymbol{q}})^2\mathrm{Im}\frac{1}{\hbar\omega-\tilde{\varepsilon}_{\boldsymbol{q}}-\Sigma^{(0)}(\boldsymbol{q};\omega+i\epsilon)+i\hbar\epsilon}\\
&\quad-\frac{\sqrt{S}}{\sqrt{2}\pi}\left[1-\frac{2\langle\mathcal{A}\rangle_0+\langle C\rangle_0}{4S}\right]\sum_{\tau=\pm}(u_{\tau\boldsymbol{Q}_{\mathrm{X,K}}+\boldsymbol{q}}+v_{\tau\boldsymbol{Q}_{\mathrm{X,K}}+\boldsymbol{q}})\\
&\quad\times\tau\mathrm{Im}\left[\frac{\Gamma_1'^{(-\frac{1}{2})}(\tau\boldsymbol{Q}_{\mathrm{X,K}}+\boldsymbol{q};\omega+i\epsilon)}{\hbar\omega-\tilde{\varepsilon}_{\tau\boldsymbol{Q}_{\mathrm{X,K}}+\boldsymbol{q}}-\Sigma^{(0)}(\tau\boldsymbol{Q}_{\mathrm{X,K}}+\boldsymbol{q};\omega+i\epsilon)+i\hbar\epsilon}-\frac{\Gamma_1''^{(-\frac{1}{2})}(\tau\boldsymbol{Q}_{\mathrm{X,K}}+\boldsymbol{q};\omega+i\epsilon)}{\hbar\omega+\tilde{\varepsilon}_{\tau\boldsymbol{Q}_{\mathrm{X,K}}+\boldsymbol{q}}+\Sigma^{(0)}(-\tau\boldsymbol{Q}_{\mathrm{X,K}}-\boldsymbol{q};\omega-i\epsilon)+i\hbar\epsilon}\right]. \quad \text{(S60)}
\end{aligned}$$

With $\Sigma^{(0)}$, $\Gamma_1'^{(-\frac{1}{2})}$, and $\Gamma_1''^{(-\frac{1}{2})}$ all away, (S60) reduces to the MLSW-ground-state dynamic structure factor

$$\begin{aligned}
S(\boldsymbol{q},\omega)&=\frac{1}{2L}\sum_{\tau=\pm}\sum_{\sigma=0,\pm}\sum_{\nu=1}^{N}v_{\boldsymbol{k}_{\nu,\sigma}}u_{\boldsymbol{k}_{\nu,\sigma}+\tau\boldsymbol{Q}_{\mathrm{X,K}}+\boldsymbol{q}}(u_{\boldsymbol{k}_{\nu,\sigma}}v_{\boldsymbol{k}_{\nu,\sigma}+\tau\boldsymbol{Q}_{\mathrm{X,K}}+\boldsymbol{q}}+v_{\boldsymbol{k}_{\nu,\sigma}}u_{\boldsymbol{k}_{\nu,\sigma}+\tau\boldsymbol{Q}_{\mathrm{X,K}}+\boldsymbol{q}})\delta\left(\hbar\omega-\tilde{\varepsilon}_{\boldsymbol{k}_{\nu,\sigma}}-\tilde{\varepsilon}_{\boldsymbol{k}_{\nu,\sigma}+\tau\boldsymbol{Q}_{\mathrm{X,K}}+\boldsymbol{q}}\right)\\
&\quad+\frac{S}{4}\left[1-\frac{2\langle\mathcal{A}\rangle_0+\langle C\rangle_0}{2S}\right]\sum_{\tau=\pm}(u_{\tau\boldsymbol{Q}_{\mathrm{X,K}}+\boldsymbol{q}}+v_{\tau\boldsymbol{Q}_{\mathrm{X,K}}+\boldsymbol{q}})^2\delta\left(\hbar\omega-\tilde{\varepsilon}_{\tau\boldsymbol{Q}_{\mathrm{X,K}}+\boldsymbol{q}}\right)\\
&\quad+\frac{S}{2}\left[1-\frac{2\langle\mathcal{A}\rangle_0-\langle C\rangle_0}{2S}\right](u_{\boldsymbol{q}}-v_{\boldsymbol{q}})^2\delta\left(\hbar\omega-\tilde{\varepsilon}_{\boldsymbol{q}}\right). \quad \text{(S61)}
\end{aligned}$$

Note that $\langle\mathcal{A}\rangle_0^{\mathrm{SC}}=S$, whereas $\langle\mathcal{A}\rangle_0^{\mathrm{DC}}=S-\delta$ and $\langle C\rangle_0^{\mathrm{DC}}=0$.

Since SC MLSWs have such a small chemical potential and therefore excitation energy that $\mu\simeq0.0069JS$ and $\tilde{\varepsilon}^{\mathrm{SC}}_{\boldsymbol{Q}_{\Gamma,\Gamma}}\simeq0.2402JS$ [Eq. (7) and Fig. 1(c1)], they overestimate a single-magnon scattering intensity in $S(\boldsymbol{Q}_{\mathrm{X,K}},\omega)$ [Fig. 2(a2)] as

$$\begin{aligned}
S(\boldsymbol{Q}_{\mathrm{X,K}},\omega)&\simeq\frac{S}{4}\left[1-\frac{2\langle\mathcal{A}\rangle_0+\langle C\rangle_0}{2S}\right](u_{-\boldsymbol{Q}_{\mathrm{X,K}}+\boldsymbol{Q}_{\mathrm{X,K}}}+v_{-\boldsymbol{Q}_{\mathrm{X,K}}+\boldsymbol{Q}_{\mathrm{X,K}}})^2\delta\left(\hbar\omega-\tilde{\varepsilon}^{\mathrm{SC}}_{-\boldsymbol{Q}_{\mathrm{X,K}}+\boldsymbol{Q}_{\mathrm{X,K}}}\right)\\
&=\left(\frac{S}{4}+\frac{1}{8}-\sum_{\sigma=0,\pm}\sum_{\nu=1}^{N}\frac{u^2_{\boldsymbol{k}_{\nu,\sigma}}+v^2_{\boldsymbol{k}_{\nu,\sigma}}+u_{\boldsymbol{k}_{\nu,\sigma}}v_{\boldsymbol{k}_{\nu,\sigma}}}{8L}\right)(u_{\boldsymbol{Q}_{\Gamma,\Gamma}}+v_{\boldsymbol{Q}_{\Gamma,\Gamma}})^2\delta\left(\hbar\omega-\tilde{\varepsilon}^{\mathrm{SC}}_{\boldsymbol{Q}_{\Gamma,\Gamma}}\right)\\
&=\left(\frac{S}{4}+\frac{1}{8}-\sum_{\sigma=0,\pm}\sum_{\nu=1}^{N}\frac{u^2_{\boldsymbol{k}_{\nu,\sigma}}+v^2_{\boldsymbol{k}_{\nu,\sigma}}+u_{\boldsymbol{k}_{\nu,\sigma}}v_{\boldsymbol{k}_{\nu,\sigma}}}{8L}\right)\left\{\frac{1}{4\tilde{\varepsilon}^{\mathrm{SC}}_{\boldsymbol{Q}_{\Gamma,\Gamma}}}\left[21JS-2\mu+\frac{(7JS)^2}{2\tilde{\varepsilon}^{\mathrm{SC}}_{\boldsymbol{Q}_{\Gamma,\Gamma}}+7JS-2\mu}\right]+\frac{1}{2}\right\}\delta\left(\hbar\omega-\tilde{\varepsilon}^{\mathrm{SC}}_{\boldsymbol{Q}_{\Gamma,\Gamma}}\right)\\
&\simeq\left(\frac{S}{4}+\frac{1}{8}+0.1545\right)\frac{7JS}{\tilde{\varepsilon}^{\mathrm{SC}}_{\boldsymbol{Q}_{\Gamma,\Gamma}}}\delta\left(\hbar\omega-\tilde{\varepsilon}^{\mathrm{SC}}_{\boldsymbol{Q}_{\Gamma,\Gamma}}\right)=0.4045\frac{7J}{2\tilde{\varepsilon}^{\mathrm{SC}}_{\boldsymbol{Q}_{\Gamma,\Gamma}}}\delta\left(\hbar\omega-\tilde{\varepsilon}^{\mathrm{SC}}_{\boldsymbol{Q}_{\Gamma,\Gamma}}\right)\left(S=\frac{1}{2}\right). \quad \text{(S62)}
\end{aligned}$$

Besides, SC MLSWs have smaller excitation energies such that $\tilde{\varepsilon}^{\rm SC}_{\pm\boldsymbol{Q}_{\rm X,K}} \simeq 0.2130JS$ [Eq. (7) and Fig. 1(c2)], and therefore they further overestimate a two-magnon scattering intensity in $S(\boldsymbol{Q}_{\rm X,\Gamma},\omega)$ [see Fig. 2(a1)] as

$$\begin{aligned} S(\boldsymbol{Q}_{\rm X,\Gamma},\omega) &\simeq v_{\boldsymbol{Q}_{\rm X,K}} u_{\boldsymbol{Q}_{\rm X,K}+\boldsymbol{Q}_{\rm X,K}+\boldsymbol{Q}_{\rm X,\Gamma}} (u_{\boldsymbol{Q}_{\rm X,K}} v_{\boldsymbol{Q}_{\rm X,K}+\boldsymbol{Q}_{\rm X,K}+\boldsymbol{Q}_{\rm X,\Gamma}} + v_{\boldsymbol{Q}_{\rm X,K}} u_{\boldsymbol{Q}_{\rm X,K}+\boldsymbol{Q}_{\rm X,K}+\boldsymbol{Q}_{\rm X,\Gamma}}) \delta\left(\hbar\omega - \tilde{\varepsilon}^{\rm SC}_{\boldsymbol{Q}_{\rm X,K}} - \tilde{\varepsilon}^{\rm SC}_{\boldsymbol{Q}_{\rm X,K}+\boldsymbol{Q}_{\rm X,K}+\boldsymbol{Q}_{\rm X,\Gamma}}\right) \\ &= v_{\boldsymbol{Q}_{\rm X,K}} u_{-\boldsymbol{Q}_{\rm X,K}} (u_{\boldsymbol{Q}_{\rm X,K}} v_{-\boldsymbol{Q}_{\rm X,K}} + v_{\boldsymbol{Q}_{\rm X,K}} u_{-\boldsymbol{Q}_{\rm X,K}}) \delta\left(\hbar\omega - \tilde{\varepsilon}^{\rm SC}_{\boldsymbol{Q}_{\rm X,K}} - \tilde{\varepsilon}^{\rm SC}_{-\boldsymbol{Q}_{\rm X,K}}\right) = \frac{(11JS)^2}{32\tilde{\varepsilon}^{\rm SC}_{\boldsymbol{Q}_{\rm X,K}} \tilde{\varepsilon}^{\rm SC}_{-\boldsymbol{Q}_{\rm X,K}}} \delta\left(\hbar\omega - \tilde{\varepsilon}^{\rm SC}_{\boldsymbol{Q}_{\rm X,K}} - \tilde{\varepsilon}^{\rm SC}_{-\boldsymbol{Q}_{\rm X,K}}\right). \end{aligned} \tag{S63}$$

On the other hand, the SC-MWDISW-ground-state dynamic structure factor is evaluated as

$$S^{\lambda\lambda'}(\boldsymbol{q},\omega) = \frac{1}{2\pi\hbar}\int_{-\infty}^{\infty} \left\langle \delta S^{\lambda}_{\boldsymbol{q}}(t) \delta S^{\lambda'}_{-\boldsymbol{q}} \right\rangle_0^{\prime\rm SC} e^{i\omega t} dt = \frac{1}{2\pi\hbar}\int_{-\infty}^{\infty} \left\langle e^{i\widetilde{\mathcal{H}}'^{\rm SC}t/\hbar} \delta S^{\lambda}_{\boldsymbol{q}} e^{-i\widetilde{\mathcal{H}}'^{\rm SC}t/\hbar} \delta S^{\lambda'}_{-\boldsymbol{q}} \right\rangle_0^{\prime\rm SC} e^{i\omega t} dt;\ \delta S^{\lambda}_{\boldsymbol{q}} = S^{\lambda}_{\boldsymbol{q}} - \left\langle S^{\lambda}_{\boldsymbol{q}} \right\rangle_0^{\prime\rm SC}, \tag{S64}$$

$$\begin{aligned} S(\boldsymbol{q},\omega) = {}& \frac{1}{2L}\sum_{\tau=\pm}\sum_{\sigma=0,\pm}\sum_{\nu=1}^{N} v_{\boldsymbol{k}_{\nu,\sigma}} u_{\boldsymbol{k}_{\nu,\sigma}+\tau\boldsymbol{Q}_{\rm X,K}+\boldsymbol{q}} (u_{\boldsymbol{k}_{\nu,\sigma}} v_{\boldsymbol{k}_{\nu,\sigma}+\tau\boldsymbol{Q}_{\rm X,K}+\boldsymbol{q}} + v_{\boldsymbol{k}_{\nu,\sigma}} u_{\boldsymbol{k}_{\nu,\sigma}+\tau\boldsymbol{Q}_{\rm X,K}+\boldsymbol{q}}) \delta\left(\hbar\omega - \tilde{\varepsilon}'^{\rm SC}_{\boldsymbol{k}_{\nu,\sigma}} - \tilde{\varepsilon}'^{\rm SC}_{\boldsymbol{k}_{\nu,\sigma}+\tau\boldsymbol{Q}_{\rm X,K}+\boldsymbol{q}}\right) \\ &+ \frac{S}{4}\left[1 - \frac{2\langle\mathcal{A}\rangle_0^{\prime\rm SC} + \langle C\rangle_0^{\prime\rm SC}}{2S}\right] \sum_{\tau=\pm} (u_{\tau\boldsymbol{Q}_{\rm X,K}+\boldsymbol{q}} + v_{\tau\boldsymbol{Q}_{\rm X,K}+\boldsymbol{q}})^2 \delta\left(\hbar\omega - \tilde{\varepsilon}'^{\rm SC}_{\tau\boldsymbol{Q}_{\rm X,K}+\boldsymbol{q}}\right) \\ &+ \frac{S}{2}\left[1 - \frac{2\langle\mathcal{A}\rangle_0^{\prime\rm SC} - \langle C\rangle_0^{\prime\rm SC}}{2S}\right] (u_{\boldsymbol{q}} - v_{\boldsymbol{q}})^2 \delta\left(\hbar\omega - \tilde{\varepsilon}'^{\rm SC}_{\boldsymbol{q}}\right). \end{aligned} \tag{S65}$$

Note that $\langle\mathcal{A}\rangle_0^{\prime\rm SC} = S$. The expression (S65) looks the same as (S61) except for $\langle\mathcal{A}\rangle_0^{\prime\rm SC}$, $\langle C\rangle_0^{\prime\rm SC}$, and $\tilde{\varepsilon}'^{\rm SC}_{\boldsymbol{k}}$ instead of $\langle\mathcal{A}\rangle_0^{\rm SC}$, $\langle C\rangle_0^{\rm SC}$, and $\tilde{\varepsilon}^{\rm SC}_{\boldsymbol{k}}$, respectively.

The $\mathcal{H}^{(\frac{1}{2})}$-driven $O(S^0)$ self-energy $\bar{\Sigma}^{(0)}_2(\boldsymbol{k};\tilde{\varepsilon}^{\rm DC}_{\boldsymbol{k}}/\hbar)$ causes a strong downward renormalization of the bare magnon energies $\tilde{\varepsilon}^{\rm DC}_{\boldsymbol{k}}$ at $k^x = \pm Q^x_{\rm K}$ and $|k^z| \lesssim \frac{Q^z_{\rm X}}{2}$. The thus-obtained DC MPSWs yield the scattering intensities

$$S(\boldsymbol{q},\omega) \simeq -\frac{S}{4\pi}\left[1 - \frac{2\langle\mathcal{A}\rangle_0^{\rm DC} + \langle C\rangle_0^{\rm DC}}{2S}\right] \sum_{\tau=\pm} \left(u_{\tau\boldsymbol{Q}_{\rm X,K}+\boldsymbol{q}} + v_{\tau\boldsymbol{Q}_{\rm X,K}+\boldsymbol{q}}\right)^2 {\rm Im} \frac{1}{\hbar\omega - \tilde{\varepsilon}^{\rm DC}_{\tau\boldsymbol{Q}_{\rm X,K}+\boldsymbol{q}} - \Sigma^{(0)}(\tau\boldsymbol{Q}_{\rm X,K}+\boldsymbol{q};\omega+i\epsilon) + i\hbar\epsilon} \tag{S66}$$

at $q^x = Q^x_\Gamma$ and $\frac{Q^z_{\rm X}}{2} \ll |q^z| \lesssim Q^z_{\rm X}$ and

$$S(\boldsymbol{q},\omega) \simeq -\frac{S}{2\pi}\left[1 - \frac{2\langle\mathcal{A}\rangle_0^{\rm DC} - \langle C\rangle_0^{\rm DC}}{2S}\right] \left(u_{\boldsymbol{q}} - v_{\boldsymbol{q}}\right)^2 {\rm Im} \frac{1}{\hbar\omega - \tilde{\varepsilon}^{\rm DC}_{\boldsymbol{q}} - \Sigma^{(0)}(\boldsymbol{q};\omega+i\epsilon) + i\hbar\epsilon} \tag{S67}$$

at $q^x = \pm Q^x_{\rm K}$ and $Q^z_\Gamma \lesssim |q^z| \lesssim \frac{Q^z_{\rm X}}{2}$ to successfully reproduce the DMRG calculations, as are illustrated with vertical arrows in Figs. 2(b1′) and 2(c1) and in Figs. 2(b2′) and 2(c2), respectively. This is not the case with SC MPSWs. $\tilde{\varepsilon}^{\rm DC}_{\boldsymbol{k}}$ owes its strong downward renormalization at $k^x = \pm Q^x_{\rm K}$ and $|k^z| \lesssim \frac{Q^z_{\rm X}}{2}$ to the cubic-interaction-driven self-energy correction $\bar{\Sigma}^{(0)}_2(\boldsymbol{k};\tilde{\varepsilon}^{\rm DC}_{\boldsymbol{k}}/\hbar)\,(<0)$ surpassing the quartic-interaction-driven one $\bar{\Sigma}^{(0)}_1(\boldsymbol{k})\,(>0)$ in magnitude [Fig. 3(a2″)]. These self-energy corrections cancel out each other at $k^x = \pm Q^x_{\rm K}$ and $|k^z| \lesssim \frac{Q^z_{\rm X}}{2}$ under the SC condition [Fig. 3(b2″)]. There is no downward renormalization of the bare magnon energies $\tilde{\varepsilon}_{\boldsymbol{k}}$ with MWDISWs either, whether SC or DC conditioned. Variationally interacting SWs are totally ignorant of cubic anharmonicities.

## S3. DOUBLE-CONSTRAINT VERSUS SINGLE-CONSTRAINT MODIFICATION SCHEMES

The DC modification scheme retains the local U(1) symmetry without spoiling the ground-state energy in the SC modification scheme. Let $\widetilde{\mathcal{H}}_{\rm harm}$ be either $\widetilde{\mathcal{H}}^{\rm SC}_{\rm harm}$ or $\widetilde{\mathcal{H}}^{\rm DC}_{\rm harm}$. Then the MSW ground-state energy $E_{\rm g}$ is written as $\langle\widetilde{\mathcal{H}}_{\rm harm}\rangle_0 = \sum_{m=1}^{2} E^{(m)} + \mu L\left(S - \delta + \frac{1}{2}\right)$ (MLSWs) or $\langle\widetilde{\mathcal{H}}_{\rm harm}\rangle_0 + \delta E^{(0)}_1 + \delta E^{(0)}_2$ (MPSWs), where $\delta$ (S34) serves to optimize the ground-state energy, while the perturbative corrections to first order in $\mathcal{H}^{(0)}$ (S40) and second order in $\mathcal{H}^{(\frac{1}{2})}$ (S39) are given by

$$\begin{aligned} \delta E^{(0)}_1 = \langle\mathcal{H}^{(0)}\rangle_0 = -JL\sum_{\sigma=\parallel,\perp}\Bigg\{ & \left[(\langle\mathcal{A}\rangle_0)^2 + (\langle\mathcal{B}_\sigma\rangle_0)^2 + (\langle\mathcal{D}_\sigma\rangle_0)^2 - (2\langle\mathcal{A}\rangle_0 + \langle C\rangle_0)\frac{\langle\mathcal{B}_\sigma\rangle_0 + \langle\mathcal{D}_\sigma\rangle_0}{2}\right]\cos\boldsymbol{Q}_{\rm X,K}\cdot\boldsymbol{\delta}_\sigma \\ & - (2\langle\mathcal{A}\rangle_0 - \langle C\rangle_0)\frac{\langle\mathcal{B}_\sigma\rangle_0 - \langle\mathcal{D}_\sigma\rangle_0}{2} - \left(\frac{\langle\mathcal{A}\rangle_0}{2} - \frac{\langle\mathcal{B}_\sigma\rangle_0 + \langle\mathcal{D}_\sigma\rangle_0}{4}\right)\cos\boldsymbol{Q}_{\rm X,K}\cdot\boldsymbol{\delta}_\sigma - \frac{\langle\mathcal{B}_\sigma\rangle_0 - \langle\mathcal{D}_\sigma\rangle_0}{4}\Bigg\}, \end{aligned} \tag{S68}$$

$$\delta E^{(0)}_2 = \prod_{\tau=0,\pm}\prod_{\mu=1}^{N}\sum_{n_{\boldsymbol{k}_{\mu,\tau}}=0}^{\infty}{}^{\prime} \frac{\left|\left\langle \prod_{\sigma=0,\pm}\prod_{\nu=1}^{N} \frac{\left(\alpha_{\boldsymbol{k}_{\nu,\sigma}}\right)^{n_{\boldsymbol{k}_{\nu,\sigma}}}}{\sqrt{n_{\boldsymbol{k}_{\nu,\sigma}}!}} \mathcal{H}^{(\frac{1}{2})} \right\rangle_0\right|^2}{-\sum_{\sigma=0,\pm}\sum_{\nu=1}^{N}\tilde{\varepsilon}_{\boldsymbol{k}_{\nu,\sigma}} n_{\boldsymbol{k}_{\nu,\sigma}}} = \sum_{\sigma'=0,\pm}\sum_{\nu'=1}^{N}\sum_{\sigma=0,\pm}\sum_{\nu=1}^{N} \frac{6|\Lambda_{+++}(\boldsymbol{k}_{\nu,\sigma}, -\boldsymbol{k}_{\nu,\sigma} - \boldsymbol{k}_{\nu',\sigma'}, \boldsymbol{k}_{\nu',\sigma'})|^2}{-\tilde{\varepsilon}_{\boldsymbol{k}_{\nu,\sigma}} - \tilde{\varepsilon}_{-\boldsymbol{k}_{\nu,\sigma}-\boldsymbol{k}_{\nu',\sigma'}} - \tilde{\varepsilon}_{\boldsymbol{k}_{\nu',\sigma'}}}. \tag{S69}$$

$\left(\sum_{\nu=1}^{N}\sum_{\sigma=0,\pm} n_{\boldsymbol{k}_{\nu,\sigma}} \neq 0\right)$

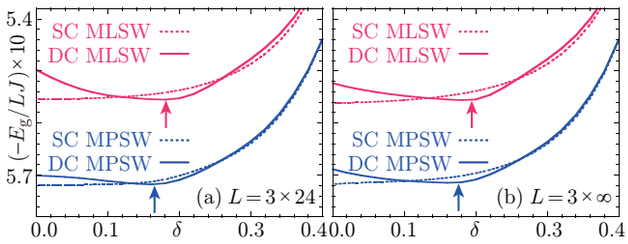



FIG. S1. MSW ground-state energies $E_g = \langle\widetilde{\mathcal{H}}_{\rm harm}\rangle_0 = \sum_{m=1}^{2} E^{(m)} + \mu L\left(S-\delta+\frac{1}{2}\right)$ (MLSW) and $E_g = \langle\widetilde{\mathcal{H}}_{\rm harm}\rangle_0 + \delta E_1^{(0)} + \delta E_2^{(0)}$ (MPSW) under the SC (7) and DC (9) modification schemes for $S=\frac{1}{2}$ at $N=24$ (a) and in the $N\to\infty$ limit (b). The optimal values of $\delta$ in the DC scheme (S34) are indicated by arrows, whereas those in the SC scheme are always zero.

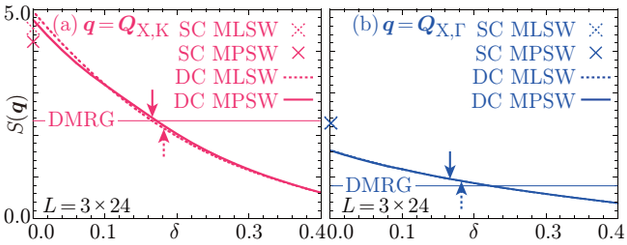



FIG. S2. DC-MSW findings as functions of $\delta$, together with SC-MSW findings just for reference, for the static structure factors $S(\boldsymbol{Q}_{\rm X,K})$ (a) and $S(\boldsymbol{Q}_{\rm X,\Gamma})$ (b) in comparison with the DMRG estimates [14] as criteria for $S=\frac{1}{2}$ at $N=24$. The optimal values of $\delta$ in the DC scheme (S34) determined in Fig. S1 are again indicated by arrows.

We plot $E_g$ as a function of $\delta$ in various manners of modifying SWs in Fig. S1. While just adding the second constraint condition in (S34) to the conventional constraint condition (S19) causes a rise in the ground-state energy, further tuning up the first one in (S34) with respect to $\delta$ cancels out this energy cost.

We further understand the necessity of boson number tuning in the DC modification scheme when we observe DC-MSW calculations of the structure factor in more detail. SC MLSWs describe the scattering intensities at $\boldsymbol{Q}_{\rm X,K}$ and $\boldsymbol{Q}_{\rm X,\Gamma}$ as (S62) and (S63), respectively, and these descriptions turn out to be such overestimates as Figs. 2(a1) and 2(a2), respectively. Their DC-MLSW replacements are such improvements as Figs. 2(b1) and 2(b2) and further developed DC-MPSW calculations are even better than them as Figs. 2(b1′) and 2(b2′), when we rely upon the DMRG findings Figs. 2(c1) and 2(c2). In order to demonstrate how important the tuning of the first constraint condition is in this context, we show in Fig. S2 DC-MSW findings as functions of $\delta$ for the static structure factor $S(\boldsymbol{q}) = \int_0^\infty S(\boldsymbol{q},\omega)d\omega$ at $\boldsymbol{Q}_{\rm X,K}$ and $\boldsymbol{Q}_{\rm X,\Gamma}$ in comparison with DMRG estimates [14]. SC-MSW findings are terrible overestimates. DC-MSW estimates without tuning the total number of emergent bosons remain too large, but they can well hit the DMRG calculations at the end, if pertinently tuned.

The DC modification scheme really makes subtle observations when supplemented by perturbative corrections. This is not the case with the SC modification scheme. In order to contrast them in more detail, it is also worth while comparing the single-CLSW excitation spectrum (5) and double-CLSW excitation continuum band $\mathcal{E}_{\boldsymbol{k};\boldsymbol{q}} \equiv \varepsilon_{\frac{\boldsymbol{k}}{2}+\boldsymbol{q}} + \varepsilon_{\frac{\boldsymbol{k}}{2}-\boldsymbol{q}}$ (Fig. S3), though no perturbative correction is available there. The lower boundary of $\mathcal{E}_{\boldsymbol{k};\boldsymbol{q}}$ is analytically available as

$$\mathcal{E}_{\boldsymbol{k};\boldsymbol{q}_{\rm min}(\boldsymbol{k})} = \begin{cases} \varepsilon_{(Q^z_{\rm X},\mp Q^x_{\rm K})} + \varepsilon_{(k^z-Q^z_{\rm X},\pm Q^x_{\rm K})} = \varepsilon_{(k^z-Q^z_{\rm X},\pm Q^x_{\rm K})} \begin{cases} = \varepsilon_{\boldsymbol{Q}_{\Gamma,\Gamma}} & \left(k^x = Q^x_\Gamma,\ k^z = Q^z_\Gamma\right) \\ < \varepsilon_{(k^z,Q^x_\Gamma)} & \left(k^x = Q^x_\Gamma,\ Q^z_\Gamma < |k^z| \le Q^z_{\rm X}\right) \end{cases} \\ \varepsilon_{(Q^z_{\rm X},\mp Q^x_{\rm K})} + \varepsilon_{(k^z-Q^z_{\rm X},\mp Q^x_{\rm K})} = \varepsilon_{(k^z-Q^z_{\rm X},\mp Q^x_{\rm K})} < \varepsilon_{(k^z,\pm Q^x_{\rm K})} & \left(k^x = \pm Q^x_{\rm K},\ |k^z| < \dfrac{Q^z_{\rm X}}{2}\right) \\ \varepsilon_{(Q^z_\Gamma,Q^x_\Gamma)} + \varepsilon_{(k^z-Q^z_\Gamma,\pm Q^x_{\rm K})} = \varepsilon_{(k^z-Q^z_\Gamma,\pm Q^x_{\rm K})} = \varepsilon_{(k^z,\pm Q^x_{\rm K})} & \left(k^x = \pm Q^x_{\rm K},\ \dfrac{Q^z_{\rm X}}{2} \le |k^z| \le Q^z_{\rm X}\right) \end{cases} . \tag{S70}$$

The CLSW spectrum contains three Nambu-Goldstone modes to be buried in its pair excitation continuum (Fig. S3). Modifying CLSWs causes a hardening of their dispersion such that $0 < \tilde{\varepsilon}^{\rm SC}_{\pm\boldsymbol{Q}_{\rm X,K}} < \tilde{\varepsilon}^{\rm SC}_{\boldsymbol{Q}_{\Gamma,\Gamma}} < \tilde{\varepsilon}^{\rm DC}_{\boldsymbol{Q}_{\Gamma,\Gamma}} < \tilde{\varepsilon}^{\rm DC}_{\pm\boldsymbol{Q}_{\rm X,K}}$ [Figs. 3(a1) to 3(b2)], and therefore any MLSW spectrum is no longer completely buried in its pair excitation continuum. DC MLSWs have larger gaps than SC MLSWs in general, $\tilde{\varepsilon}^{\rm SC}_{\boldsymbol{Q}_{\Gamma,\Gamma}} < \tilde{\varepsilon}^{\rm DC}_{\boldsymbol{Q}_{\Gamma,\Gamma}}$ and $\tilde{\varepsilon}^{\rm SC}_{\pm\boldsymbol{Q}_{\rm X,K}} < \tilde{\varepsilon}^{\rm DC}_{\pm\boldsymbol{Q}_{\rm X,K}}$, and therefore succeed in yielding such subtle observations as are illustrated with vertical arrows in Figs. 2(b1′) and 2(b2′). On the other hand, having in mind that $v_{\boldsymbol{Q}_{\rm X,K}} = \sqrt{\frac{11}{2}}JSa < \sqrt{7}JSa = v_{\boldsymbol{Q}_{\Gamma,\Gamma}}$, DC MLSWs with $\tilde{\varepsilon}^{\rm DC}_{\boldsymbol{Q}_{\Gamma,\Gamma}} < \tilde{\varepsilon}^{\rm DC}_{\pm\boldsymbol{Q}_{\rm X,K}}$ are stabler than SC MLSWs with $\tilde{\varepsilon}^{\rm SC}_{\pm\boldsymbol{Q}_{\rm X,K}} < \tilde{\varepsilon}^{\rm SC}_{\boldsymbol{Q}_{\Gamma,\Gamma}}$, i.e., the single-DC (SC)-MLSW branch comes below the lower edge of the double-DC (SC) -MLSW continuum in a major (minor) part of the Brillouin zone (Table S1). That is why under the successful DC modification scheme, the inequality condition of bare magnons being kinematically unstable towards decays into pairs of other magnons occupies a part of the Brillouin zone far smaller than the region of the lowest-order self-energy corrections to bare magnons having an imaginary part, implying a novel *mixed instability*.

In sum, only when doubly constrained and perturbed, SWs succeed in revealing such complicated dynamics $S(\boldsymbol{q},\omega)$ as a consequence of cubic dominant anharmonicities at the zone boundaries $(k^z,\pm Q^x_{\rm K})$ with $|k^z| \lesssim \frac{Q^z_{\rm X}}{2}$ [Fig. 3(a2″)]. MLSWs miss anharmonicities. MWDISWs are still ignorant of cubic anharmonicities. SC MPSWs leave their cubic and quartic anharmonicities to cancel out each other [Fig. 3(b2″)]. Besides these, SC MSWs all fail to give reasonable gaps at the zone center and corners and therefore end up with too strong $S(\boldsymbol{q},\omega)$ intensities at the zone boundaries [Figs. 2(a1) to 2(a1″) and 2(a2) to 2(a2″)]. DC MSWs are generally much better than SC MSWs at describing magnon hardening effects [Figs. 2(b1), 2(b1′), 2(b2), and 2(b2′)]. In Table S2 we summarize to what extent various MSW schemes are successful in describing three major properties.

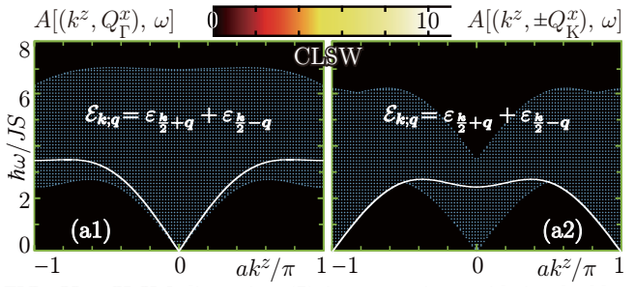



FIG. S3. CLSW dispersion (5) in comparison with its double-excitation continuum $\mathcal{E}_{k;q} \equiv \varepsilon_{\frac{k}{2}+q} + \varepsilon_{\frac{k}{2}-q}$ for $S = \frac{1}{2}$ in the $N \to \infty$ limit, which is shown in the same format as Figs. 3(a1) to 3(b2′) so as to be easy to compare. The CLSW spectral function reads $A(\boldsymbol{k}, \omega) = \delta(\hbar\omega - \varepsilon_{\boldsymbol{k}})$.

TABLE S1. The shaded regions in Figs. 3(a1″) to 3(b2″), where every MLSW excitation is unstable with its energy $\tilde{\varepsilon}_{\boldsymbol{k}}$ exceeding the minimum of the two-magnon continuum $\widetilde{\mathcal{E}}_{k;q} \equiv \tilde{\varepsilon}_{\frac{k}{2}+q} + \tilde{\varepsilon}_{\frac{k}{2}-q}$ [see Figs. 3(a1) to 3(b2)].

| | $k^x = Q^x_\Gamma$ | $k^x = \pm Q^x_K$ |
|---|---|---|
| SC MLSW | $0.2083 < \left\lvert\frac{ak^z}{\pi}\right\rvert \le 1$ | $\left\lvert\frac{ak^z}{\pi}\right\rvert < 0.4479$ |
| DC MLSW | $0.6771 < \left\lvert\frac{ak^z}{\pi}\right\rvert \le 1$ | $\left\lvert\frac{ak^z}{\pi}\right\rvert < 0.2812$ |

TABLE S2. Assessment of various MSW descriptions.

| Scheme (to which order in what manner) | | | Zone-center magnon hardening | Zone-corner magnon hardening | Zone-boundary anharmonicities |
|---|---|---|---|---|---|
| SC | MLSW | (harmonic) | insufficient | insufficient | missing |
| | MPSW | (perturbed) | insufficient | insufficient | cancel out |
| | MWDISW | (variational) | underestimate | overestimate | insufficient |
| DC | MLSW | (harmonic) | sufficient | sufficient | missing |
| | MPSW | (perturbed) | sufficient | sufficient | sufficient |


[1] Takahashi M., *J. Phys. Soc. Jpn.*, **58** (1989) 1524.
[2] Takahashi M., *Phys. Rev. B*, **40** (1989) 2494.
[3] Hirsch J. E. and Tang S., *Phys. Rev. B*, **40** (1989) 4769.
[4] Tang S., Lazzouni M. E. and Hirsch J. E., *Phys. Rev. B*, **40** (1989) 5000.
[5] Yamamoto S., *Phys. Rev. B*, **69** (2004) 064426.
[6] Yamamoto S., Hori H., Furukawa Y., Nishisaka Y., Sumida Y., Yamada K., Kumagai K., Asano T. and Inagaki Y., *J. Phys. Soc. Jpn.*, **75** (2006) 074703.
[7] Yamamoto S. and Ohara J., *J. Phys. Commun.*, **7** (2023) 065004.
[8] Noriki Y. and Yamamoto S., *J. Phys. Soc. Jpn.*, **86** (2017) 034714.
[9] Yamamoto S. and Noriki Y., *Phys. Rev. B*, **99** (2019) 094412.
[10] Lehmann H., *Nuovo Cimento*, **11** (1954) 342.
[11] Fetter A. L. and Walecka J. D., *Quantum Theory of Many-Particle Systems* (McGraw-Hill, New York, 1971).
[12] Wick G. C., *Phys. Rev.*, **80** (1950) 268.
[13] Mourigal M., Fuhrman W. T., Chernyshev A. L. and Zhitomirsky M. E., *Phys. Rev. B*, **88** (2013) 094407.
[14] Nishimoto S. and Arikawa M., *Phys. Rev. B*, **78** (2008) 054421.